

DYNAMIC NEURAL NETWORK-BASED ROBUST CONTROL METHODS FOR
UNCERTAIN NONLINEAR SYSTEMS

By

HUYEN T. DINH

A DISSERTATION PRESENTED TO THE GRADUATE SCHOOL
OF THE UNIVERSITY OF FLORIDA IN PARTIAL FULFILLMENT
OF THE REQUIREMENTS FOR THE DEGREE OF
DOCTOR OF PHILOSOPHY

UNIVERSITY OF FLORIDA

2012

© 2012 Huyen T. Dinh

To my beautiful daughter *Anh Tran*, my loving husband *Thong Tran*, and my dear parents *Hop Pham* and *Tung Dinh*, for their unwavering support and constant encouragement

ACKNOWLEDGMENTS

I would like to express my deepest gratitude to my advisor, Dr. Warren E. Dixon, for his excellent guidance, caring, patience and support in the four years of my doctoral study. As an advisor, he exposed me to the vast and exciting research area of nonlinear control and motivated me to work on Dynamic Neural Network-based control applications. He encouraged me to explore my own ideas and helped me grow as an independent researcher. I highly appreciate all his caring and support as an understanding boss during my maternity time.

I would like to extend my gratitude to my committee members, Dr. Prabir Barooah, Dr. Joshep Wilson, and Dr. Mrinal Kumar, for insightful comments and many valuable suggestions to improve the presentation and contents of this dissertation.

I would also like to thank all my coworkers at the Nonlinear Controls and Robotics Lab for their various forms of support during my graduate study. Their warm friendship has enriched my life.

From the bottom of my heart, I would like to thank my parents for their support and belief in me. Without their support, encouragement and unconditional love, I would never be able to finish my dissertation. Also, I would like to thank and apologize to my daughter, who was born before this dissertation was completed and spend most of her time with my mother to allow me to focus. I am deeply sorry for the time we spend apart. Finally, I would like to thank my husband for his constant patience and unwavering love.

TABLE OF CONTENTS

	<u>page</u>
ACKNOWLEDGMENTS	4
LIST OF TABLES	7
LIST OF FIGURES	8
LIST OF ABBREVIATIONS	9
ABSTRACT	10
CHAPTER	
1 INTRODUCTION	12
1.1 Motivation and Problem Statement	12
1.2 Dissertation Outline	17
1.3 Contributions	18
2 BACKGROUND ON NEURAL NETWORKS	23
2.1 Neural Networks	23
2.2 Multi-layer Feedforward Neural Networks	24
2.3 Dynamic Neural Networks	27
3 DYNAMIC NEURAL NETWORK-BASED ROBUST IDENTIFICATION AND CONTROL OF A CLASS OF NONLINEAR SYSTEMS	30
3.1 Dynamic System and Properties	30
3.2 Robust Identification using Dynamic Neural Networks	31
3.3 Robust Trajectory Tracking using RISE feedback	34
3.4 Lyapunov Stability Analysis for DNN-based Identification and Control	38
3.5 Simulation	42
3.6 Conclusion	46
4 DYNAMIC NEURAL NETWORK-BASED ROBUST OBSERVERS FOR UNCER- TAIN NONLINEAR SYSTEMS	47
4.1 Dynamic System and Properties	47
4.2 Estimation Objective	49
4.3 Robust Observer using Dynamic Neural Networks	50
4.4 Lyapunov Stability Analysis	54
4.5 Extension for High-order Uncertain Nonlinear Systems	58
4.6 Experiment and Simulation Results	60
4.7 Conclusion	65

5	GLOBAL OUTPUT FEEDBACK TRACKING CONTROL FOR UNCERTAIN SECOND-ORDER NONLINEAR SYSTEMS	67
5.1	Dynamic System and Properties	67
5.2	Estimation and Control Objectives	68
5.3	DNN-based Robust Observer	69
5.4	Robust Adaptive Tracking Controller	72
5.5	Lyapunov Stability Analysis for DNN-based Observation and Control	75
5.6	Experiment Results	78
5.7	Conclusion	79
6	OUTPUT FEEDBACK CONTROL FOR AN UNCERTAIN NONLINEAR SYSTEM WITH SLOWLY VARYING INPUT DELAY	82
6.1	Dynamic System and Properties	82
6.2	Estimation and Control Objectives	83
6.3	Robust DNN Observer Development	84
6.4	Robust Tracking Control Development	86
6.5	Lyapunov Stability Analysis for DNN-based Observation and Control	88
6.6	Simulation Results	93
6.7	Conclusion	95
7	CONCLUSION AND FUTURE WORKS	97
7.1	Dissertation Summary	97
7.2	Future Work	99
APPENDIX		
A	DYNAMIC NEURAL NETWORK-BASED ROBUST IDENTIFICATION AND CONTROL OF A CLASS OF NONLINEAR SYSTEMS	101
A.1	Proof of the Inequality in Eq. (3–12)	101
A.2	Proof of the Inequality in Eq. (3–23)	101
A.3	Proof of the Inequality in Eqs. (3–25) and (3–26)	102
A.4	Proof of the Inequality in Eq. (3–32)	103
B	DYNAMIC NEURAL NETWORK-BASED GLOBAL OUTPUT FEEDBACK TRACKING CONTROL FOR UNCERTAIN SECOND-ORDER NONLINEAR SYSTEMS	105
REFERENCES		
BIOGRAPHICAL SKETCH		
		114

LIST OF TABLES

<u>Table</u>	<u>page</u>
4-1 Transient ($t = 0 - 1$ sec) and steady state ($t = 1 - 10$ sec) velocity estimation errors $\hat{\dot{x}}(t)$ for different velocity estimation methods in presence of noise 50dB.	65
5-1 Steady-state RMS errors and torques for each of the analyzed control designs.	79
6-1 Link1 and Link 2 RMS tracking errors and RMS estimation errors.	95
6-2 RMS errors for cases of uncertainty in time-varying delay seen by the plant as compared to the delay of the controller.	95

LIST OF FIGURES

<u>Figure</u>	<u>page</u>
2-1 Nonlinear model of a neuron	24
2-2 Two-layer NN	25
2-3 Hopfield DNN circuit structure	27
3-1 The architecture of the MLDNN.	32
3-2 Robust identification-based trajectory tracking control.	36
3-3 Link 1 and link 2 tracking errors.	44
3-4 Link 1 and Link 2 position identification errors.	44
3-5 Control inputs of the link 1 and link 2.	45
3-6 Link 1 and Link 2 feedforward component of the control input.	45
4-1 The experimental testbed consists of a two-link robot. The links are mounted on two NSK direct-drive switched reluctance motors.	60
4-2 Velocity estimate $\hat{x}(t)$ using (a) [1], (b) [2], (c) the proposed method, and (d) the center difference method on a two-link experiment testbed.	62
4-3 The steady-state velocity estimate $\hat{x}(t)$ using (a) [1], (b) [2], (c) the proposed method, and (d) the center difference method on a two-link experiment testbed.	63
4-4 Frequency analysis of velocity estimation $\hat{x}(t)$ using (a) [1], (b) [2], (c) the proposed method, and (d) the center difference method on a two-link experiment testbed.	63
4-5 The steady-state velocity estimation error $\tilde{x}(t)$ using (a) [1], (b) [2], (c) the proposed method, and (d) the center difference method on simulations, in presence of sensor noise (SNR 60dB). The right figures (e)-(h) indicate the respective frequency analysis of velocity estimation $\hat{x}(t)$	65
5-1 The tracking errors $e(t)$ of (a) Link 1 and (b) Link 2 using classical PID, robust dis- continuous OFB controller [1], and proposed controller.	79
5-2 Control inputs for Link 1 and Link 2 using (a), (b) classical PID, (c), (d) robust dis- continuous OFB controller [1], and (e), (f) the proposed controller.	80
5-3 Velocity estimation $\dot{x}(t)$ using (a) DNN-based observer and (b) numerical backwards difference.	81
6-1 Simulation results with 10% magnitude and 10% offset variance in time-delay	96

LIST OF ABBREVIATIONS

DNN	Dynamic Neural Network
LK	Lyapunov-Krasovskii
LP	Linear-in-parameter
MLNN	Multi-layer Neural Network
NN	Neural Network
OFB	Output Feedback
RISE	Robust Integral of the Sign of the Error
RMS	Root Mean Squares
UUB	Uniformly Ultimately Bounded

Abstract of Dissertation Presented to the Graduate School
of the University of Florida in Partial Fulfillment of the
Requirements for the Degree of Doctor of Philosophy

DYNAMIC NEURAL NETWORK-BASED ROBUST CONTROL METHODS FOR
UNCERTAIN NONLINEAR SYSTEMS

By

Huyen T. Dinh

August 2012

Chair: Warren E. Dixon

Major: Mechanical Engineering

Neural networks (NNs) have proven to be effective tools for identification, estimation and control of complex uncertain nonlinear systems. As a natural extension of feedforward NNs with the capability to approximate nonlinear functions, dynamic neural networks (DNNs) can be used to approximate the behavior of dynamic systems. DNNs distinguish themselves from static feedforward NNs in that they have at least one feedback loop and their representation is described by differential equations. Because of internal state feedback, DNNs are known to provide faster learning and exhibit improved computational capability in comparison to static feedforward NNs.

In this dissertation, a DNN architecture is utilized to approximate uncertain nonlinear systems as a means to develop identification methods and observers for estimation and control. In Chapter 3, an identification-based control method is presented, wherein a multilayer DNN is used in conjunction with a sliding mode term to approximate the input-output behavior of a plant while simultaneously tracking a desired trajectory. This result is achieved by combining the DNN-identification strategy with a RISE (Robust Integral of the Sign of the Error) controller. In Chapters 4 and 5, a class of second-order uncertain nonlinear systems with partially unmeasurable states is considered. A DNN-based observer is developed to estimate the missing states in Chapter 4, and the DNN-based observer is developed for an output feedback (OFB) tracking control method in Chapter 5. In Chapter 6, an OFB control method is developed for uncertain nonlinear systems with time-varying input delays. In all developed approaches, weights of the

DNN can be adjusted on-line: no off-line weight update phase is required. Chapter 7 concludes the proposal by summarizing the work and discussing some future problems that could be further investigated.

CHAPTER 1 INTRODUCTION

1.1 Motivation and Problem Statement

Based on their approximation properties, NNs have proven to be effective tools for identification, estimation and control of complex uncertain nonlinear systems. Feedforward NNs have been extensively used for adaptive control: NNs are cascaded into the controlled system and the NN weights are directly adjusted through an adaptive update law that is a function of the tracking error [3–5]. Contrary to feedforward NNs, the neurons of DNNs receive not only external input (e.g., tracking error) but also internal state feedback. Feedforward and feedback connections allow information in DNNs to propagate in two directions: from input neurons to outputs and vice versa [6]. Since DNNs exhibit dynamic behavior, they can be used as dynamic models to represent nonlinear systems, unlike feedforward NNs which can only approximate nonlinear functions in a system. From a computational perspective, a DNN with state feedback may provide more computational advantages than a static feedforward NN [7]. Funahashi and Nakamura [8] and Polycarpou [9] proved that DNNs could approximate the input-output behavior of a plant with arbitrary accuracy.

Narendra [10] proposed the idea of using DNNs for identification of nonlinear systems, wherein the identification models (DNNs) have the same structure as the plant but contain NNs with adjustable weights. The DNN-based learning paradigm involves the identification of the input-output behavior of the plant and the use of the resulting identification model to adjust the parameters of the controller [10]. In [11], recurrent higher order NNs are used for identification of nonlinear systems, where the dynamical neurons are distributed throughout the network. Rovithakis and Christodoulou [12] used singular perturbation to investigate the stability and robustness properties of the DNN identifier, and designed a state feedback law to track a reference model. In [13], a Hopfield-type DNN is used to identify a single input/single output (SISO) system, and the identifier is used in the controller to feedback linearize the system, which is then controlled using a PID controller. Poznyak used a parallel Hopfield-type NN for

identification and trajectory tracking [14, 15] and proved bounded Lyapunov stability of the identification and tracking errors in presence of modeling errors. Ren et al. [16] proposed a DNN structure for identification and control of nonlinear systems by using just the input/output measurements. The Hopfield-type DNN is widely used because of its simple structure and desirable stability properties [7, 17]. However, its structure only includes the single-layer NN, so its approximation capability is limited in comparison with a multi-layer DNN. A multi-layer DNN with stable learning laws is used in [18] for nonlinear system identification. However, all of the previous DNN methods are limited to uniformly ultimately bounded results, because of the residual function approximation error. In contrast, Chapter 3 proposes a modified DNN identifier structure to prove that the identification error is asymptotically regulated with only typical gradient weight update laws, and a controller including a DNN-identifier term and a robust feedback term (RISE) is used to ensure asymptotic tracking of the system along a desired trajectory. Both asymptotic identification and asymptotic tracking are achieved simultaneously while the DNN weights are adapted on-line.

Typical identification-based control approaches [12, 16, 19, 20] require the system states to be completely measurable. However, full state feedback is not always available in many practical systems. In the absence of sensors, the requirement of full-state feedback for the controller is typically fulfilled by using *ad hoc* numerical differentiation techniques, which can aggravate the problem of noise, leading to unusable state estimates. Several nonlinear observers are proposed in literature to estimate unmeasurable states. For instance, sliding mode observers were designed for general nonlinear systems by Slotine *et al.* in [21], for robot manipulators by Canudas de Wit *et al.* in [22], and for mechanical systems subject to impacts by Mohamed *et al.* in [23]. However, all these observers require exact model knowledge to compensate for nonlinearities in the system. Model-based observers are also proposed in [24] and [25] which require a high-gain to guarantee convergence of the estimation error to zero. The observers introduced in [26] and [27] are both applied for Lagrangian dynamic systems to estimate the velocity, and asymptotic convergence to the true velocity is obtained. However, the symmetric

positive-definiteness of the inertia matrix and the skew-symmetric property of the Coriolis matrix are required. Model knowledge is required in [26] and a partial differential equation needs to be solved to compute the observers. In [27], the system dynamics must be expressed in a non-minimal model and only mass and inertia parameters are unknown in the system.

The design of robust observers for uncertain nonlinear systems is considered in [1, 28, 29]. In [28], a second-order sliding mode observer for uncertain systems using a super-twisting algorithm is developed, where a nominal model of the system is assumed to be available and estimation errors are proven to converge in finite-time to a bounded set around the origin. In [29], the proposed observer can guarantee that the state estimates converge exponentially fast to the actual state, if there exists a vector function satisfying a complex set of matching conditions. In [1], one of the first asymptotic velocity observers is developed for general second-order systems, where the estimation error is proven to asymptotically converge. However, all nonlinear uncertainties in [1] are damped out by a sliding mode term resulting in high frequency state estimates. A NN approach that uses the universal approximation property is investigated for use in an adaptive observer design in [30]. However, estimation errors in [30] are only guaranteed to be bounded due to function reconstruction inaccuracies. Inspired by [1] and [30], a robust adaptive DNN-based observer is introduced in Chapter 4, where the DNN is used to approximate the uncertain system, a dynamic filter works in junction with the DNN to reconstruct the unmeasurable state, and a sliding mode term is added to the observer to compensate for the approximation error and exogenous disturbance. Asymptotic estimation is proven by a Lyapunov-based stability analysis and illustrated by experiments and simulations.

In addition to OFB observers, various OFB controllers have also been developed. OFB controllers using model-based observers were developed in [31–33]. In [31], Berghuis *et al.* designed an observer and a controller for robot models using a passivity approach for both positioning and tracking objectives based on the condition that the system dynamics are exactly known. Do *et al.* in [32] considered observer-based OFB control for unicycle-type mobile robots to stabilize the system and track a desired trajectory. In [33], a controller based on an

observer-based integrator backstepping technique was proposed for a revolute manipulator with known dynamics, and a semi-global exponential stability result for the link position tracking error and the velocity observation error was achieved. A disadvantage of these approaches is the requirement of exact model knowledge. OFB control for systems with parametric uncertainties has been developed in [34–37]. A linear observer is used in [34] to estimate the angular velocity of a rigid robot arm which is required to satisfy the linear-in-parameters (LP) condition, and uniform ultimate boundedness of the tracking and observation errors is obtained. Adaptive OFB control for robot manipulators satisfying the LP condition which achieves semi-global asymptotic tracking results is considered in [35–37]. The difference between these approaches is the joint velocity is estimated by an observer in [35], while a filter is used for velocity estimation in [36] and [37]. An extension of [36] and [37] to obtain a global asymptotic tracking result was introduced in [38]. However, a limitation of such previous adaptive OFB control approaches is that only LP uncertainties are considered. As a result, if uncertainties in the system do not satisfy the LP condition or if the system is affected by disturbances, the results will reduce to a uniformly ultimately bounded (UUB) result. The condition of linear dependence upon unknown parameters can be relaxed by introducing a NN or fuzzy logic in the observer structure as in [30, 39–43]; however, both estimation and tracking errors are only guaranteed to be bounded due to the existence of reconstruction errors. The first semi-global asymptotic OFB tracking result for second-order dynamic systems under the condition that uncertain dynamics are first-order differentiable was introduced in [1] with a novel filter design. All of the uncertain nonlinearities in [1] are damped out by a sliding mode term, so the discontinuous controller requires high-gain. The OFB control approach in Chapter 5 is motivated by [1] and the observer design in Chapter 4. In this approach, the DNN-based observer is used to estimate the unmeasurable state of the system; the controller, including the state estimation, NN, and sliding mode terms are used to yield trajectory tracking. Both asymptotic estimation of the unmeasurable state and asymptotic tracking of the desired trajectory are achieved simultaneously. Experiments demonstrate the performance of the developed approach.

For many practical systems, time delay is inevitable. The torque generated by an internal combustion engine can be delayed due to fuel-air mixing, ignition delays, cylinder pressure force propagation (see, e.g., [44, 45]), or communication delays in remote control applications where time is required to transmit information used for feedback control (see, e.g., master-slave teleoperation of robot in [46–50]). Unfortunately, time delay is a source of instability and can decrease system performance.

Delay in the control input (i.e, actuator delay) is an issue that has attracted significant attention. Various stability analysis methods and control design techniques have been developed for systems with input delays. For nonlinear systems, Lyapunov-Krasovskii (LK) functional-based methods (cf. [51–53]) and Lyapunov-Razumikhin methods (cf. [54–56]) are the most widely used tools to investigate the stability of a system affected by time delays. Compared with frequency domain methods that check if all roots of the characteristic equation of a retarded or neutral partial differential equation have negative real parts [57, 58], limiting its applicability to only linear time-invariant systems with exact model knowledge, the Krasovskii-type and Razumikhin-type approaches can be applied for uncertain nonlinear systems with time-varying delays. Comparing between the Razumikhin-type and LK functional-type techniques reveals that the Razumikhin methods can be considered as a particular but more conservative case of Krasovskii methods, where Razumikhin methods can be applied to arbitrarily large, bounded time-varying delays ($0 \leq \tau(t) < \infty$), whereas the Krasovskii methods require a bounded derivative of the delays ($\dot{\tau}(t) \leq \varphi < 1$). However, the Razumikhin approach requires input-to-state stability of the nominal system without delay.

Various full-state feedback controllers have been developed that are based on LK or Razumikhin stability criterion for nonlinear systems with input delays. Approaches in [59–63] provide control methods for uncertain nonlinear systems with known and unknown constant time-delays. However, time-delays are likely to vary in practice. Several methods for nonlinear systems with time-varying input delays have been recently investigated. Linearized controllers in [64, 65] are only valid within a region around the linearization point. A controller developed

in [66], which is an extension of [61, 67], deals with forward complete nonlinear systems with time-varying input delay under an assumption that the plant is asymptotically stable in the absence of the input delay. In [66], an invertible infinite dimensional backstepping transformation is used to yield an asymptotically stable system. An Euler-Lagrange system with a slowly varying input delay is considered in [68], where full state feedback is required. However, if only system output is available for feedback, how to design a controller to handle both the lack of the state and the time-varying delay of the input is rarely investigated. Studies in [69–71] address the OFB control problem for nonlinear systems with constant input delay by linearization method. A spacecraft, flexible-joint robot and rigid robot with constant time delay are considered in [69–71], respectively, where the objectives are to design OFB controllers to stabilize the systems around a set point. The controllers are first designed for delay-free linearized systems, then robustness to the delay is proven provided certain delay dependent conditions hold true. To the author’s knowledge, an OFB control method for nonlinear systems with time-varying input delay and tracking control objectives is still an open problem.

1.2 Dissertation Outline

Chapter 1 serves as an introduction. The motivation, problem statement, literature review, the contributions and the proposed research plan of the dissertation are discussed in this chapter.

Chapter 2 provides a background discussion on NNs, reviewing multi-layer neural network (MLNN) and DNN structures, their learning laws, and their approximation properties.

Chapter 3 provides a methodology for DNN-based identification and tracking control. The identifier structure is modified by adding a robust sliding mode term to account for the reconstruction error, hence the input-output behavior of the identifier is proven to asymptotically track the input-output behavior of the system. The controller, including information from the identifier and the RISE feedback term is proposed to guarantee asymptotic tracking of the system to the desired trajectory. The performance of the identification and control is illustrated through simulations.

Chapter 4 illustrates a novel robust adaptive observer design for second-order uncertain nonlinear systems. The observer is designed based on a DNN to approximate the uncertain system, a dynamic filter to provide a surrogate for the unmeasurable state, and a sliding mode term to cancel out the approximation error and exogenous disturbance. The asymptotic estimation result is proven by Lyapunov-based stability analysis and illustrated by experiments and simulations.

Chapter 5 develops an OFB control approach for second-order uncertain nonlinear systems, where the DNN-based observer is used to estimate the unmeasurable state of the system and the controller includes the state estimation, NN, and sliding mode terms to force the system to track a desired trajectory. Both asymptotic estimation of the unmeasurable state and asymptotic tracking of the desired trajectory are achieved simultaneously. Experiment results demonstrate the performance of the developed approach.

Chapter 6 considers OFB control method for uncertain nonlinear systems affected by time-varying input delays and additive disturbances. The delay is assumed to be bounded and slowly varying. The DNN-based observer works in junction with the controller to provide an estimate for the unmeasurable state. UUB estimation of the unmeasurable state and UUB tracking in the presence of model uncertainty, disturbances, and time delays are proven by a Lyapunov-based stability analysis.

Chapter 7 describes the possible directions that could extend the outcomes of the work in this dissertation.

1.3 Contributions

The contributions in this dissertation are provided in Chapters 3-6.

Chapter 3: DNN-based robust identification and control of a class of nonlinear systems: The focus of this chapter is the development of an indirect control strategy (identification-based control) for a class of uncertain nonlinear systems. A modified DNN structure is proposed where a multi-layer DNN is combined with an identification error-based sliding mode term. Unlike most DNN results which consider a single-layer Hopfield-type series-parallel configuration of the DNN, this method considers a parallel multi-layer DNN configuration, which has the

advantage of providing better approximation accuracy [15]. The additional sliding mode term is used to robustly account for exogenous bounded disturbances, modeling errors, and the function reconstruction errors of the DNN. This modified DNN structure allows identification of uncertain nonlinear systems while ensuring robustness to external disturbances. The idea of robust identification of nonlinear systems was first proposed by Poznyak [72], who used a sliding mode term in the algebraic weight update laws and ensured regulation of the identification error to zero. Huang and Lewis [73] used a high gain robustifying term in the DNN structure to prove UUB stability of nonlinear systems with time-delay. However, the proposed use of the sliding mode term in the DNN structure is novel and advantageous since it provides robustness to matched disturbances in the system without the need to modify the weight update laws. Asymptotic convergence of the identification error is also guaranteed. The identifier is developed to facilitate the design of the controller for the purpose of trajectory tracking. The controller consists of a DNN-identifier term and a robust feedback term (RISE) [74, 75] to ensure asymptotic tracking of the system along a desired trajectory. Asymptotic tracking is a contribution over previous results, where only bounded stability of the tracking error could be proven due to the presence of modeling and function reconstruction errors of the DNN. The use of the continuous RISE term is preferred over the sliding mode term in the feedback controller to avoid chattering and other side-effects associated with using a discontinuous control strategy. One of the assumptions in the use of the RISE feedback technique is that the disturbance terms are bounded by known constants and their derivatives be bounded by either a constant or a linear combination of the states. To satisfy these boundedness assumptions, a bounded, user-defined sample state is introduced in the design of the weight update laws for the DNN. No offline identification stage is required, and both the controller and the identifier operate simultaneously in real-time.

Chapter 4: DNN-based robust observers for second-order uncertain nonlinear systems: The challenge to obtain asymptotic estimation stems from the fact that to robustly account for disturbances, feedback of the unmeasurable error and its estimate are required. Typically, feedback of the unmeasurable error is derived by taking the derivative of the measurable state

and manipulating the resulting dynamics (e.g., this is the approach used in methods such as [1] and [30]). However, such an approach provides a linear feedback term of the unmeasurable state. Hence, a sliding mode term could not be simply added to the NN structure of the result in [30] to yield an asymptotic result, because it would require the signum of the unmeasurable state, and it does not seem clear how this nonlinear function of the unmeasurable state can be injected in the closed-loop error system using traditional methods. Likewise, it is not clear how to simply add a NN-based feedforward estimation of the nonlinearities in results such as [1] because of the need to inject nonlinear functions of the unmeasurable state. The novel approach used in this chapter avoids this issue by using nonlinear (sliding mode) feedback of the measurable state, and then exploiting the recurrent nature of a DNN structure to inject terms that cancel cross terms associated with the unmeasurable state. The approach is facilitated by using the filter structure of the controller in [1] and a novel stability analysis. The stability analysis is based on the idea of segregating the nonlinear uncertainties into terms which can be upper-bounded by constants and terms which can be upper-bounded by states. The terms upper-bounded by states can be canceled by linear feedback of the measurable errors, while the terms upper-bounded by constants are partially rejected by the sign feedback (of the measurable state) and partially eliminated by the novel DNN-based weight update laws. The contribution of this chapter over previous results is that the observer is designed for uncertain nonlinear systems, and the on-line approximation of the unmeasurable uncertain nonlinearities via the DNN structure should heuristically improve the performance of methods that only use high-gain feedback. Asymptotic convergence of the estimated states to the real states is proven using a Lyapunov-based analysis for a general second-order system. An extension of the proposed observer for a high-order system is shown, whereas, the output of the n^{th} order system is assumed to be measurable up to $n - 1$ derivatives. The developed observer can be used separately from the controller even if the relative degree between the control input and the output is arbitrary. Simulation and experiment results on a two-link robot manipulator show the effectiveness of the proposed observer when compared with

a standard numerical central differentiation algorithm, the high gain observer proposed in [2], and the observer in [1].

Chapter 5: DNN-based global output feedback tracking control for second-order uncertain nonlinear systems: In this chapter, a DNN-based observer-controller is proposed for uncertain nonlinear systems affected by bounded external disturbances, to achieve a two-fold result: asymptotic estimation of unmeasurable states and asymptotic tracking control. Asymptotic estimation of unmeasurable states is exploited from DNN-based observer design introduced in Chapter 4; however, asymptotic tracking is not simply obtained by replacing the estimation state with the unmeasurable state in the control law. The challenge is that the disturbances are again included in the open-loop tracking error system. To robustly account for disturbances, both linear and nonlinear feedback of the unmeasurable tracking error are required. The linear feedback is utilized from the linear feedback of unmeasurable estimation error, as in Chapter 4. However, it is not clear how to inject the nonlinear feedback of the unmeasurable tracking error from the measurable state and the estimation state. The approach used in Chapter 5 avoids this issue by using the sliding mode feedback of the measurable tracking error combined with the novel stability analysis. A modified version of the filter introduced in [1] is used to estimate the output derivative. Modification in the definition of the filtered estimation and tracking errors is utilized. A combination of a NN feedforward term, along with estimated state feedback and sliding mode terms are designed for the controller. The DNN observer adapts on-line for nonlinear uncertainties and should heuristically perform better than a robust feedback observer. New weight update laws for the DNN based on the estimation error, tracking error and filter output are proposed. Asymptotic regulation of the estimation error and asymptotic tracking are achieved.

Chapter 6: Output Feedback Control for an Uncertain Nonlinear System with Slowly Varying Input Delay: The challenge to design an OFB control for uncertain nonlinear systems with time-varying input delays stems from two questions: how to inject the negative feedback of the state through the delayed input, and how to account for the delayed state which is

introduced into the closed-loop system by the input. Normally, with full-state feedback methods as in [63, 68], the answer for the first question is the use of a predictor term which can provide a free delay input to the system and the solution for the second question is the use of an auxiliary LK functional, which is the integral over a delay time interval of the norm square of the state, hence, the time derivative of the LK functional can provide a negative feedback term of the norm square of the delayed state which itself cancels all state delay terms. However, with OFB control, the difficulty is that the corresponding state is unmeasurable so it can not indirectly feedback into the system via the predictor term. The approach to solve the issue in this chapter is motivated from the use of a DNN-based observer in [76] and [77] to include a negative feedback of an unmeasurable estimation error signal into the closed-loop system via a dynamic filter, then a controller is designed based on the difference residual between the unmeasurable state with the unmeasurable error signal, where this residual is measurable. Hence, finally through the predictor term, the residual without delay is added to the closed-loop system along with the error signal to form the negative feedback of the unmeasurable state. To deal with the delayed residual injected to the system, similarly, an auxiliary LK functional including the norm square of the residual term is used, then UUB tracking and estimation results are proven by Lyapunov-based techniques.

In this chapter, an OFB control for a second-order uncertain nonlinear system with additive disturbances is developed to compensate for both the inaccessibility of all states and the time-varying delay of the input. The delay is assumed to be bounded and slowly varying. A DNN-based observer with on-line update algorithms is used to provide a surrogate for the unmeasurable state, a predictor term is utilized to inject a delay free control into the analysis, and LK functionals are used to facilitate the design and stability analysis. The developed controller achieves simultaneously UUB estimation of the unmeasurable state and UUB tracking results, despite the lack of full state feedback, the time-varying input delay, uncertainties, and exogenous disturbances in the plant dynamics. A numerical simulation for a two-link robot manipulator is provided to examine the performance of the proposed method.

CHAPTER 2 BACKGROUND ON NEURAL NETWORKS

2.1 Neural Networks

In this chapter, a brief background on artificial NNs is provided. NN structures, learning methods, and approximation properties are included. The structures of both multilayer NNs and DNNs are described.

A NN is a massively parallel distributed processor composed of simple processing units that have a natural propensity for storing experiential knowledge and making it available for use. A NN resembles the brain in two respects [78]:

1. Knowledge is acquired by the network from its environment through a learning process.
2. Interneuron connection strengths, known as synaptic weights, are used to store the acquired knowledge.

The procedure for the learning process is called a learning algorithm. Its function is to modify the synaptic weights of the network to attain a desired design objective. The weight modification equips the method for NN design and implementation. Facilitating identification, estimation, and control for a wide class of nonlinear systems, NNs offer several useful properties and capabilities:

1. **NONLINEARITY.** A NN is constructed from an interconnection of nonlinear neurons, so it is itself nonlinear. This is an important property, especially if the underlying mechanism is inherently nonlinear.
2. **INPUT-OUTPUT MAPPING.** The synaptic weights (free parameters) of the network are modified to minimize the difference between the desired response and the actual response of the network produced by the input signal in accordance with appropriate criterion. Hence, the NN can adapt to construct the desired input - output mapping.
3. **ADAPTIVITY.** NNs have a built-in capability to adapt their weights based on design criterion. The on-line learning algorithm can lead the network to adapt in real time.

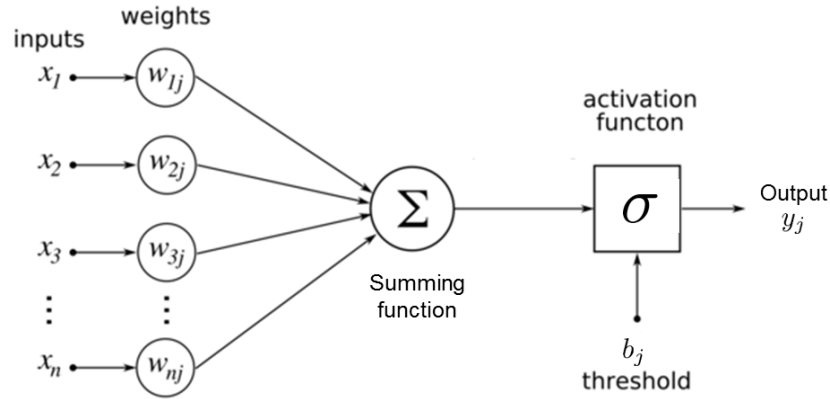


Figure 2-1. Nonlinear model of a neuron

A neuron is the fundamental unit for the operation of a NN. Its model is shown in Fig. 2-1 with three basic elements:

1. A set of synapses links, with each element characterized by its own weight,
2. An adder for summing the input signals multiplied by their respective weights,
3. A nonlinear activation function transforming the adder output into the output of the neuron.

In mathematical terms, the neuron can be described as

$$y_j = \sigma \left(\sum_{i=1}^n w_{ij}x_i + b_j \right),$$

where x_1, x_2, \dots, x_n are the input signals, $w_{1j}, w_{2j}, \dots, w_{nj}$ are the respective synaptic weights of neuron j , b_j is the bias, $\sigma(\cdot)$ is the activation function, and y_j is the output signal of the neuron. The activation function $\sigma(\cdot)$ is often chosen as hard limit, linear threshold, sigmoid, hyperbolic tangent, augmented ratio of squares, or radial basis functions.

The way in which neurons of a NN are interconnected determines its structure. In the following, the structure for a multilayer feedforward neural network (MLNN) and the structure for a DNN are considered.

2.2 Multi-layer Feedforward Neural Networks

Multi-layer feedforward NNs distinguishes itself by the presence of one or more hidden layers in addition to input and output layers. The neurons in each layer have the output of the preceding layer as their inputs. If each neuron in each layer is connected to every neuron in the

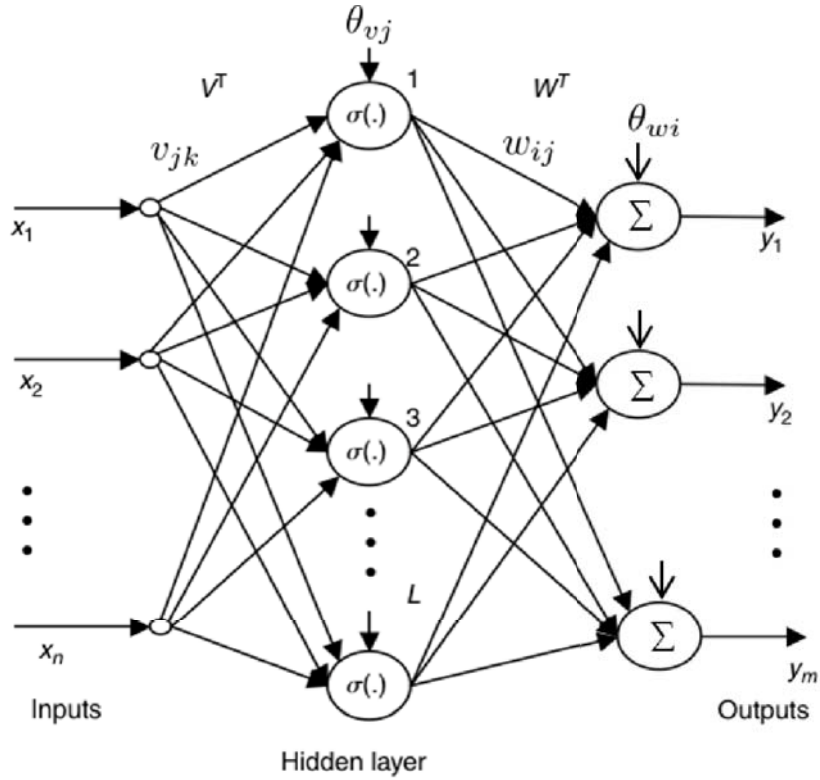


Figure 2-2. Two-layer NN

adjacent forward layer, then the NN is fully connected. The most common structure of MLNNs is a two-layer NN, shown in Fig. 2-2.

A mathematical formula describing a two-layer NN is given by

$$y_i = \sum_{j=1}^L \left[w_{ij} \sigma \left(\sum_{k=1}^n v_{jk} x_k + \theta_{vj} \right) + \theta_{wi} \right], \quad i = 1, 2, \dots, m.$$

The NN can be rewritten in matrix form as

$$y = W^T \sigma(V^T x),$$

where the output vector is $y = [y_1 \ y_2 \ \dots \ y_m]^T \in \mathbb{R}^m$, the input vector is $x = [1 \ x_1 \ x_2 \ \dots \ x_n]^T \in \mathbb{R}^{n+1}$, the activation vector defined for a vector $\xi = [\xi_1 \ \xi_2 \ \dots \ \xi_L]^T$ is $\sigma(\xi) = [1 \ \sigma(\xi_1) \ \sigma(\xi_2) \ \dots \ \sigma(\xi_L)]^T \in \mathbb{R}^{L+1}$

\mathbb{R}^{L+1} , and the weight matrices W, V contain the thresholds in the first columns as

$$W = \begin{bmatrix} \theta_{w1} & w_{11} & \dots & w_{1L} \\ \theta_{w2} & w_{21} & \dots & w_{2L} \\ \vdots & \vdots & & \vdots \\ \theta_{wm} & w_{m1} & \dots & w_{mL} \end{bmatrix}^T \in \mathbb{R}^{(L+1) \times m}, \quad V = \begin{bmatrix} \theta_{v1} & v_{11} & \dots & v_{1n} \\ \theta_{v2} & v_{21} & \dots & v_{2n} \\ \vdots & \vdots & & \vdots \\ \theta_{vL} & v_{L1} & \dots & v_{Ln} \end{bmatrix}^T \in \mathbb{R}^{(n+1) \times L}.$$

The weights of NNs can be tuned by many techniques. A common weight-tuning algorithm is the gradient algorithm based on the backpropagated error. A continuous version of backpropagation tuning is given by

$$\dot{W} = \Gamma_w \sigma(V^T x_d) E^T, \quad \dot{V} = \Gamma_v x_d (\sigma'^T W E)^T,$$

where Γ_w, Γ_v are the design gains, the backpropagated error $E = y_d - y$, with $y_d \in \mathbb{R}^m$ is the desired NN output in response to the reference input $x_d \in \mathbb{R}^n$, and $y \in \mathbb{R}^m$ is the actual NN output. The term $\sigma'(\cdot)$ is the derivative of the activation function $\sigma(\cdot)$, which can be calculated easily. For example, if the activation function is chosen as the sigmoid function, the term $\sigma'(\cdot)$ is equal to

$$\sigma' \equiv \text{diag} \{ \sigma(V^T x_d) \} [I - \text{diag} \{ \sigma(V^T x_d) \}].$$

Approximation using two-layer NNs:

Let $f(x)$ be a general smooth function from \mathbb{R}^n to \mathbb{R}^m . As long as x is restricted to a compact set S of \mathbb{R}^n , there exist NN weights and thresholds such that

$$f(x) = W^T \sigma(V^T x) + \varepsilon,$$

for some number L of hidden-layer neurons. The universal function approximation property holds for a large class of activation functions and the functional reconstruction error ε can be made arbitrarily small by increasing the number of nodes in the network structure. Generally, ε decreases as L increases. In fact, for any positive number ε_N , there exist weights and an L such that $\|\varepsilon\| < \varepsilon_N$, for all $x \in S$. Further details are provided in [78] and [46].

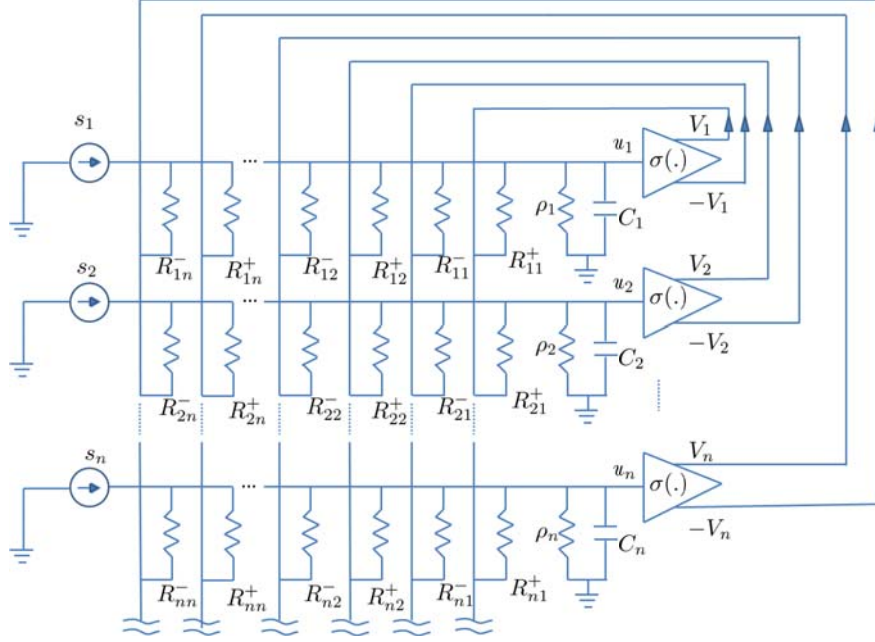


Figure 2-3. Hopfield DNN circuit structure

2.3 Dynamic Neural Networks

DNNs distinguish themselves from other types of NNs (static MLNNs) in that they have at least one feedback loop. The feedback loops result in a nonlinear dynamical behavior of DNNs. A DNN structure that contains state feedback may provide more computational advantages than a static neural structure, which contains only a feedforward neural structure. In general, a small feedback system is equivalent to a large and possibly infinite feedforward system [79]. A very well known DNN structure is the Hopfield structure [17, 80], which can be implemented by an electronic circuit. A continuous-time Hopfield DNN containing n units is described by the following differential equations [7]:

$$\text{State equation : } C_i \frac{dx_i(t)}{dt} = -\frac{x_i(t)}{R_i} + \sum_{j=1}^n w_{ij} y_j(t) + s_i(t), \quad i = 1, 2, \dots, n,$$

$$\text{Output equation : } y_i(t) = \sigma_i(x_i(t)).$$

This nonlinear system can be implemented by an analog RC (resistance-capacitance) network circuit as shown in Fig. 2-3, where $u_i = x_i$ is the input voltage of the i th amplifier, $V_i = \sigma_i(u_i)$ is

the output of the i th amplifier, the parameter R_i is defined as

$$\frac{1}{R_i} = \frac{1}{\rho_i} + \sum_{j=1}^n \frac{1}{R_{ij}},$$

and the weight parameter w_{ij} as

$$w_{ij} = \begin{cases} +\frac{1}{R_{ij}}, & R_{ij} \text{ is connected to } V_j \\ -\frac{1}{R_{ij}}, & R_{ij} \text{ is connected to } -V_j \end{cases}.$$

This system can be written in matrix form as

$$\frac{dx}{dt} = Ax + W_1 \sigma(x) + W_2 u,$$

where

$$x = [x_1 \ x_2 \ \dots \ x_n]^T,$$

$$\sigma(x) = [\sigma(x_1) \ \sigma(x_2) \ \dots \ \sigma(x_n)]^T,$$

$$u = [s_1 \ s_2 \ \dots \ s_n]^T,$$

and

$$A = \begin{bmatrix} -\frac{1}{R_1 C_1} & 0 & \dots & 0 \\ 0 & -\frac{1}{R_2 C_2} & \dots & 0 \\ \vdots & \vdots & & \vdots \\ 0 & 0 & \dots & -\frac{1}{R_n C_n} \end{bmatrix}, \quad W_1 = \begin{bmatrix} \frac{w_{11}}{C_1} & \frac{w_{12}}{C_1} & \dots & \frac{w_{1n}}{C_1} \\ \frac{w_{21}}{C_2} & \frac{w_{22}}{C_2} & \dots & \frac{w_{2n}}{C_2} \\ \vdots & \vdots & & \vdots \\ \frac{w_{n1}}{C_n} & \frac{w_{n2}}{C_n} & \dots & \frac{w_{nn}}{C_n} \end{bmatrix},$$

$$W_2 = \begin{bmatrix} \frac{1}{C_1} & 0 & \dots & 0 \\ 0 & \frac{1}{C_2} & \dots & 0 \\ \vdots & \vdots & & \vdots \\ 0 & 0 & \dots & \frac{1}{C_n} \end{bmatrix}.$$

Approximation using DNNs:

The approximation capability for nonlinear system behaviors with DNNs is documented in literature. The first proof based on natural extension of the function approximation properties of static NNs is shown in [81] and [8], hence the input of DNNs is limited for time belonging to a closed set. The second proof uses a system representation operator to derive conditions for the approximation validity by a DNN. It has been extensively analyzed by I. W. Sandberg, both for continuous and discrete time [82–84]. All approaches introduced in Chapters 3 - 6 prove the approximation capability of DNNs based on the extension of the function approximation properties of NNs and Lyapunov stability analysis.

CHAPTER 3
DYNAMIC NEURAL NETWORK-BASED ROBUST IDENTIFICATION AND CONTROL OF
A CLASS OF NONLINEAR SYSTEMS

A methodology for DNN identification-based control of uncertain nonlinear systems is proposed. The multi-layer DNN structure is modified by the addition of a sliding mode term to robustly account for exogenous disturbances and DNN reconstruction errors. Weight update laws are proposed which guarantee asymptotic regulation of the identification error. A recently developed robust feedback technique (RISE) is used in conjunction with the DNN identifier for asymptotic tracking of a desired trajectory. Both the identifier and the controller operate simultaneously in real time. Numerical simulations for a two-link robot are provided to examine the stability and performance of the developed method.

3.1 Dynamic System and Properties

Consider a control-affine nonlinear system of the form

$$\dot{x} = f(x) + g(x)u(t) + d(t), \quad (3-1)$$

where $x(t) \in \mathbb{R}^n$ is the measurable state with a finite initial condition $x(0) = x_0$, $u(t) \in \mathbb{R}^m$ is the control input, $f(x) \in \mathbb{R}^n$ is an unknown C^1 function, locally Lipschitz in x , $g(x) \in \mathbb{R}^{n \times m}$, and $d(t) \in \mathbb{R}^n$ is an exogenous disturbance. The following assumptions about the system in (3-1) will be utilized in the subsequent development.

Assumption 3.1. *The input matrix $g(x)$ is known, bounded and has full-row rank.*

Assumption 3.2. *The disturbance $d(t)$ and its first and second time derivatives are bounded, i.e. $d(t), \dot{d}(t), \ddot{d}(t) \in \mathcal{L}_\infty$.*

The universal approximation property of the MLNN states that given any continuous function $F : \mathbb{S} \rightarrow \mathbb{R}^n$, where \mathbb{S} is a compact set, there exist ideal weights θ^* , such that the output of the NN, $\hat{F}(\cdot, \theta)$ approximates $F(\cdot)$ to an arbitrary accuracy [85]. Hence, the unknown nonlinearity in (3-1) can be replaced by a MLNN, and the system can be represented as

$$\dot{x} = A_s x + W^T \sigma(V^T x) + \varepsilon + gu + d, \quad (3-2)$$

where the universal approximation property of the MLNNs [86, 87] is used to approximate the function $f(x) - A_s x$ as

$$f(x) - A_s x = W^T \sigma(V^T x) + \varepsilon.$$

In (4–3), $A_s \in \mathbb{R}^{n \times n}$ is Hurwitz, $W \in \mathbb{R}^{N \times n}$ and $V \in \mathbb{R}^{n \times N}$ are bounded constant ideal weight matrices of the DNN having N hidden layer neurons, $\sigma(\cdot) \in \mathbb{R}^N$ is the activation function (sigmoid, hyperbolic tangent etc.), and $\varepsilon(x) \in \mathbb{R}^n$ is the function reconstruction error. The feedback of the state $x(t)$ as the input of the MLNN $W^T \sigma(V^T x)$ makes the whole system in the structure of a multi-layer DNN. The following assumptions on the DNN model of the system in (3–2) will be utilized for the stability analysis.

Assumption 3.3. *The ideal NN weights are bounded by known positive constants [46] i.e.*

$$\|W\| \leq \bar{W} \text{ and } \|V\| \leq \bar{V}.$$

Assumption 3.4. *The activation function $\sigma(\cdot)$ and its derivatives with respect to its arguments are bounded [46].*

Assumption 3.5. *The function reconstruction errors and its first and second derivatives are bounded [46], as $\|\varepsilon(x)\| \leq \bar{\varepsilon}_1$, $\|\dot{\varepsilon}(x, \dot{x})\| \leq \bar{\varepsilon}_2$, $\|\ddot{\varepsilon}(x, \dot{x}, \ddot{x})\| \leq \bar{\varepsilon}_3$.*

Since the initial state x_0 is assumed to be bounded and the continuous controller $u(t)$ is subsequently designed to guarantee that the system state $x(t)$ is always bounded, the function $f(x) - A_s x$ can be defined on a compact set; hence the NN universal approximation property holds. With the selection of the activation function as the sigmoid and/or hyperbolic tangent functions, Assumption 3.4 is satisfied.

3.2 Robust Identification using Dynamic Neural Networks

To identify the unknown nonlinear system in (3–1), the following MLDNN architecture is proposed

$$\dot{\hat{x}} = A_s \hat{x} + \hat{W} \sigma(\hat{V}^T \hat{x}) + g u + k \tilde{x} + \beta \operatorname{sgn}(\tilde{x}), \quad (3-3)$$

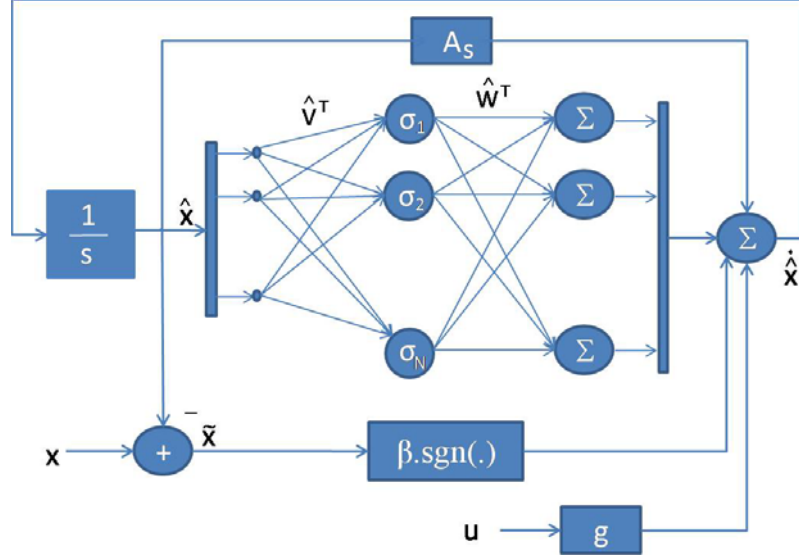


Figure 3-1. The architecture of the MLDNN.

where $\hat{x}(t) \in \mathbb{R}^n$ is the state of the DNN, $\hat{W}(t) \in \mathbb{R}^{N \times n}$ and $\hat{V}(t) \in \mathbb{R}^{n \times N}$ are the weight estimates, $\beta \in \mathbb{R}$ is a positive constant control gain, and $\tilde{x}(t) \in \mathbb{R}^n$ is the identification error defined as

$$\tilde{x} \triangleq x - \hat{x}. \quad (3-4)$$

The architecture of the DNN is shown in Fig. 3-1.

Considering $d \triangleq 0$ in (3-1), [9] proved that for some finite initial condition and $u \in \mathcal{U} \subset \mathbb{R}^m$, where \mathcal{U} is some compact set, then for a finite $T > 0$, there exists ideal weights W, V such that for all $u \in \mathcal{U}$ the DNN state and the state of the plant satisfy

$$\max_{t \in [0, T]} \|\hat{x}(t) - x(t)\| \leq \varepsilon_x,$$

where $\varepsilon_x \in \mathbb{R}$ is a positive constant. A contribution of this chapter is the addition of a robust sliding mode term to the classical DNN structure [9, 15, 17], which robustly accounts for the bounded disturbance $d(t)$ and the NN function reconstruction error $\varepsilon(x)$ to guarantee asymptotic convergence of the identification error to zero, as seen from the subsequent stability analysis.

The identification objective is to prove that the input-output behavior of the DNN approximates the input-output behavior of the plant. Quantitatively, the aim is to regulate the

identification error in (3–4). The closed-loop dynamics of the identification error in (3–4) are obtained by using (3–2) and (3–3) as

$$\begin{aligned}\dot{\tilde{x}} &= \dot{x} - \dot{\hat{x}} \\ &= A_s \tilde{x} + W^T \sigma(V^T x) - \hat{W}^T \sigma(\hat{V}^T \hat{x}) + \varepsilon + d - \beta \operatorname{sgn}(\tilde{x}).\end{aligned}\quad (3-5)$$

Adding and subtracting the term $W^T \sigma(\hat{V}^T \hat{x})$ yields

$$\dot{\tilde{x}} = A_s \tilde{x} + W^T \sigma(V^T x) - W^T \sigma(\hat{V}^T \hat{x}) + \tilde{W}^T \sigma(\hat{V}^T \hat{x}) + \varepsilon + d - \beta \operatorname{sgn}(\tilde{x}), \quad (3-6)$$

where $\tilde{W}(t) \triangleq W - \hat{W}(t) \in \mathbb{R}^{N \times n}$ is the estimate mismatch for the ideal NN weight.

To facilitate the subsequent analysis, the term $W^T \sigma(V^T x^*)$ is added and subtracted to (3–6), where $x^*(t) \in \mathbb{R}^n$ is a sample state selected such that $x^{*(i)}(t) \in \mathcal{L}_\infty$, $i = 0, 1, 2$, where $(\cdot)^{(i)}(t)$ denotes the i^{th} derivative with respect to time. Based on the fact that the Taylor series of the vector function $\sigma(V^T x^*)$ in the neighborhood of $\hat{V}^T x^*$ is

$$\sigma(V^T x^*) = \sigma(\hat{V}^T x^*) + \sigma'(\hat{V}^T x^*) \tilde{V}^T x^* + O(\tilde{V}^T x^*)^2, \quad (3-7)$$

where $\sigma'(\hat{V}^T x^*) \triangleq d\sigma(\xi)/d(\xi)|_{\xi=\hat{V}^T x^*}$, $\tilde{V}(t) \triangleq V - \hat{V}(t) \in \mathbb{R}^{n \times N}$ and $O(\tilde{V}^T x^*)^2$ is the higher order term, (3–6) can be represented as

$$\begin{aligned}\dot{\tilde{x}} &= A_s \tilde{x} + W^T \tilde{\sigma}_1 + W^T \tilde{\sigma}_2 + W^T \sigma'(\hat{V}^T x^*) \tilde{V}^T x^* + W^T O(\tilde{V}^T x^*)^2 \\ &\quad + \tilde{W}^T \sigma(\hat{V}^T \hat{x}) + \varepsilon + d - \beta \operatorname{sgn}(\tilde{x}),\end{aligned}\quad (3-8)$$

where the terms $\tilde{\sigma}_1$ and $\tilde{\sigma}_2$ are defined as $\tilde{\sigma}_1 \triangleq \sigma(V^T x) - \sigma(V^T x^*)$, $\tilde{\sigma}_2 \triangleq \sigma(\hat{V}^T x^*) - \sigma(\hat{V}^T \hat{x})$.

Rearranging the terms in (3–8) yields

$$\dot{\tilde{x}} = A_s \tilde{x} + \hat{W}^T \sigma'(\hat{V}^T x^*) \tilde{V}^T x^* + \tilde{W}^T \sigma(\hat{V}^T \hat{x}) + h - \beta \operatorname{sgn}(\tilde{x}), \quad (3-9)$$

where $h(x, x^*, \hat{x}, \hat{W}, \hat{V}, \varepsilon, d) \in \mathbb{R}^n$ can be considered as a disturbance term defined as

$$h \triangleq W^T \tilde{\sigma}_1 + W^T \tilde{\sigma}_2 + W^T O(\tilde{V}^T x^*)^2 + \varepsilon + d + \tilde{W}^T \sigma'(\hat{V}^T x^*) \tilde{V}^T x^*. \quad (3-10)$$

The weight update laws for the DNN are designed using the subsequent stability analysis as

$$\begin{aligned}\dot{\hat{W}} &= \Gamma_1 \text{proj} [\sigma(\hat{V}^T \hat{x}) \tilde{x}^T], \\ \dot{\hat{V}} &= \Gamma_2 \text{proj} [x^* \tilde{x}^T \hat{W}^T \sigma'(\hat{V}^T x^*)],\end{aligned}\tag{3-11}$$

where $\Gamma_1 \in \mathbb{R}^{N \times N}$ and $\Gamma_2 \in \mathbb{R}^{n \times n}$ are constant symmetric positive-definite adaptation gains, and $\text{proj}(\cdot)$ is a smooth projection operator [88, 89] used to guarantee that the weight estimates $\hat{W}(t)$ and $\hat{V}(t)$ remain bounded.

Remark 3.1. The sample state $x^*(t)$ is introduced in the weight update laws (3-11) to satisfy the assumptions required for the subsequently designed RISE-based controller (3-16). The RISE feedback term requires that the disturbance terms be bounded by known constants and their derivatives be bounded by either a constant or a linear combination of the states [75]. These assumptions are satisfied if there is a bounded signal, with bounded derivatives (like $x^*(t)$) in (3-11), rather than $x(t)$ or $\hat{x}(t)$ which cannot be proven to be bounded prior to the stability analysis.

Using Assumptions 3.2, 3.3-3.5, the Taylor series expansion in (3-7), and the $\text{proj}(\cdot)$ algorithm in (3-11), the disturbance term $h(\cdot)$ in (3-10) can be bounded as¹

$$\|h\| \leq \bar{h},\tag{3-12}$$

where \bar{h} is a known constant.

3.3 Robust Trajectory Tracking using RISE feedback

The control objective is to force the system state $x(t)$ to asymptotically track a desired time-varying trajectory $x_d(t) \in \mathbb{R}^n$, despite uncertainties and external disturbances in the system. The desired trajectory $x_d(t)$ is assumed to be bounded such that $x_d^{(i)}(t) \in \mathcal{L}_\infty$, $i = 0, 1, 2$. To quantify

¹ See Appendix A.1 for detail

the tracking objective, the tracking error $e(t) \in \mathbb{R}^n$ is defined as

$$e \triangleq x - x_d. \quad (3-13)$$

The filtered tracking error $r(t) \in \mathbb{R}^n$ for (3-13) is defined as

$$r = \dot{e} + \alpha e, \quad (3-14)$$

where $\alpha \in \mathbb{R}$ denotes a positive constant. Since $r(t)$ contains acceleration terms, it is unmeasurable. Substituting the system dynamics from (3-2) and using (3-13) and (3-14), the following expression is obtained

$$r = (A_s + \alpha I)e + W^T \sigma(V^T x) + \varepsilon + d + gu - \dot{x}_d + A_s x_d, \quad (3-15)$$

where $I \in \mathbb{R}^{n \times n}$ is an identity matrix. The control input $u(t)$ is now designed as a composition of the DNN term and the RISE feedback term as

$$u = g^+(\dot{x}_d - A_s x_d - \hat{W}^T \sigma(\hat{V}^T x_d) - \mu), \quad (3-16)$$

where $g(x)^+$ is the right Moore-Penrose pseudoinverse of the matrix $g(x)$, and $\mu(t) \in \mathbb{R}^n$ is the RISE term defined as the generalized solution to [90]

$$\dot{\mu} \triangleq (k_{tr} + k_{\mu})r + \beta_1 \text{sgn}(e), \quad (3-17)$$

where $k_{tr}, k_{\mu}, \beta_1 \in \mathbb{R}$ are constant positive control gains and $\text{sgn}(\cdot)$ denotes the signum function defined as

$$\text{sgn}(e) \triangleq [\text{sgn}(e_1) \text{sgn}(e_2) \dots \text{sgn}(e_n)]^T.$$

Remark 3.2. Since the input matrix $g(x)$ is assumed to be known, bounded and full-row rank (Assumption 3.1), the right pseudoinverse $g(x)^+$ is calculated as $g(x)^+ = g(x)^T (g(x)g(x)^T)^{-1}$ and satisfies $g(x)g(x)^+ = I$, where I is the identity matrix.

The controller in (3-16) and the DNN identifier developed in (3-3) operate simultaneously in real-time. A block diagram of the identifier-controller system is shown in Fig. 3-2.

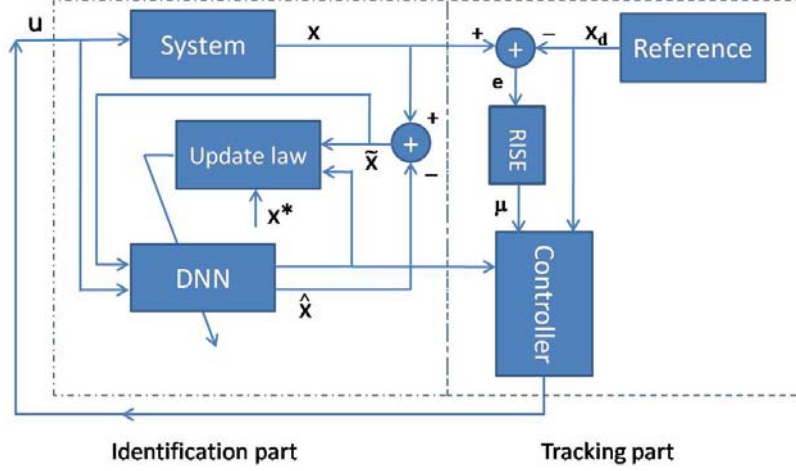


Figure 3-2. Robust identification-based trajectory tracking control.

Substituting the control (3-16) into (3-15), the closed-loop system becomes

$$r = (A_s + \alpha I)e + W^T \sigma(V^T x) - \hat{W}^T \sigma(\hat{V}^T x_d) + \varepsilon + d - \mu. \quad (3-18)$$

To facilitate the subsequent stability analysis, the time derivative of (3-18) is calculated as

$$\begin{aligned} \dot{r} = & (A_s + \alpha I)\dot{e} + W^T \sigma'(V^T x)V^T \dot{x} - \dot{\hat{W}}^T \sigma(\hat{V}^T x_d) - \hat{W}^T \sigma'(\hat{V}^T x_d)\dot{\hat{V}}^T x_d \\ & - \hat{W}^T \sigma'(\hat{V}^T x_d)\dot{\hat{V}}^T x_d + \dot{\varepsilon} + \dot{d} - (k_{tr} + k_{\mu})r - \beta_1 \text{sgn}(e). \end{aligned} \quad (3-19)$$

Rearranging the terms in (3-19) yields

$$\dot{r} = \tilde{N} + N - e - (k_{tr} + k_{\mu})r - \beta_1 \text{sgn}(e), \quad (3-20)$$

where the auxiliary function $\tilde{N}(e, r, \hat{W}, \hat{V}, t) \in \mathbb{R}^n$ is defined as

$$\begin{aligned} \tilde{N} = & (A_s + \alpha I)(r - \alpha e) + W^T \sigma'(V^T x)V^T (r - \alpha e) \\ & - \dot{\hat{W}}^T \sigma(\hat{V}^T x_d) - \hat{W}^T \sigma'(\hat{V}^T x_d)\dot{\hat{V}}^T x_d + e, \end{aligned} \quad (3-21)$$

and $N(x, \hat{W}, \hat{V}, t) \in \mathbb{R}^n$ is segregated into two parts as

$$N = N_D + N_B, \quad (3-22)$$

where $N_D(t) \in \mathbb{R}^n$ is defined as

$$N_D = \dot{d} + \dot{e},$$

and $N_B(x, \hat{W}, \hat{V}, t) \in \mathbb{R}^n$ is defined as

$$N_B = W^T \sigma'(V^T x) V^T \dot{x}_d - \hat{W}^T \sigma'(\hat{V}^T x_d) \hat{V}^T \dot{x}_d.$$

The function $\tilde{N}(\cdot)$ in (3–21) can be upper bounded as²

$$\|\tilde{N}\| \leq \zeta_1 \|z\|, \quad (3-23)$$

where $z(\tilde{x}, e, r) \in \mathbb{R}^{3n}$ is defined as

$$z \triangleq [\tilde{x}^T \quad e^T \quad r^T]^T, \quad (3-24)$$

and the bounding function $\rho(\cdot) \in \mathbb{R}$ is a positive, globally invertible, non-decreasing function.

Based on Assumptions 3.2, 3.3-3.5, and (3–11), the following bounds can be developed³

$$\begin{aligned} \|N_D\| &\leq \zeta_2, & \|N_B\| &\leq \zeta_3, \\ \|N\| &\leq \zeta_2 + \zeta_3. \end{aligned} \quad (3-25)$$

Further, the bounds for the time derivatives of $N_D(\cdot)$ and $N_B(\cdot)$ are developed as

$$\|\dot{N}_D\| \leq \zeta_4, \quad \|\dot{N}_B\| \leq \zeta_5 + \zeta_6 \|z\|, \quad (3-26)$$

where $\zeta_i \in \mathbb{R}$, ($i = 1, 2, \dots, 6$) are computable positive constants. To facilitate the subsequent

stability analysis, $y(z, P, Q) \in \mathbb{R}^{3n+2}$ is defined as

$$y \triangleq [z^T \quad \sqrt{P} \quad \sqrt{Q}]^T. \quad (3-27)$$

² See Appendix A.2 for proof

³ See Appendix A.3 for detail

In (3–27), the auxiliary function $P(t) \in \mathbb{R}$ is defined as

$$P \triangleq \beta_1 \sum_{j=1}^n |e_j(0)| - e^T(0)N(0) - L + L(0), \quad (3-28)$$

where the subscript $j = 1, 2, \dots, n$ denotes the j^{th} element of $e(0)$, and the auxiliary function $L(z, N) \in \mathbb{R}$ is generated as

$$\dot{L} \triangleq r^T(N - \beta_1 \text{sgn}(e)) - \beta_2 \|z\|^2, \quad (3-29)$$

where $\beta_1, \beta_2 \in \mathbb{R}$ are positive constants chosen according to the sufficient conditions

$$\beta_1 > \zeta_2 + \zeta_3 + \frac{\zeta_4}{\alpha} + \frac{\zeta_5}{\alpha} \quad \beta_2 > \zeta_6. \quad (3-30)$$

The derivative $\dot{P}(t) \in \mathbb{R}$ can be expressed as

$$\dot{P} = -\dot{L} = -r^T(N - \beta_1 \text{sgn}(e)) + \beta_2 \|z\|^2. \quad (3-31)$$

Provided the sufficient conditions in (3–30) are satisfied, the following inequality can be obtained

$$L \leq \beta_1 \sum_{j=1}^n |e_j(0)| - e^T(0)N(0) + L(0), \quad (3-32)$$

which can be used to conclude that $P(t) \geq 0^4$. The auxiliary function $Q(\tilde{W}, \tilde{V}) \in \mathbb{R}$ in (3–27) is defined as

$$Q \triangleq \frac{1}{2} \text{tr}(\tilde{W}^T \Gamma_1^{-1} \tilde{W}) + \frac{1}{2} \text{tr}(\tilde{V}^T \Gamma_2^{-1} \tilde{V}). \quad (3-33)$$

Since Γ_1 and Γ_2 are constant, symmetric, and positive definite matrix, $Q(\cdot) \geq 0$.

3.4 Lyapunov Stability Analysis for DNN-based Identification and Control

Theorem 3.1. *The DNN-based identifier and controller proposed in (3–3) and (3–16), respectively, and the weight update laws for the DNN designed in (3–11) ensure that all system signals*

⁴ See Appendix A.4 for proof

are bounded and that the identification and tracking errors are regulated in the sense that

$$\|\tilde{x}(t)\| \rightarrow 0, \quad \|e(t)\| \rightarrow 0 \quad \text{as} \quad t \rightarrow \infty,$$

provided the control gains k_{tr} , k_μ introduced in (3–17) are selected sufficiently large, the gain conditions in (3–30) are satisfied, and the following sufficient gain conditions are satisfied

$$\beta > \bar{h} \quad \lambda > \beta_2 + \frac{\zeta_1^2}{4k_{tr}}, \quad (3-34)$$

where β , \bar{h} , ζ_1 , β_2 , and λ are introduced in (3–3), (3–12), (3–23), (3–29), and (3–41), respectively.

Proof. Consider the Lyapunov candidate function $V_L(y, t) : \mathbb{R}^{3n+2} \times [0, \infty) \rightarrow \mathbb{R}$, which is a positive definite function defined as

$$V_L \triangleq \frac{1}{2} \tilde{x}^T \tilde{x} + \frac{1}{2} r^T r + \frac{1}{2} e^T e + P + Q, \quad (3-35)$$

and satisfies the following inequalities:

$$U_1(y) \leq V_L(y, t) \leq U_2(y),$$

where the continuous positive definite functions $U_1(y)$, $U_2(y) \in \mathbb{R}$ are defined as

$$U_1(y) \triangleq \frac{1}{2} \|y\|^2, \quad U_2(y) \triangleq \|y\|^2.$$

Let $\dot{y} = h(y, t)$ represent the closed-loop differential equations in (3–9), (3–14), (3–20), (3–31), where $h(y, t) \in \mathbb{R}^{3n+2}$ denotes the right-hand side of the closed-loop error signals.

Using Filippov’s theory of differential inclusion [91–94], the existence of solutions can be established for $\dot{y} \in K[h](y, t)$, where $K[h] \triangleq \bigcap_{\delta > 0} \bigcap_{\mu M = 0} \overline{\text{co}}h(B(y, \delta) - M, t)$, where $\bigcap_{\mu M = 0}$ denotes the intersection of all sets M of Lebesgue measure zero, $\overline{\text{co}}$ denotes convex closure, and $B(y, \delta) = \{w \in \mathbb{R}^{3n+2} \mid \|y - w\| < \delta\}$. The right hand side of the differential equation, $h(y, t)$, is continuous except for the Lebesgue measure zero set of times $t \in [t_0, t_f]$ when $e(t) = 0$ or $\tilde{x}(t) = 0$. Hence, the set of time instances for which $\dot{y}(t)$ is not defined is Lebesgue negligible.

The absolutely continuous solution $y(t) = y(t_0) + \int_{t_0}^t \dot{y}(t)dt$ does not depend on the value of $\dot{y}(t)$ on a Lebesgue negligible set of time-instances [95]. Under Filippov's framework, a generalized Lyapunov stability theory can be used (see [94, 96–98] for further details) to establish strong stability of the closed-loop system $\dot{y} = h(y, t)$. The generalized time derivative of (3–35) exists almost everywhere (a.e.), i.e. for almost all $t \in [t_0, t_f]$, and $\dot{V}_L(y) \in^{a.e.} \dot{\tilde{V}}_L(y)$ where

$$\dot{\tilde{V}}_L = \xi \in \partial V_L(y) \xi^T K \left[\dot{\tilde{x}}^T \ e^T \ r^T \ \frac{1}{2} P^{-\frac{1}{2}} \dot{P} \ \frac{1}{2} Q^{-\frac{1}{2}} \dot{Q} \right]^T, \quad (3-36)$$

where ∂V_L is the generalized gradient of $V_L(y)$ [96]. Since $V_L(y)$ is locally Lipschitz continuous regular and smooth in y , (3–36) can be simplified as [97]

$$\begin{aligned} \dot{\tilde{V}}_L &= \nabla V_L^T K \left[\dot{\tilde{x}}^T \ e^T \ r^T \ \frac{1}{2} P^{-\frac{1}{2}} \dot{P} \ \frac{1}{2} Q^{-\frac{1}{2}} \dot{Q} \right]^T \\ &= \left[\tilde{x}^T \ e^T \ r^T \ 2P^{\frac{1}{2}} \ 2Q^{\frac{1}{2}} \right] K \left[\dot{\tilde{x}}^T \ e^T \ r^T \ \frac{1}{2} P^{-\frac{1}{2}} \dot{P} \ \frac{1}{2} Q^{-\frac{1}{2}} \dot{Q} \right]^T. \end{aligned}$$

Using the calculus for $K[\cdot]$ from [98] (Theorem 1, Properties 2, 5, 7), and substituting the dynamics from (3–9), (3–14), (3–20), (3–31) and (3–33), $\dot{\tilde{V}}_L(y)$ can be rewritten as

$$\begin{aligned} \dot{\tilde{V}}_L &\subset \tilde{x}^T (A_s \tilde{x} + \hat{W}^T \sigma'(\hat{V}^T x^*) \tilde{V}^T x^* + \tilde{W}^T \sigma(\hat{V}^T \hat{x}) + h - \beta \text{sgn}(\tilde{x})) \\ &\quad + r^T (\tilde{N} + N - e - (k_{tr} + k_\mu)r - \beta_1 \text{sgn}(e)) + e^T (r - \alpha e) \\ &\quad - r^T (N - \beta_1 \text{sgn}(e)) + \beta_2 \|z\|^2 - \text{tr}(\tilde{W}^T \Gamma_1^{-1} \dot{\hat{W}}) - \text{tr}(\tilde{V}^T \Gamma_2^{-1} \dot{\hat{V}}). \end{aligned} \quad (3-37)$$

Using the fact that $K[\text{sgn}(e)] = \text{SGN}(e)$ [98], such that $\text{SGN}(e_i) = 1$ if $e_i > 0$, $[-1, 1]$ if $e_i = 0$, and -1 if $e_i < 0$, (the subscript i denotes the i^{th} element), and similarly $K[\text{sgn}(\tilde{x})] = \text{SGN}(\tilde{x})$, the set in (3–37) reduces to the scalar inequality, since the RHS is continuous a.e., i.e., the RHS is continuous except for the Lebesgue measure zero set of times when $e_i(t) = 0$ or $\tilde{x}_i(t) = 0$ for any $i = 1, 2, \dots, n$. Substituting the weight update laws in (3–11) and canceling common terms, the above expression is simplified as

$$\dot{\tilde{V}}_L \stackrel{a.e.}{\leq} \tilde{x}^T A_s \tilde{x} + \tilde{x}^T h - \beta \tilde{x}^T \text{sgn}(\tilde{x}) + r^T \tilde{N} - r^T (k_{tr} + k_\mu)r - \alpha e^T e + \beta_2 \|z\|^2. \quad (3-38)$$

Taking the upper bound of (3–38), the following expression is obtained

$$\begin{aligned} \dot{\tilde{V}}_L \stackrel{a.e.}{\leq} & -k_\mu \|r\|^2 - \alpha \|e\|^2 + \lambda_{\min}\{A_s\} \|\tilde{x}\|^2 - k_{tr} \|r\|^2 \\ & + \bar{h} \|\tilde{x}\| - \beta \sum_{j=1}^n |\tilde{x}_j| + \|\tilde{N}\| \|r\| + \beta_2 \|z\|^2, \end{aligned}$$

where $\lambda_{\min}\{\cdot\}$ is the minimum eigenvalue of a matrix. Now, using the fact that $\sum_{j=1}^n |\tilde{x}_j| \geq \|\tilde{x}\|$,

and (3–23), $\dot{\tilde{V}}_L$ can be further upper bounded as

$$\begin{aligned} \dot{\tilde{V}}_L \stackrel{a.e.}{\leq} & -k_\mu \|r\|^2 - \alpha \|e\|^2 + \lambda_{\min}\{A_s\} \|\tilde{x}\|^2 \\ & - \left[k_{tr} \|r\|^2 - \zeta_1 \|z\| \|r\| \right] + \beta_2 \|z\|^2 - (\beta - \bar{h}) \|\tilde{x}\|. \end{aligned} \quad (3–39)$$

Choosing β to satisfy the condition in (3–34), and completing the squares on the bracketed terms, the expression in (3–39) can be further upper bound as

$$\dot{\tilde{V}}_L \stackrel{a.e.}{\leq} - \left(\lambda - \beta_2 - \frac{\zeta_1^2}{4k_{tr}} \right) \|z\|^2, \quad (3–40)$$

where

$$\lambda \triangleq \min\{k_\mu, \alpha, -\lambda_{\min}\{A_s\}\}. \quad (3–41)$$

Based on (3–40), we can state that

$$\dot{\tilde{V}}_L \stackrel{a.e.}{\leq} -U(y) \quad (3–42)$$

where $U(y) = c \|z\|^2$, for some positive constant $c \in \mathbb{R}$, is a continuous positive semi-definite function. From (3–35) and (3–42), $V_L(y, t) \in \mathcal{L}_\infty$; hence, $\tilde{x}(t)$, $e(t)$, $r(t)$, $P(t)$, and $Q(t) \in \mathcal{L}_\infty$; since $e(t)$, $r(t) \in \mathcal{L}_\infty$, using (3–14), $\dot{e}(t) \in \mathcal{L}_\infty$. Moreover, since $x_d(t)$, $\dot{x}_d(t) \in \mathcal{L}_\infty$ by assumption, and $e(t)$, $\dot{e}(t) \in \mathcal{L}_\infty$, so $x(t)$, $\dot{x}(t) \in \mathcal{L}_\infty$ by using (3–13). Since $x(t)$, $\dot{x}(t)$, $f(x)$, $d(t) \in \mathcal{L}_\infty$, from (3–1), $u(t) \in \mathcal{L}_\infty$. The fact that $u(t) \in \mathcal{L}_\infty$ and $\hat{W}(t)$, $\sigma(\cdot) \in \mathcal{L}_\infty$ by the *proj*(\cdot) algorithm, indicates $\mu(t) \in \mathcal{L}_\infty$ by (3–16). Similarly, since both $x(t)$, $\tilde{x}(t) \in \mathcal{L}_\infty$ so $\hat{x}(t) \in \mathcal{L}_\infty$ by using (3–4); moreover, by using (3–3), $\hat{x}(t) \in \mathcal{L}_\infty$; hence, $\tilde{x}(t) \in \mathcal{L}_\infty$ from (3–5). Using $\dot{d}(t)$, $\dot{e}(t) \in \mathcal{L}_\infty$ by Assumptions 3.2, 3.5, $\hat{W}(t)$, $\hat{V}(t) \in \mathcal{L}_\infty$ by using the update laws (3–11), $W, V \in \mathcal{L}_\infty$ by Assumption 3.3, and the boundedness of the function $\sigma(\cdot)$ and $sgn(\cdot)$, we can prove that

$\dot{r}(t) \in \mathcal{L}_\infty$ from (3–19); then $\dot{z}(t) = [\dot{\tilde{x}} \ \dot{e}^T \ \dot{r}^T]^T \in \mathcal{L}_\infty$. Hence, $U(y)$ is uniformly continuous. It can be concluded that

$$c \|z\|^2 \rightarrow 0 \text{ as } t \rightarrow \infty.$$

Based on the definition of $z(t)$, both the identification error $\tilde{x}(t) \rightarrow 0$ and the tracking error $e(t) \rightarrow 0$ as $t \rightarrow \infty$. \square

3.5 Simulation

The following dynamics of a two link robot manipulator are considered for the simulations:

$$M(q)\ddot{q} + V_m(q, \dot{q})\dot{q} + F_d\dot{q} + \tau_d(t) = u(t), \quad (3-43)$$

where $q = [q_1 \ q_2]^T$ are the angular positions (*rad*) and $\dot{q} = \begin{bmatrix} \dot{q}_1 & \dot{q}_2 \end{bmatrix}^T$ are the angular velocities (*rad/s*) of the two links respectively. $M(q)$ is the inertia matrix and $V_m(q, \dot{q})$ is the centripetal-Coriolis matrix, defined as

$$M \triangleq \begin{bmatrix} p_1 + 2p_3c_2 & p_2 + p_3c_2 \\ p_2 + p_3c_2 & p_2 \end{bmatrix},$$

$$V_m \triangleq \begin{bmatrix} -p_3s_2\dot{q}_2 & -p_3s_2(\dot{q}_1 + \dot{q}_2) \\ p_3s_2\dot{q}_1 & 0 \end{bmatrix},$$

where $p_1 = 3.473 \text{ kg} \cdot \text{m}^2$, $p_2 = 0.196 \text{ kg} \cdot \text{m}^2$, $p_3 = 0.242 \text{ kg} \cdot \text{m}^2$, $c_2 = \cos(x_2)$, $s_2 = \sin(x_2)$, $F_d = \text{diag}\{5.3, 1.1\} \text{ Nm} \cdot \text{sec}$ are the models for dynamic and static friction, respectively, and τ_d is the external disturbance. The matrix $M(q)$ is assumed to be known, and other matrices $V_m(q, \dot{q})$, F_d are unknown.

The system (3–43) is represented to the form of the considered systems (3–1) as

$$\dot{x} = A_s x + B f(x) - B M(x)^{-1} \tau_d + B M(x)^{-1} u, \quad (3-44)$$

where the new measurable state vector $x \in \mathbb{R}^4$ defined as $x \triangleq [q^T \ \dot{q}^T]^T$, a constant matrix $B \triangleq [0_{2 \times 2} \ I_{2 \times 2}]^T \in \mathbb{R}^{4 \times 2}$ with $I_{n \times n}$, $0_{n \times n}$ are the $n \times n$ dimensional identity matrix and zero matrix, the

unknown vector function $f(x) \in \mathbb{R}^2$ is defined as $f(x) \triangleq -A_1q - A_2\dot{q} - M(q)^{-1} \{V_m(q, \dot{q})\dot{q} + F_d\dot{q}\}$

with $A_1, A_2 \in \mathbb{R}^{2 \times 2}$ are known constant matrices such that the matrix $A_s \in \mathbb{R}^{4 \times 4}$ defined as

$$A_s \triangleq \begin{bmatrix} 0_{2 \times 2} & I_{2 \times 2} \\ A_1 & A_2 \end{bmatrix} \text{ is Hurwitz. The proposed DNN identifier is in the form as}$$

$$\dot{\hat{x}} = A_s \hat{x} + B \hat{W} \sigma(\hat{V}^T \hat{x}) + B M(x)^{-1} u + \beta \text{sgn}(\tilde{x}).$$

The objective of two links is to track desired trajectories given as

$$q_{1d} = 0.52 \sin(2t)(1 - \exp(-0.01t^3)) \text{ rad},$$

$$q_{2d} = q_{1d} \text{ rad}.$$

To quantify the tracking objective, the tracking error $e_1(t) \in \mathbb{R}^2$ is defined as $e_1 \triangleq q - q_d$, where

$q_d(t) \triangleq [q_{1d} \ q_{2d}]^T$, and filtered tracking errors, denoted by $e_2(t)$, $r(t) \in \mathbb{R}^2$ are also defined

as $e_2 \triangleq \dot{e}_1 + \alpha e_1$, $r \triangleq \dot{e}_2 + \alpha e_2$. The relationship between $r(t)$, $x(t)$, and $x_d(t) \triangleq [q_d^T \ \dot{q}_d^T]^T$ is

$r_{1r} = \Lambda \{\dot{x} - \dot{x}_d + \alpha(x - x_d)\}$, where $\Lambda = [\alpha I_{n \times n} \ I_{n \times n}]$. The controller $u(t) \in \mathbb{R}^2$ is designed as

$$u \triangleq M(x) \{ \Lambda(\dot{x}_d - A_s x_d) - \hat{W}^T \sigma(\hat{V}^T x_d) - \mu \}$$

with $\mu(t) \in \mathbb{R}^2$ is the RISE term defined as the generalized solution to $\dot{\mu}(t) \triangleq kr + \beta_1 \text{sgn}(e_2)$.

The control gains are chosen as $k = \text{diag}([10 \ 15])$, $\alpha = \text{diag}([10 \ 35 \ 25 \ 5])$, $\beta_1 = 25$, $\beta = \text{diag}([1 \ 1 \ 30 \ 35])$, and $\Gamma_w = I_{15 \times 15}$, $\Gamma_v = I_{2 \times 2}$, where $I_{n \times n}$ denotes an identity matrix of appropriate dimensions. The NNs are designed to have 15 hidden layer neurons and the NN weights are initialized as uniformly distributed random numbers in the interval $[-0.1, 0.1]$. The initial conditions of the system and the identifier are chosen as $q_0 = [-0.3 \ 0.2]^T$, $\dot{q}_0 = [0 \ 0]^T$, and $\hat{x}_0 = [0 \ 0 \ 0 \ 0]^T$, respectively.

Figures 3-3 and 3-4 show the tracking errors and state identification errors for link 1 and link 2 during a 8s simulation period respectively. Both tracking and identification errors have good transient responses and converge to zero quickly. The control input is shown in Fig. 3-5, the

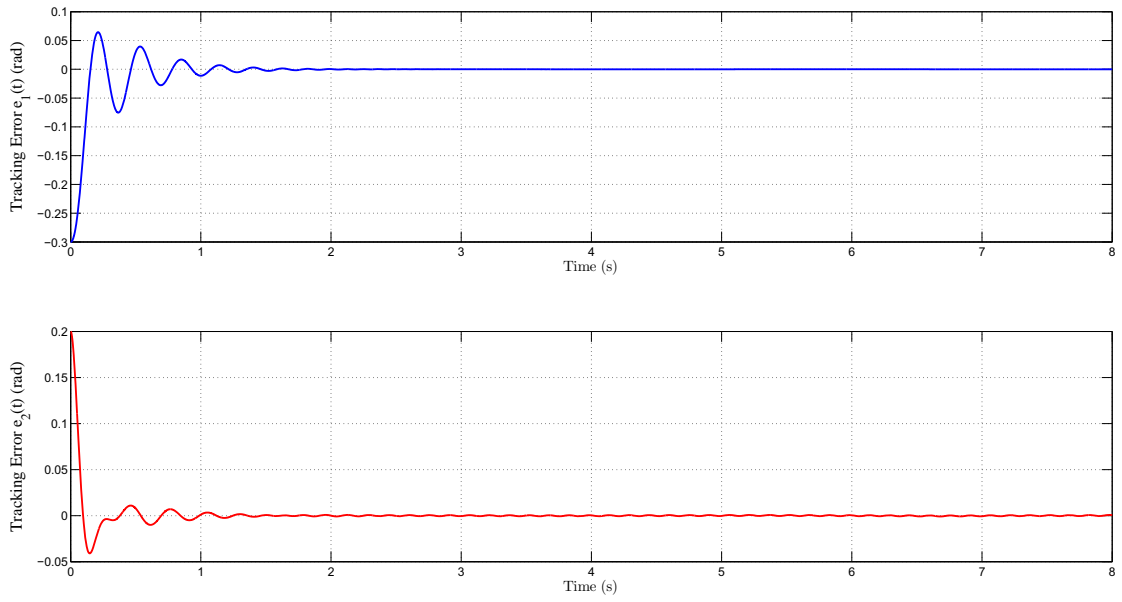


Figure 3-3. Link 1 and link 2 tracking errors.

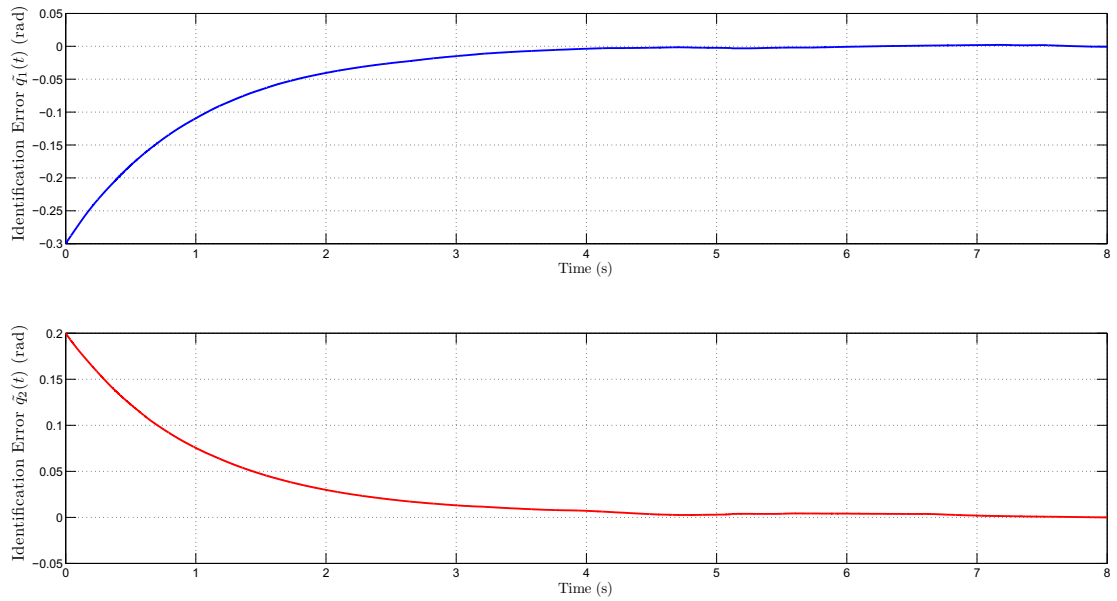


Figure 3-4. Link 1 and Link 2 position identification errors.

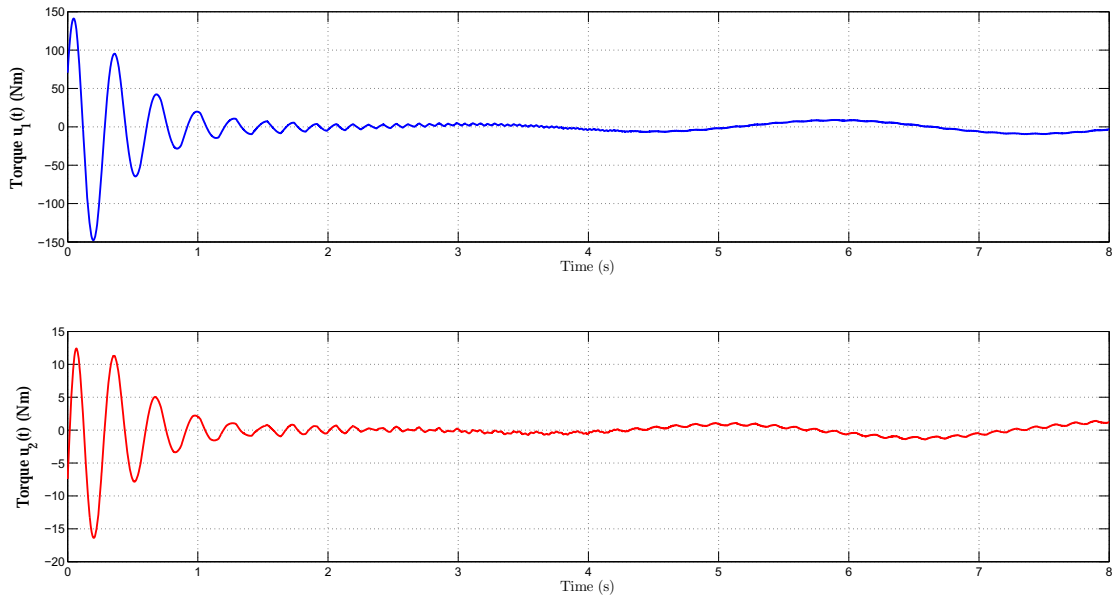


Figure 3-5. Control inputs of the link 1 and link 2.

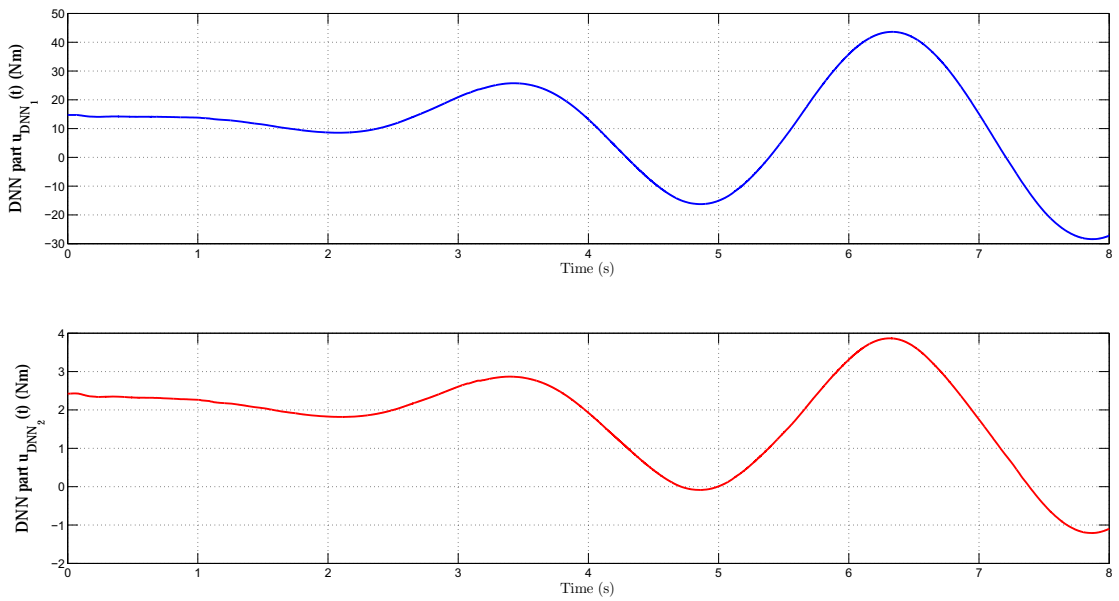


Figure 3-6. Link 1 and Link 2 feedforward component of the control input.

control input is a continuous signal. Fig. 3-6 shows the NN feedforward part in the control input. Both control input $u(t)$ and the NN feedforward part are bounded.

3.6 Conclusion

A DNN-based robust identification and control method for a family of control-affine nonlinear systems is proposed. The novel use of the sliding mode term in the DNN structure guarantees asymptotic convergence of the DNN state to the state of the plant. The controller is comprised of a DNN identifier term to account for uncertain nonlinearities in the system and a continuous RISE feedback term to account for external disturbances. Asymptotic trajectory tracking is achieved, unlike previous results in literature where only bounded stability is obtained due to DNN reconstruction errors.

CHAPTER 4
DYNAMIC NEURAL NETWORK-BASED ROBUST OBSERVERS FOR UNCERTAIN
NONLINEAR SYSTEMS

A DNN-based robust observer for uncertain nonlinear systems is developed in this chapter. The observer structure consists of a DNN to estimate the system dynamics on-line, a dynamic filter to estimate the unmeasurable state and a sliding mode feedback term to account for modeling errors and exogenous disturbances. The observed states are proven to asymptotically converge to the system states of second-order systems through a Lyapunov-based analysis. Similar results are extended to higher-order systems. Simulations and experiments on a two-link robot manipulator are performed to show the effectiveness of the proposed method in comparison to several other state estimation methods.

4.1 Dynamic System and Properties

Consider a second order control affine nonlinear system given in MIMO Brunovsky form as

$$\begin{aligned}\dot{x}_1 &= x_2, \\ \dot{x}_2 &= f(x) + G(x)u + d, \\ y &= x_1,\end{aligned}\tag{4-1}$$

where $y(t) \in \mathbb{R}^n$ is the measurable output with a finite initial condition $y(0) = y_0$, $u(t) \in \mathbb{R}^m$ is the control input, $x(t) = [x_1(t)^T \ x_2(t)^T]^T \in \mathbb{R}^{2n}$ is the state of the system, $f(x) : \mathbb{R}^{2n} \rightarrow \mathbb{R}^{2n}$, $G(x) : \mathbb{R}^{2n} \rightarrow \mathbb{R}^{n \times m}$ are unknown continuous functions, and $d(t) \in \mathbb{R}^n$ is an external disturbance. The following assumptions about the system in (4-1) will be utilized in the observer development.

Assumption 4.1. *The state $x(t)$ is bounded, i.e, $x_1(t), x_2(t) \in \mathcal{L}_\infty$, and is partially measurable, i.e, only $x_1(t)$ is measurable.*

Assumption 4.2. *The unknown functions $f(x), G(x)$ and the control input $u(t)$ are C^1 , and $u(t), \dot{u}(t) \in \mathcal{L}_\infty$.*

Assumption 4.3. *The disturbance $d(t)$ is differentiable, and $d(t), \dot{d}(t) \in \mathcal{L}_\infty$.*

Based of the universal approximation property of MLNNs, the unknown functions $f(x), G(x)$ in (4-1) can be replaced by MLNNs as

$$\begin{aligned} f(x) &= W_f^T \sigma_f(V_{f_1}^T x_1 + V_{f_2}^T x_2) + \varepsilon_f(x), \\ g_i(x) &= W_{gi}^T \sigma_{gi}(V_{gi_1}^T x_1 + V_{gi_2}^T x_2) + \varepsilon_{gi}(x), \end{aligned} \quad (4-2)$$

where $W_f \in \mathbb{R}^{L_f+1 \times n}$, $V_{f_1}, V_{f_2} \in \mathbb{R}^{n \times L_f}$ are unknown ideal weight matrices of the MLNN having L_f hidden layer neurons, $g_i(x)$ is the i^{th} column of the matrix $G(x)$, $W_{gi} \in \mathbb{R}^{L_{gi}+1 \times n}$, $V_{gi_1}, V_{gi_2} \in \mathbb{R}^{n \times L_{gi}}$ are also unknown ideal weight matrices of the MLNN having L_{gi} hidden layer neurons, $i = 1 \dots m$, $\sigma_f(t) \in \mathbb{R}^{L_f+1}$ and $\sigma_{gi}(t) \in \mathbb{R}^{L_{gi}+1}$ defined as $\sigma_f \triangleq \sigma_f(V_{f_1}^T x_1 + V_{f_2}^T x_2)$, $\sigma_{gi} \triangleq \sigma_{gi}(V_{gi_1}^T x_1 + V_{gi_2}^T x_2)$ are the activation functions (sigmoid, hyperbolic tangent, etc.), and $\varepsilon_f(x), \varepsilon_{gi}(x) \in \mathbb{R}^n, i = 1 \dots m$ are the function reconstruction errors. Using (4-2) and Assumption 4.2, the system in (4-1) can be represented as

$$\begin{aligned} \dot{x}_1 &= x_2, \\ \dot{x}_2 &= W_f^T \sigma_f + \varepsilon_f + d + \sum_{i=1}^m [W_{gi}^T \sigma_{gi} + \varepsilon_{gi}] u_i, \end{aligned} \quad (4-3)$$

where $u_i(t) \in \mathbb{R}$ is the i^{th} element of the control input vector $u(t)$. The following assumptions will be used in the observer development and stability analysis.

Assumption 4.4. *The ideal NN weights are bounded by known positive constants [46], i.e.*

$\|W_f\| \leq \bar{W}_f, \|V_{f_1}\| \leq \bar{V}_{f_1}, \|V_{f_2}\| \leq \bar{V}_{f_2}, \|W_{gi}\| \leq \bar{W}_{gi}, \|V_{gi_1}\| \leq \bar{V}_{gi_1},$ and $\|V_{gi_2}\| \leq \bar{V}_{gi_2}, i = 1 \dots m,$ where $\|\cdot\|$ denotes Frobenius norm for a matrix and Euclidean norm for a vector.

Assumption 4.5. *The activation functions $\sigma_f(\cdot), \sigma_{gi}(\cdot)$ and their derivatives with respect to its arguments, $\sigma_f'(\cdot), \sigma_{gi}'(\cdot), \sigma_f''(\cdot), \sigma_{gi}''(\cdot), i = 1 \dots m,$ are bounded [46].*

Assumption 4.6. *The function reconstruction errors $\varepsilon_f(\cdot), \varepsilon_{gi}(\cdot),$ and its first derivatives with respect to their arguments are bounded, with $i = 1 \dots m$ [46].*

4.2 Estimation Objective

The estimation objective is to prove that the estimated state $\hat{x}(t)$ converges to the system state $x(t)$. To facilitate the subsequent analysis, the estimation error $\tilde{x}(t) \in \mathbb{R}^n$ is defined as

$$\tilde{x} \triangleq x_1 - \hat{x}_1. \quad (4-4)$$

To compensate for the lack of direct measurements of $x_2(t)$, an auxiliary estimation error is defined as

$$r \triangleq \dot{\tilde{x}} + \alpha\tilde{x} + \eta, \quad (4-5)$$

where $\alpha \in \mathbb{R}$ is a positive constant control gain, and $\eta(t) \in \mathbb{R}^n$ is an output of the dynamic filter [1]

$$\eta = p - (k + \alpha)\tilde{x}, \quad (4-6)$$

$$\dot{p} = -(k + 2\alpha)p - \tilde{x}_f + ((k + \alpha)^2 + 1)\tilde{x}, \quad (4-7)$$

$$\dot{\tilde{x}}_f = p - \alpha\tilde{x}_f - (k + \alpha)\tilde{x}, \quad (4-8)$$

$$p(0) = (k + \alpha)\tilde{x}(0), \quad \tilde{x}_f(0) = 0,$$

where $\tilde{x}_f(t) \in \mathbb{R}^n$ is an auxiliary output of the filter, $p(t) \in \mathbb{R}^n$ is used as an internal filter variable, and $k \in \mathbb{R}$ is a positive constant gain. The estimation error $r(t)$ is not measurable, since the expression in (4-5) depends on $\dot{\tilde{x}}(t)$. The second order dynamic filter to estimate the system velocity was first proposed for the OFB control in [1]. The filter in (4-6)-(4-8) admits the estimation error $\tilde{x}(t)$ as its input and produces two signal outputs $\tilde{x}_f(t)$ and $\eta(t)$. The auxiliary signal $p(t)$ is utilized to only generate the signal $\eta(t)$ without involving the derivative of the estimation error $\dot{\tilde{x}}(t)$ which is unmeasurable. Hence, the filter can be physically implemented. A difficulty to obtain asymptotic estimation is that the filtered estimation error $r(t)$ is not available for feedback. The relation between two filter outputs is $\eta = \dot{\tilde{x}}_f + \alpha\tilde{x}_f$, and this relationship is utilized to generate the feedback of $r(t)$. Since taking time derivative of $r(t)$, the term $\ddot{\tilde{x}}_f(t)$

appears implicitly inside $\dot{\eta}(t)$, and consequently, the unmeasurable term $\dot{\tilde{x}}(t)$ which can be replaced by $r(t)$ is introduced.

4.3 Robust Observer using Dynamic Neural Networks

The following MLDNN architecture is proposed to observe the system in (4-1)

$$\begin{aligned}\dot{\hat{x}}_1 &= \hat{x}_2, \\ \dot{\hat{x}}_2 &= \hat{W}_f^T \hat{\sigma}_f + \sum_{i=1}^m \hat{W}_{gi}^T \hat{\sigma}_{gi} u_i + v,\end{aligned}\quad (4-9)$$

where $\hat{x}(t) = [\hat{x}_1(t)^T \hat{x}_2(t)^T]^T \in \mathbb{R}^{2n}$ is the state of the DNN observer, $\hat{W}_f(t) \in \mathbb{R}^{L_f+1 \times n}$, $\hat{V}_{f_1}(t), \hat{V}_{f_2}(t) \in \mathbb{R}^{n \times L_f}$, $\hat{W}_{gi}(t) \in \mathbb{R}^{L_{gi}+1 \times n}$, $\hat{V}_{gi_1}(t), \hat{V}_{gi_2}(t) \in \mathbb{R}^{n \times L_{gi}}$, $i = 1 \dots m$, are the weight estimates, $\hat{\sigma}_f(t) \in \mathbb{R}^{L_f+1}$, and $\hat{\sigma}_{gi}(t) \in \mathbb{R}^{L_{gi}+1}$ defined as $\hat{\sigma}_f \triangleq \sigma_f(\hat{V}_{f_1}^T \hat{x}_1 + \hat{V}_{f_2}^T \hat{x}_2)$, $\hat{\sigma}_{gi} \triangleq \sigma_{gi}(\hat{V}_{gi_1}^T \hat{x}_1 + \hat{V}_{gi_2}^T \hat{x}_2)$, and $v(t) \in \mathbb{R}^n$ is a function to be determined to provide robustness to account for the function reconstruction errors and external disturbances. In (4-9), the feed-forward NN terms $\hat{W}_f(t)^T \hat{\sigma}_f(t)$, $\hat{W}_{gi}(t)^T \hat{\sigma}_{gi}(t)$ use internal feedback of the observer states $\hat{x}(t)$, hence this observer has a DNN structure. The DNN has a recurrent feedback loop, and is proven to be able to approximate dynamic systems with any arbitrary degree of accuracy [8], [9]. This property motivates the DNN-based observer design. The DNN is automatically trained to estimate system dynamics by the weight update laws based on the state, weight estimates, and the filter output.

Taking the derivative of (4-6) and using the definitions (4-5)-(4-8) yields

$$\dot{\eta} = -(k + \alpha)r - \alpha\eta + \tilde{x} - \tilde{x}_f. \quad (4-10)$$

The closed-loop dynamics of the derivative of the filtered estimation error in (4-5) is determined from (4-3)-(4-5) and (4-10) as

$$\begin{aligned}\dot{r} &= W_f^T \sigma_f - \hat{W}_f^T \hat{\sigma}_f + \sum_{i=1}^m [W_{gi}^T \sigma_{gi} - \hat{W}_{gi}^T \hat{\sigma}_{gi}] u_i + \varepsilon_f + \sum_{i=1}^m \varepsilon_{gi} u_i \\ &+ d - v + \alpha(r - \alpha\tilde{x} - \eta) - (k + \alpha)r - \alpha\eta + \tilde{x} - \tilde{x}_f.\end{aligned}\quad (4-11)$$

The robust disturbance rejection term $v(t)$ is designed based on the subsequent analysis as

$$v = -[\gamma(k + \alpha) + 2\alpha]\eta + (\gamma - \alpha^2)\tilde{x} + \beta_1 \text{sgn}(\tilde{x} + \tilde{x}_f), \quad (4-12)$$

where $\gamma, \beta_1 \in \mathbb{R}$ are positive constant control gains. Adding and subtracting $W_f^T \sigma_f(\hat{V}_{f_1}^T x_1 + \hat{V}_{f_2}^T x_2) + \hat{W}_f^T \sigma_f(\hat{V}_{f_1}^T x_1 + \hat{V}_{f_2}^T x_2) + \sum_{i=1}^m [W_{gi}^T \sigma_{gi}(\hat{V}_{gi_1}^T x_1 + \hat{V}_{gi_2}^T x_2) + \hat{W}_{gi}^T \sigma_{gi}(\hat{V}_{gi_1}^T x_1 + \hat{V}_{gi_2}^T x_2)]u_i$ and substituting $v(t)$ from (4-12), the expression in (4-11) can be rewritten as

$$\dot{r} = \tilde{N} + N - kr - \beta_1 \text{sgn}(\tilde{x} + \tilde{x}_f) + \gamma(k + \alpha)\eta - \gamma\tilde{x}, \quad (4-13)$$

where the auxiliary function $\tilde{N}(x_1, x_2, \hat{x}_1, \hat{x}_2, \tilde{x}_f, \hat{W}_f, \hat{V}_{f_1}, \hat{V}_{f_2}, \hat{W}_{gi}, \hat{V}_{gi_1}, \hat{V}_{gi_2}, t) \in \mathbb{R}^n$ is defined as

$$\tilde{N} \triangleq \hat{W}_f^T [\sigma_f(\hat{V}_{f_1}^T x_1 + \hat{V}_{f_2}^T x_2) - \hat{\sigma}_f] + \tilde{x} - \tilde{x}_f + \sum_{i=1}^m \hat{W}_{gi}^T [\sigma_{gi}(\hat{V}_{gi_1}^T x_1 + \hat{V}_{gi_2}^T x_2) - \hat{\sigma}_{gi}]u_i, \quad (4-14)$$

and $N(x_1, x_2, \hat{W}_f, \hat{V}_{f_1}, \hat{V}_{f_2}, \hat{W}_{gi}, \hat{V}_{gi_1}, \hat{V}_{gi_2}, t) \in \mathbb{R}^n$ is segregated into two parts as

$$N \triangleq N_1 + N_2. \quad (4-15)$$

In (4-15), $N_1(x_1, x_2, \hat{W}_f, \hat{V}_{f_1}, \hat{V}_{f_2}, \hat{W}_{gi}, \hat{V}_{gi_1}, \hat{V}_{gi_2}, t)$, $N_2(x_1, x_2, \hat{W}_f, \hat{V}_{f_1}, \hat{V}_{f_2}, \hat{W}_{gi}, \hat{V}_{gi_1}, \hat{V}_{gi_2}, t) \in \mathbb{R}^n$ are defined as

$$\begin{aligned} N_1 &\triangleq \tilde{W}_f^T \sigma_f'[\tilde{V}_{f_1}^T x_1 + \tilde{V}_{f_2}^T x_2] + W_f^T O(\tilde{V}_{f_1}^T x_1 + \tilde{V}_{f_2}^T x_2)^2 + \varepsilon_f + d + \sum_{i=1}^m \varepsilon_{gi} u_i \\ &\quad + \sum_{i=1}^m \tilde{W}_{gi}^T \sigma_{gi}'[\tilde{V}_{gi_1}^T x_1 + \tilde{V}_{gi_2}^T x_2]u_i + \sum_{i=1}^m W_{gi}^T O(\tilde{V}_{gi_1}^T x_1 + \tilde{V}_{gi_2}^T x_2)^2 u_i, \\ N_2 &\triangleq \tilde{W}_f^T \sigma_f(\hat{V}_{f_1}^T x_1 + \hat{V}_{f_2}^T x_2) + \hat{W}_f^T \sigma_f'[\tilde{V}_{f_1}^T x_1 + \tilde{V}_{f_2}^T x_2] \\ &\quad + \sum_{i=1}^m \tilde{W}_{gi}^T \sigma_{gi}(\hat{V}_{gi_1}^T x_1 + \hat{V}_{gi_2}^T x_2)u_i + \sum_{i=1}^m \hat{W}_{gi}^T \sigma_{gi}'[\tilde{V}_{gi_1}^T x_1 + \tilde{V}_{gi_2}^T x_2]u_i, \end{aligned} \quad (4-16)$$

where $\tilde{W}_f(t) \triangleq W_f - \hat{W}_f(t) \in \mathbb{R}^{L_f+1 \times n}$, $\tilde{V}_{f_1}(t) \triangleq V_{f_1} - \hat{V}_{f_1}(t) \in \mathbb{R}^{n \times L_f}$, $\tilde{V}_{f_2}(t) \triangleq V_{f_2} - \hat{V}_{f_2}(t) \in \mathbb{R}^{n \times L_f}$, $\tilde{W}_{gi}(t) \triangleq W_{gi} - \hat{W}_{gi}(t) \in \mathbb{R}^{L_{gi}+1 \times n}$, $\tilde{V}_{gi_1}(t) \triangleq V_{gi_1} - \hat{V}_{gi_1}(t) \in \mathbb{R}^{n \times L_{gi}}$, $\tilde{V}_{gi_2}(t) \triangleq V_{gi_2} - \hat{V}_{gi_2}(t) \in \mathbb{R}^{n \times L_{gi}}$, $i = 1 \dots m$, are the estimate mismatches for the ideal NN weights; $O(\tilde{V}_{f_1}^T x_1 + \tilde{V}_{f_2}^T x_2)^2(t) \in \mathbb{R}^{L_f+1}$, $O(\tilde{V}_{gi_1}^T x_1 + \tilde{V}_{gi_2}^T x_2)^2(t) \in \mathbb{R}^{L_{gi}+1}$ are the higher order terms in the Taylor series of the vector

functions $\sigma_f(\cdot)$, $\sigma_{gi}(\cdot)$ in the neighborhood of $\hat{V}_{f_1}^T x_1 + \hat{V}_{f_2}^T x_2$ and $\hat{V}_{g_{i1}}^T x_1 + \hat{V}_{g_{i2}}^T x_2$, respectively, as

$$\begin{aligned}\sigma_f &= \sigma_f(\hat{V}_{f_1}^T x_1 + \hat{V}_{f_2}^T x_2) + \sigma'_f[\tilde{V}_{f_1}^T x_1 + \tilde{V}_{f_2}^T x_2] + O(\tilde{V}_{f_1}^T x_1 + \tilde{V}_{f_2}^T x_2)^2, \\ \sigma_{gi} &= \sigma_{gi}(\hat{V}_{g_{i1}}^T x_1 + \hat{V}_{g_{i2}}^T x_2) + \sigma'_{gi}[\tilde{V}_{g_{i1}}^T x_1 + \tilde{V}_{g_{i2}}^T x_2] + O(\tilde{V}_{g_{i1}}^T x_1 + \tilde{V}_{g_{i2}}^T x_2)^2,\end{aligned}\quad (4-17)$$

where the terms $\sigma'_f(t)$, $\sigma'_{gi}(t)$ are defined as $\sigma'_f \triangleq \sigma'_f(\hat{V}_{f_1}^T x_1 + \hat{V}_{f_2}^T x_2) = d\sigma_f(\theta)/d\theta|_{\theta=\hat{V}_{f_1}^T x_1 + \hat{V}_{f_2}^T x_2}$ and $\sigma'_{gi} \triangleq \sigma'_{gi}(\hat{V}_{g_{i1}}^T x_1 + \hat{V}_{g_{i2}}^T x_2) = d\sigma_{gi}(\theta)/d\theta|_{\theta=\hat{V}_{g_{i1}}^T x_1 + \hat{V}_{g_{i2}}^T x_2}$. To facilitate the subsequent analysis, an auxiliary function $\hat{N}_2(\hat{x}_1, \hat{x}_2, \hat{W}_f, \hat{V}_{f_1}, \hat{V}_{f_2}, \hat{W}_{gi}, \hat{V}_{g_{i1}}, \hat{V}_{g_{i2}}, t) \in \mathbb{R}^n$ is defined by replacing terms $x_1(t), x_2(t)$ in $N_2(\cdot)$ by $\hat{x}_1(t), \hat{x}_2(t)$, respectively.

The weight update laws for the DNN in (4-9) are developed based on the subsequent stability analysis as

$$\begin{aligned}\dot{\hat{W}}_f &= \text{proj}[\Gamma_{wf} \hat{\sigma}_f(\tilde{x} + \tilde{x}_f)^T], \\ \dot{\hat{V}}_{f_1} &= \text{proj}[\Gamma_{vf_1} \hat{x}_1(\tilde{x} + \tilde{x}_f)^T \hat{W}_f^T \hat{\sigma}'_f], \\ \dot{\hat{V}}_{f_2} &= \text{proj}[\Gamma_{vf_2} \hat{x}_2(\tilde{x} + \tilde{x}_f)^T \hat{W}_f^T \hat{\sigma}'_f], \\ \dot{\hat{W}}_{gi} &= \text{proj}[\Gamma_{wgi} \hat{\sigma}_{gi} u_i(\tilde{x} + \tilde{x}_f)^T], \quad i = 1 \dots m \\ \dot{\hat{V}}_{g_{i1}} &= \text{proj}[\Gamma_{vg_{i1}} \hat{x}_1 u_i(\tilde{x} + \tilde{x}_f)^T \hat{W}_{gi}^T \hat{\sigma}'_{gi}], \quad i = 1 \dots m \\ \dot{\hat{V}}_{g_{i2}} &= \text{proj}[\Gamma_{vg_{i2}} \hat{x}_2 u_i(\tilde{x} + \tilde{x}_f)^T \hat{W}_{gi}^T \hat{\sigma}'_{gi}], \quad i = 1 \dots m\end{aligned}\quad (4-18)$$

where $\Gamma_{wf} \in \mathbb{R}^{(L_f+1) \times (L_f+1)}$, $\Gamma_{wgi} \in \mathbb{R}^{(L_{gi}+1) \times (L_{gi}+1)}$, $\Gamma_{vf_1}, \Gamma_{vf_2}, \Gamma_{vg_{i1}}, \Gamma_{vg_{i2}} \in \mathbb{R}^{n \times n}$, are constant symmetric positive-definite adaptation gains, the terms $\hat{\sigma}'_f(t)$, $\hat{\sigma}'_{gi}(t)$ are defined as $\hat{\sigma}'_f \triangleq \sigma'_f(\hat{V}_{f_1}^T \hat{x}_1 + \hat{V}_{f_2}^T \hat{x}_2) = d\sigma_f(\theta)/d\theta|_{\theta=\hat{V}_{f_1}^T \hat{x}_1 + \hat{V}_{f_2}^T \hat{x}_2}$, $\hat{\sigma}'_{gi} \triangleq \sigma'_{gi}(\hat{V}_{g_{i1}}^T \hat{x}_1 + \hat{V}_{g_{i2}}^T \hat{x}_2) = d\sigma_{gi}(\theta)/d\theta|_{\theta=\hat{V}_{g_{i1}}^T \hat{x}_1 + \hat{V}_{g_{i2}}^T \hat{x}_2}$, and $\text{proj}(\cdot)$ is a smooth projection operator [88], [89] used to guarantee that the weight estimates $\hat{W}_f(t), \hat{V}_{f_1}(t), \hat{V}_{f_2}(t), \hat{W}_{gi}(t), \hat{V}_{g_{i1}}(t)$, and $\hat{V}_{g_{i2}}(t)$ remain bounded.

Using (4-4)-(4-8), Assumptions 4.1-4.2 and 4.4-4.5, the $\text{proj}(\cdot)$ algorithm in (4-18) and the Mean Value Theorem, the auxiliary function $\tilde{N}(\cdot)$ in (4-14) can be upper-bounded as

$$\|\tilde{N}\| \leq \zeta_1 \|z\|, \quad (4-19)$$

where $z(\tilde{x}, \tilde{x}_f, \eta, r) \in \mathbb{R}^{4n}$ is defined as

$$z \triangleq [\tilde{x}^T \ \tilde{x}_f^T \ \eta^T \ r^T]^T. \quad (4-20)$$

Based on (4-4)-(4-8), Assumptions 4.1-4.6, the Taylor series expansion in (4-17) and the weight update laws in (4-18), the following bounds can be developed

$$\begin{aligned} \|N_1\| &\leq \zeta_2, \quad \|N_2\| \leq \zeta_3, \\ \|\dot{N}\| &\leq \zeta_4 + \rho(\|z\|) \|z\|, \\ \|\tilde{N}_2\| &\leq \zeta_5 \|z\|, \end{aligned} \quad (4-21)$$

where $\zeta_i \in \mathbb{R}, i = 1 \dots 5$, are computable positive constants, $\rho(\cdot) \in \mathbb{R}$ is a positive, globally invertible, non-decreasing function, and $\tilde{N}_2(\tilde{x}, \tilde{x}_f, \hat{W}_f, \hat{V}_{f_1}, \hat{V}_{f_2}, \hat{W}_{gi}, \hat{V}_{gi_1}, \hat{V}_{gi_2}, u) \triangleq N_2(\cdot) - \hat{N}_2(\cdot)$.

To facilitate the subsequent stability analysis, let $\mathcal{D} \subset \mathbb{R}^{4n+2}$ be a domain containing $y(z, P, Q) = 0$, where $y(z, P, Q) \in \mathbb{R}^{4n+2}$ is defined as

$$y \triangleq [z^T \ \sqrt{P} \ \sqrt{Q}]^T. \quad (4-22)$$

In (4-22), the auxiliary function $P(t) \in \mathbb{R}$ is the Filippov solution to the differential equation

$$\begin{aligned} \dot{P} &\triangleq -L, \\ P(0) &\triangleq \beta_1 \sum_{j=1}^n \left| \tilde{x}_j(0) + \tilde{x}_{f_j}(0) \right| - (\tilde{x}(0) + \tilde{x}_f(0))^T N(0), \end{aligned} \quad (4-23)$$

where the subscript $j = 1, 2, \dots, n$ denotes the j^{th} element of $\tilde{x}(0)$ or $\tilde{x}_f(0)$, and the auxiliary function $L(z, N_1, N_2) \in \mathbb{R}$ is defined as

$$L \triangleq r^T (N_1 - \beta_1 \text{sgn}(\tilde{x} + \tilde{x}_f)) + (\tilde{x} + \tilde{x}_f)^T N_2 - \sqrt{2\rho(\|z\|)} \|z\|^2, \quad (4-24)$$

where $\beta_1 \in \mathbb{R}$ is a positive constant chosen according to the sufficient condition

$$\beta_1 > \max(\zeta_2 + \zeta_3, \zeta_2 + \frac{\zeta_4}{\alpha}), \quad (4-25)$$

where $\zeta_i, i = 2, 3, 4$ are introduced in (4-21). Provided the sufficient condition in (4-25) is satisfied, the following inequality can be obtained $P(t) \geq 0$ ¹. The auxiliary function $Q(\tilde{W}_f, \tilde{V}_{f_1}, \tilde{V}_{f_2}, \tilde{W}_{gi}, \tilde{V}_{gi_1}, \tilde{V}_{gi_2}) \in \mathbb{R}$ in (4-22) is defined as

$$Q \triangleq \frac{\alpha}{2} \text{tr}(\tilde{W}_f^T \Gamma_{wf}^{-1} \tilde{W}_f) + \frac{\alpha}{2} \text{tr}(\tilde{V}_{f_1}^T \Gamma_{vf_1}^{-1} \tilde{V}_{f_1}) + \frac{\alpha}{2} \text{tr}(\tilde{V}_{f_2}^T \Gamma_{vf_2}^{-1} \tilde{V}_{f_2}) \\ + \frac{\alpha}{2} \sum_{i=1}^m \text{tr}(\tilde{W}_{gi}^T \Gamma_{wgi}^{-1} \tilde{W}_{gi}) + \frac{\alpha}{2} \sum_{i=1}^m \text{tr}(\tilde{V}_{gi_1}^T \Gamma_{vgi_1}^{-1} \tilde{V}_{gi_1}) + \frac{\alpha}{2} \sum_{i=1}^m \text{tr}(\tilde{V}_{gi_2}^T \Gamma_{vgi_2}^{-1} \tilde{V}_{gi_2}), \quad (4-26)$$

where $\text{tr}(\cdot)$ denotes the trace of a matrix. Since the gains $\Gamma_{wf}, \Gamma_{wgi}, \Gamma_{vf_1}, \Gamma_{vf_2}, \Gamma_{vgi_1}, \Gamma_{vgi_2}$ are symmetric, positive-definite matrices, $Q(\cdot) \geq 0$.

4.4 Lyapunov Stability Analysis

Theorem 4.1. *The DNN-based observer proposed in (4-9) along with its weight update laws in (4-18) ensures asymptotic estimation in sense that*

$$\|\tilde{x}(t)\| \rightarrow 0 \text{ and } \|x_2(t) - \hat{x}_2(t)\| \rightarrow 0 \text{ as } t \rightarrow \infty$$

provided the control gain $k = k_1 + k_2$ introduced in (4-6)-(4-8) is selected sufficiently large based on the initial conditions of the states², the gain condition in (4-25) is satisfied, and the following sufficient conditions are satisfied

$$\gamma > \alpha \zeta_5^2 + \frac{1}{2\alpha}, k_1 > \frac{1}{2}, \text{ and } \lambda > \frac{\zeta_1^2}{4\sqrt{2}k_2}, \quad (4-27)$$

where

$$\lambda \triangleq \frac{1}{\sqrt{2}} \left[\min(\alpha(\gamma - \alpha \zeta_5^2), k_1) - \frac{1}{2} \right], \quad (4-28)$$

and ζ_1, ζ_5 are introduced in (4-19) and (4-21), respectively.

¹ See Appendix A.4 and B for proof

² See the subsequent proof

Proof. Consider the Lyapunov candidate function $V_L(y) : \mathcal{D} \rightarrow \mathbb{R}$, which is a Lipschitz continuous regular positive definite function defined as

$$V_L \triangleq \frac{\gamma}{2} \tilde{x}^T \tilde{x} + \frac{\gamma}{2} \tilde{x}_f^T \tilde{x}_f + \frac{\gamma}{2} \eta^T \eta + \frac{1}{2} r^T r + P + Q, \quad (4-29)$$

which satisfies the following inequalities:

$$U_1(y) \leq V_L(y) \leq U_2(y). \quad (4-30)$$

In (4-30), $U_1(y), U_2(y) \in \mathbb{R}$ are continuous positive definite functions defined as

$$U_1(y) \triangleq \min\left(\frac{\gamma}{2}, \frac{1}{2}\right) \|y\|^2,$$

$$U_2(y) \triangleq \max\left(\frac{\gamma}{2}, 1\right) \|y\|^2.$$

The generalized time derivative of (4-29) exists almost everywhere (a.e.), and $\dot{V}_L(y) \in^{a.e.} \dot{\tilde{V}}_L(y)$ (see Chapter 3 for further details) where

$$\dot{\tilde{V}}_L = \underset{\xi \in \partial V_L(y)}{\dot{\xi}^T} K \begin{bmatrix} \dot{\tilde{x}}^T & \dot{\tilde{x}}_f^T & \dot{\eta}^T & \dot{r}^T & \frac{1}{2} P^{-\frac{1}{2}} \dot{P} & \frac{1}{2} Q^{-\frac{1}{2}} \dot{Q} \end{bmatrix}^T, \quad (4-31)$$

where ∂V_L is the generalized gradient of $V_L(y)$ [96]. Since $V_L(y)$ is locally Lipschitz continuous regular and smooth in y , (4-31) can be simplified as [97]

$$\begin{aligned} \dot{\tilde{V}}_L &= \nabla V_L^T K \begin{bmatrix} \dot{\tilde{x}}^T & \dot{\tilde{x}}_f^T & \dot{\eta}^T & \dot{r}^T & \frac{1}{2} P^{-\frac{1}{2}} \dot{P} & \frac{1}{2} Q^{-\frac{1}{2}} \dot{Q} \end{bmatrix}^T \\ &= \begin{bmatrix} \gamma \tilde{x}^T & \gamma \tilde{x}_f^T & \gamma \eta^T & r^T & 2P^{\frac{1}{2}} & 2Q^{\frac{1}{2}} \end{bmatrix} K [\Psi]^T, \end{aligned}$$

where

$$\Psi \triangleq \begin{bmatrix} \dot{\tilde{x}}^T & \dot{\tilde{x}}_f^T & \dot{\eta}^T & \dot{r}^T & \frac{1}{2} P^{-\frac{1}{2}} \dot{P} & \frac{1}{2} Q^{-\frac{1}{2}} \dot{Q} \end{bmatrix}.$$

Using the calculus for $K[\cdot]$ from [98] (Theorem 1, Properties 2, 5, 7), and substituting the dynamics from (4-5), (4-7)-(4-10), (4-13), (4-23), (4-24) and (4-26) and adding and subtracting

$\alpha(\tilde{x} + \tilde{x}_f)^T \dot{\hat{N}}_2$ and using (4-16), $\dot{\tilde{V}}_L(y)$ can be rewritten as

$$\begin{aligned}
\dot{\tilde{V}}_L \subset & \gamma \tilde{x}^T (r - \alpha \tilde{x} - \eta) + \gamma \tilde{x}_f^T (\eta - \alpha \tilde{x}_f) + \gamma \eta^T [-(k + \alpha)r - \alpha \eta + \tilde{x} - \tilde{x}_f] \\
& + r^T [\tilde{N} + N - \beta_1 K [\text{sgn}(\tilde{x} + \tilde{x}_f)]] - kr + \gamma(k + \alpha)\eta \\
& - \gamma r^T \tilde{x} - r^T (N_1 - \beta_1 K [\text{sgn}(\tilde{x} + \tilde{x}_f)]) - (\tilde{x} + \tilde{x}_f)^T N_2 + \sqrt{2}\rho(\|z\|) \|z\|^2 \\
& - \alpha(\tilde{x} + \tilde{x}_f)^T \dot{\hat{N}}_2 + \alpha(\tilde{x} + \tilde{x}_f)^T \{ \tilde{W}_f^T \hat{\sigma}_f + \hat{W}_f^T \hat{\sigma}'_f [\tilde{V}_{f_1}^T \hat{x}_1 + \tilde{V}_{f_2}^T \hat{x}_2] \\
& + \sum_{i=1}^m \tilde{W}_{gi}^T \hat{\sigma}_{gi} u_i + \sum_{i=1}^m \hat{W}_{gi}^T \hat{\sigma}'_{gi} [\tilde{V}_{gi_1}^T \hat{x}_1 + \tilde{V}_{gi_2}^T \hat{x}_2] u_i \} \\
& - \alpha \text{tr}(\tilde{W}_f^T \Gamma_{wf}^{-1} \dot{\hat{W}}_f) - \alpha \text{tr}(\tilde{V}_{f_1}^T \Gamma_{vf_1}^{-1} \dot{\hat{V}}_{f_1}) - \alpha \text{tr}(\tilde{V}_{f_2}^T \Gamma_{vf_2}^{-1} \dot{\hat{V}}_{f_2}) \\
& - \alpha \sum_{i=1}^m \text{tr}(\tilde{W}_{gi}^T \Gamma_{wg}^{-1} \dot{\hat{W}}_{gi}) - \alpha \sum_{i=1}^m \text{tr}(\tilde{V}_{gi_1}^T \Gamma_{vgi_1}^{-1} \dot{\hat{V}}_{gi_1}) - \alpha \sum_{i=1}^m \text{tr}(\tilde{V}_{gi_2}^T \Gamma_{vgi_2}^{-1} \dot{\hat{V}}_{gi_2}).
\end{aligned} \tag{4-32}$$

Using the fact that $K[\text{sgn}(\tilde{x} + \tilde{x}_f)] = \text{SGN}(\tilde{x} + \tilde{x}_f)$ (see Chapter 3 for further details), the set in (4-32) can reduce to the scalar inequality. Substituting the weight update laws in (4-18) and canceling common terms, the above expression can be upper bounded as

$$\begin{aligned}
\dot{\tilde{V}}_L \stackrel{a.e.}{\leq} & -\alpha \gamma \tilde{x}^T \tilde{x} - \alpha \gamma \tilde{x}_f^T \tilde{x}_f - \alpha \gamma \eta^T \eta - kr^T r \\
& + \alpha(\tilde{x} + \tilde{x}_f)^T \dot{\hat{N}}_2 + r^T \tilde{N} + \sqrt{2}\rho(\|z\|) \|z\|^2.
\end{aligned} \tag{4-33}$$

Using (4-19), (4-21), the fact that

$$\alpha \zeta_5 \|\tilde{x} + \tilde{x}_f\| \|z\| \leq \alpha^2 \zeta_5^2 \|\tilde{x}\|^2 + \alpha^2 \zeta_5^2 \|\tilde{x}_f\|^2 + \frac{1}{2} \|z\|^2,$$

substituting $k = k_1 + k_2$, and completing the squares, the expression in (4-33) can be further bounded as

$$\begin{aligned}
\dot{\tilde{V}}_L \stackrel{a.e.}{\leq} & -\alpha(\gamma - \alpha \zeta_5^2) \|\tilde{x}\|^2 - \alpha(\gamma - \alpha \zeta_5^2) \|\tilde{x}_f\|^2 - \alpha \gamma \|\eta\|^2 \\
& - k_1 \|r\|^2 + \left(\frac{1}{2} + \frac{\zeta_1^2}{4k_2} + \sqrt{2}\rho(\|z\|) \right) \|z\|^2.
\end{aligned}$$

Provided the sufficient conditions in (4-27) are satisfied, the above expression can be rewritten as

$$\dot{V} \stackrel{a.e.}{\leq} -\sqrt{2}\left(\lambda - \frac{\zeta_1^2}{4\sqrt{2}k_2} - \rho(\|z\|)\right) \|z\|^2 \stackrel{a.e.}{\leq} -U(y) \quad \forall y \in \mathcal{D}, \quad (4-34)$$

where λ is defined in (4-28) and $U(y) = c \|z\|^2$, for some positive constant c , is a continuous positive semi-definite function which is defined on the domain

$$\mathcal{D} \triangleq \left\{ y(t) \in \mathbb{R}^{4n+2} \mid \|y(t)\| \leq \rho^{-1}\left(\lambda - \frac{\zeta_1^2}{4\sqrt{2}k_2}\right) \right\}.$$

The size of the domain \mathcal{D} can be increased by increasing the gains k and α . The inequalities in (4-30) and (4-34) show that $V(y) \in \mathcal{L}_\infty$ in the domain \mathcal{D} ; hence, $\tilde{x}(t), \tilde{x}_f(t), \eta(t), r(t), P(t)$ and $Q(t) \in \mathcal{L}_\infty$ in \mathcal{D} ; (4-5)-(4-10) are used to show that $\dot{\tilde{x}}(t), \dot{\tilde{x}}_f(t), \dot{\eta}(t) \in \mathcal{L}_\infty$ in \mathcal{D} . Since $x_1(t), x_2(t) \in \mathcal{L}_\infty$ by Assumption 4.1, $\hat{x}_1(t), \hat{x}_2(t) \in \mathcal{L}_\infty$ in \mathcal{D} using (4-4). Since $\tilde{x}(t), \tilde{x}_f(t), \eta(t) \in \mathcal{L}_\infty$ in \mathcal{D} , using (4-12), $v(t) \in \mathcal{L}_\infty$ in \mathcal{D} . Since $W_f, W_{gi}, \sigma_f(\cdot), \sigma_{gi}(\cdot), \varepsilon_f(\cdot), \varepsilon_{gi}(\cdot) \in \mathcal{L}_\infty, i = 1 \dots m$, by Assumptions 4.4-4.6, the control input $u(t)$ and the disturbance $d(t)$ are bounded by Assumptions 4.2-4.3, and $\hat{W}_f(t), \hat{W}_{gi}(t) \in \mathcal{L}_\infty, i = 1 \dots m$, by the use of the $proj(\cdot)$ algorithm, from (4-11), $\dot{r}(t) \in \mathcal{L}_\infty$ in \mathcal{D} ; then $\dot{z}(t) \in \mathcal{L}_\infty$ in \mathcal{D} , by using (4-20). Hence, $U(y)$ is uniformly continuous in \mathcal{D} . Let $\mathcal{S} \subset \mathcal{D}$ denote a set defined as

$$\mathcal{S} \triangleq \left\{ y(t) \in \mathcal{D} \mid U_2(y(t)) < \varepsilon_1 \left(\rho^{-1} \left(\lambda - \frac{\zeta_1^2}{4\sqrt{2}k_2} \right) \right)^2 \right\}. \quad (4-35)$$

The region of attraction in (4-35) can be made arbitrarily large to include any initial condition by increasing the control gains k and α (i.e., a semi-global type of stability result), and hence

$$c \|z\|^2 \rightarrow 0 \quad \text{as } t \rightarrow \infty \quad \forall y(0) \in \mathcal{S}.$$

Based on the definition of $z(t)$ the following result can be proven

$$\|\tilde{x}(t)\|, \|\eta(t)\|, \|r(t)\| \rightarrow 0 \quad \text{as } t \rightarrow \infty \quad \forall y(0) \in \mathcal{S}.$$

From (4-5), it can be further shown that

$$\left\| \dot{\tilde{x}}(t) \right\| \rightarrow 0 \text{ as } t \rightarrow \infty \quad \forall y(0) \in \mathcal{L}.$$

□

4.5 Extension for High-order Uncertain Nonlinear Systems

The proposed method can be extended for a N^{th} order uncertain nonlinear system as

$$\begin{aligned} \dot{x}_1 &= x_2, \\ &\vdots \\ \dot{x}_{N-1} &= x_N, \\ \dot{x}_N &= f(x) + G(x)u + d, \\ y &= x_1, \end{aligned} \tag{4-36}$$

where $x(t) = [x_1^T(t) x_2^T(t) \dots x_N^T(t)]^T \in \mathbb{R}^{Nn}$ is the system state, the system output $y(t) \in \mathbb{R}^n$ is measurable up to $N - 1^{th}$ derivatives, i.e. $x_i(t)$, $i = 1, 2, \dots, N - 1$ are measurable, and $x_N(t)$ is unmeasurable, and the unknown functions $f(x)$, $G(x)$, the control input $u(t)$ and the disturbance $d(t)$ are introduced in (4-1).

Given the system in (4-36), the observer in (4-9) can be extended as

$$\begin{aligned} \dot{\hat{x}}_1 &= \hat{x}_2, \\ &\vdots \\ \dot{\hat{x}}_{N-1} &= \hat{x}_N, \\ \dot{\hat{x}}_N &= \hat{W}_f^T \hat{\sigma}_f + \sum_{i=1}^m \hat{W}_{gi}^T \hat{\sigma}_{gi} u_i + v, \end{aligned} \tag{4-37}$$

where $\hat{x}(t) = [\hat{x}_1^T(t) \hat{x}_2^T(t) \dots \hat{x}_N^T(t)]^T \in \mathbb{R}^{Nn}$ is the state of the DNN observer, $\hat{W}_f(t)$, $\hat{V}_{fj}(t)$, $\hat{W}_{gi}(t)$, $\hat{V}_{gi_j}(t)$, $i = 1 \dots m$, $j = 1 \dots N$, and $\hat{\sigma}_f(t)$, $\hat{\sigma}_{gi}(t)$ are introduced in (4-9) and the robust control term

$v(t) \in \mathbb{R}^n$ is modified as

$$v \triangleq -[\gamma K + 2\alpha_{N-1}] \eta + (\gamma - \alpha_{N-1}^2) \tilde{x}_{N-1} + \beta_1 \text{sgn}(\tilde{x}_{N-1} + \tilde{x}_f). \quad (4-38)$$

In (4-38), $K, \gamma, \alpha_{N-1}, \beta_1 \in \mathbb{R}$ are positive constant gains, and $\tilde{x}_f(t), \eta(t) \in \mathbb{R}^n$ are outputs of the modified dynamic filter

$$\begin{aligned} \eta &= p - K\tilde{x}_{N-1}, \\ \dot{p} &= -(K + \alpha_{N-1})p - \tilde{x}_f + (K^2 + 1)\tilde{x}_{N-1}, \\ \dot{\tilde{x}}_f &= p - \alpha_{N-1}\tilde{x}_f - K\tilde{x}_{N-1}, \\ p(0) &= K\tilde{x}_{N-1}(0), \quad \tilde{x}_f(0) = 0. \end{aligned} \quad (4-39)$$

The estimation error $\tilde{x}_1(t) \in \mathbb{R}^n$ and the following filtered estimation errors $\tilde{x}_i(t) \in \mathbb{R}^n, i = 1, \dots, N-1$ are defined as

$$\begin{aligned} \tilde{x}_1 &\triangleq x_1 - \hat{x}_1, \\ \tilde{x}_2 &\triangleq \dot{\hat{x}}_1 + \alpha_1 \tilde{x}_1, \\ \tilde{x}_i &\triangleq \dot{\hat{x}}_{i-1} + \alpha_{i-1} \tilde{x}_{i-1} + \tilde{x}_{i-2}, \quad i = 3, \dots, N-1, \\ r &\triangleq \dot{\hat{x}}_{N-1} + \alpha_{N-1} \tilde{x}_{N-1} + \eta, \end{aligned} \quad (4-40)$$

where $\alpha_i \in \mathbb{R}, i = 1, 2, \dots, N-2$, are positive constant control gains. Note that the signals $\tilde{x}_i(t), i = 1, \dots, N-1$ are measurable, whereas, the filtered estimation error $r(t)$ in (4-40) is not measurable, since it depends on $x_N(t)$. The weight update laws for the DNN in (4-37) are developed as

$$\begin{aligned} \dot{\hat{W}}_f &= \text{proj}[\Gamma_{wf} \hat{\sigma}_f(\tilde{x}_{N-1} + \tilde{x}_f)^T], \\ \dot{\hat{V}}_{fj} &= \text{proj}[\Gamma_{vfj} \hat{x}_j(\tilde{x}_{N-1} + \tilde{x}_f)^T \hat{W}_f^T \hat{\sigma}'_f], \\ \dot{\hat{W}}_{gi} &= \text{proj}[\Gamma_{wgi} \hat{\sigma}_{gi} u_i(\tilde{x}_{N-1} + \tilde{x}_f)^T], \\ \dot{\hat{V}}_{gij} &= \text{proj}[\Gamma_{vgij} \hat{x}_j u_i(\tilde{x}_{N-1} + \tilde{x}_f)^T \hat{W}_{gi}^T \hat{\sigma}'_{gi}], \end{aligned}$$



Figure 4-1. The experimental testbed consists of a two-link robot. The links are mounted on two NSK direct-drive switched reluctance motors.

where $i = 1 \dots m$, $j = 1 \dots N$, Γ_{wf} , Γ_{wgi} , Γ_{vfj} , Γ_{vgij} , $\hat{\sigma}'_f(t)$, $\hat{\sigma}'_{gi}(t)$ are introduced in (4-18).

A similar stability analysis can be used to prove that

$$\|\tilde{x}_i(t)\|, \|\eta(t)\|, \|r(t)\| \rightarrow 0 \text{ as } t \rightarrow \infty, \quad i = 1, 2, \dots, N-1.$$

From (4-40), it can be further shown that

$$\left\| x_1^{(N)}(t) - \hat{x}_1^{(N)}(t) \right\| \rightarrow 0 \text{ as } t \rightarrow \infty.$$

4.6 Experiment and Simulation Results

Experiments and simulations on a two-link robot manipulator (Fig. 4-1) are performed to compare the proposed method with several other estimation methods. The testbed is composed of a two-link direct drive revolute robot consisting of two aluminum links. The motor encoders provide position measurements with a resolution of 614400 pulses/revolution. Two aluminum links are mounted on a 240 Nm (first link) and a 20 Nm (second link) switched reluctance motor. Data acquisition and control implementation were performed in real-time using QNX at a

frequency of 1.0 kHz. The two-link revolute robot is modeled with the following dynamics:

$$M(x)\ddot{x} + V_m(x, \dot{x})\dot{x} + F_d\dot{x} + F_s(\dot{x}) = u(t), \quad (4-41)$$

where $x = \begin{bmatrix} x_1 & x_2 \end{bmatrix}^T$ are the angular positions (*rad*) and $\dot{x} = \begin{bmatrix} \dot{x}_1 & \dot{x}_2 \end{bmatrix}^T$ are the angular velocities (*rad/s*) of the two links respectively. In (4-41), $M(x)$ is the inertia matrix and $V_m(x, \dot{x})$ is the centripetal-Coriolis matrix, defined as

$$M \triangleq \begin{bmatrix} p_1 + 2p_3c_2 & p_2 + p_3c_2 \\ p_2 + p_3c_2 & p_2 \end{bmatrix},$$

$$V_m \triangleq \begin{bmatrix} -p_3s_2\dot{x}_2 & -p_3s_2(\dot{x}_1 + \dot{x}_2) \\ p_3s_2\dot{x}_1 & 0 \end{bmatrix}. \quad (4-42)$$

In (4-41) and (4-42), parameters for simulation are chosen as the best-guess of the testbed model as $p_1 = 3.473 \text{ kg} \cdot \text{m}^2$, $p_2 = 0.196 \text{ kg} \cdot \text{m}^2$, $p_3 = 0.242 \text{ kg} \cdot \text{m}^2$, $c_2 = \cos(x_2)$, $s_2 = \sin(x_2)$. $F_d = \text{diag}\{5.3, 1.1\} \text{ Nm} \cdot \text{sec}$ and $F_s(\dot{x}) = \text{diag}\{8.45 \tanh(\dot{x}_1), 2.35 \tanh(\dot{x}_2)\} \text{ Nm}$ are the models for dynamic and static friction, respectively. The system in (4-41) can be rewritten as

$$\ddot{x} = f(x, \dot{x}) + G(x, \dot{x})u + d,$$

where $d(t) \in \mathbb{R}^2$ is the additive exogenous disturbance and $f(x, \dot{x}) \in \mathbb{R}^2$, and $G(x, \dot{x}) \in \mathbb{R}^{2 \times 2}$ are defined as

$$f(x, \dot{x}) = M^{-1}(-V_m - F_d)\dot{x} - F_s, \quad G(x, \dot{x}) = M^{-1}.$$

The control input is chosen as a PD controller to track a desired trajectory $x_d(t) = [0.5 \sin(2t) \ 0.5 \cos(2t)]^T$, as $u(t) = 20(x(t) - x_d(t)) + 10(\dot{x}(t) - \dot{x}_d(t))$, where the angular velocity $\dot{x}(t)$ used only in the control law is determined numerically by a standard backwards difference algorithm. The objective is to design an observer $\hat{\dot{x}}(t)$ to asymptotically estimate the angular velocities $\dot{x}(t)$ using only the measurements of angular positions $x(t)$. The control gains for the experiment are chosen as $k = 7$, $\alpha = 7$, $\gamma = 8$, $\beta_1 = 6$, and $\Gamma_{wf} = \Gamma_{wg1} = \Gamma_{wg2} = 3\mathbb{I}_{8 \times 8}$,

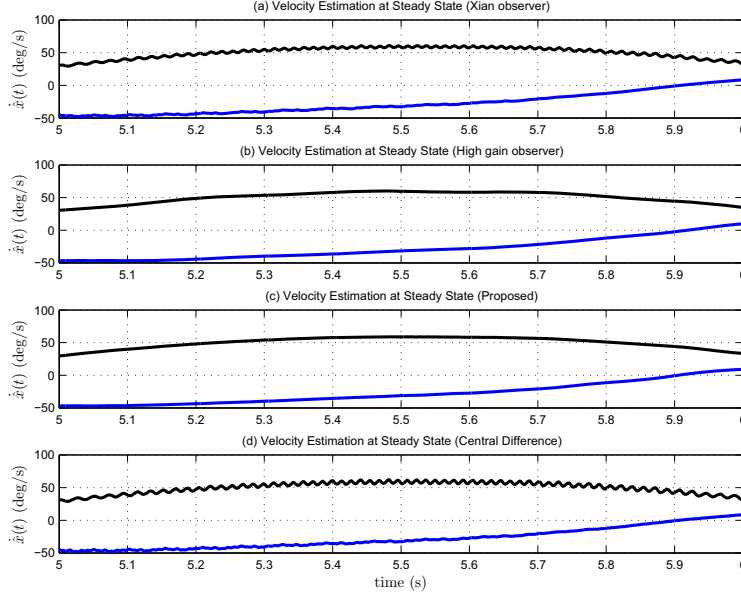


Figure 4-2. Velocity estimate $\hat{x}(t)$ using (a) [1], (b) [2], (c) the proposed method, and (d) the center difference method on a two-link experiment testbed.

$\Gamma_{vf} = \Gamma_{vg1} = \Gamma_{vg2} = 3\mathbb{I}_{2 \times 2}$, where $\mathbb{I}_{n \times n}$ denotes an identity matrix of appropriate dimensions.

The NNs are designed to have seven hidden layer neurons and the NN weights are initialized as uniformly distributed random numbers in the interval $[-1, 1]$. The initial conditions of the system and the identifier are chosen as $x(t) = [0 \ 0]^T$, $\dot{x}(t) = [0 \ 0]^T$ and $\hat{x}(t) = \hat{\dot{x}}(t) = [0 \ 0]^T$, respectively.

A global asymptotic velocity observer for uncertain nonlinear systems was developed by Xian et al. [1] as

$$\dot{\hat{x}} = p + K_0 \tilde{x}, \quad \dot{p} = K_1 \text{sgn}(\tilde{x}) + K_2 \tilde{x},$$

and a high gain (HG) observer that is asymptotic as the gain goes to infinity was developed in [2]

$$\dot{\hat{x}} = z_h + \frac{\alpha_{h1}}{\epsilon_{h1}} \tilde{x}, \quad \dot{z}_h = \frac{\alpha_{h2}}{\epsilon_{h2}} \tilde{x}.$$

Both these designs are based on a purely robust feedback strategy. A contribution of this work is the addition of a feed-forward adaptive component to compensate for the uncertain dynamics. To gauge the benefit of this approach, the proposed observer is compared with the observers in [1] and [2]. Control gains for the observer in [1] are chosen as $K_0 = 10$, $K_1 = 6$, and $K_2 = 10$, and control gains for the HG observer are chosen as $\alpha_1 = 0.6$, $\alpha_2 = 25$, $\epsilon_1 = 0.01$, and $\epsilon_2 = 0.015$.

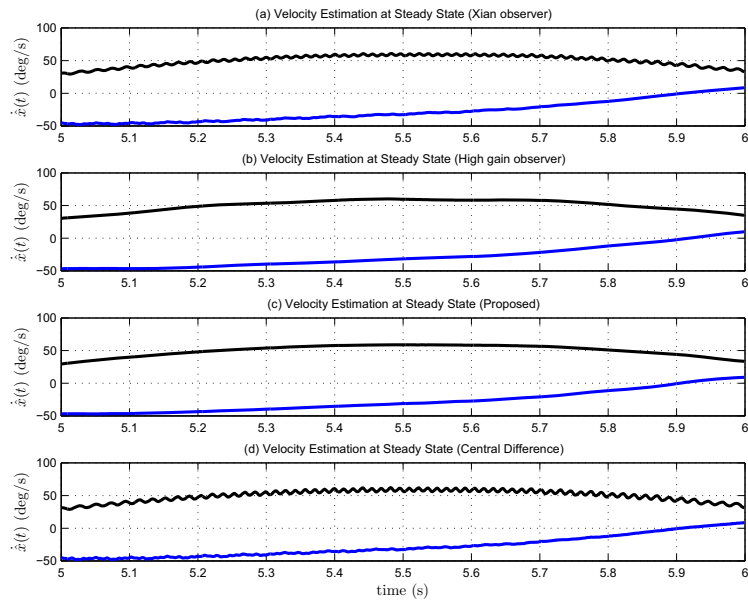


Figure 4-3. The steady-state velocity estimate $\hat{x}(t)$ using (a) [1], (b) [2], (c) the proposed method, and (d) the center difference method on a two-link experiment testbed.

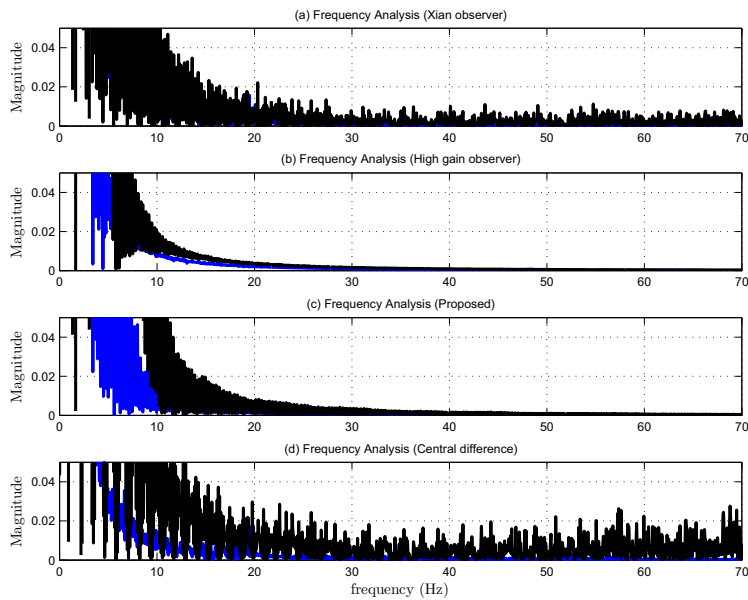


Figure 4-4. Frequency analysis of velocity estimation $\hat{x}(t)$ using (a) [1], (b) [2], (c) the proposed method, and (d) the center difference method on a two-link experiment testbed.

To make the comparison feasible, the gains of all observers are tuned to get the steady state root mean squares (RMS) of position estimation errors to be approximately equal 0.17 for a settling time of 1 second. The experiment results for the velocity estimators in [1], [2], and the proposed method are compared with the central difference algorithm. The results are shown in Figs. 4-2 and 4-3. It is observed that the velocity estimates of the proposed observer and observer in [2] look similar, but the transient response of the proposed method is improved over the observer in [2]; moreover, both methods lower frequency content than the observer in [1] and the central difference method. To illustrate the lower frequency response of the proposed method compared to [1] and the central difference method, the frequency analysis plots of the experiment results are shown in Fig. 4-4. Fig. 4-4 illustrates that the velocity estimation using [1] and central difference methods include higher frequency signals than the proposed method or the approach in [2].

Given the lack of velocity sensors in the two-link experiment testbed to verify the velocity estimates, a simulation was performed using the dynamics in (4-41). To examine the effect of noise, white Gaussian noise with SNR 60 dB is added to the position measurements. Fig. 4-5 shows the simulation results for the steady-state velocity estimation errors and the respective frequency analysis for the velocity estimate of the observer in [1], the observer in [2], the developed method, and the central difference method. Table 4-1 gives a comparison of the transient and steady state RMS velocity estimation errors for these different methods. Results of the standard numerical central differentiation algorithm are significantly worse than the other methods in the presence of noise as seen from Fig. 4-5 and Table 4-1. Although, simulation results for [2] and the developed method are comparable, differences exist in the structure of the observers and proof of convergence of the estimates. The observer in [2] is a purely robust feedback technique and the estimation result is proven to be asymptotic as the gains tend to infinity. On the other hand, the proposed method is a robust adaptive observer with a DNN structure to learn the system uncertainties, combining a dynamic filter and a robust sliding mode structure, thus guaranteeing asymptotic convergence with finite gains. Further, the observer in [1]

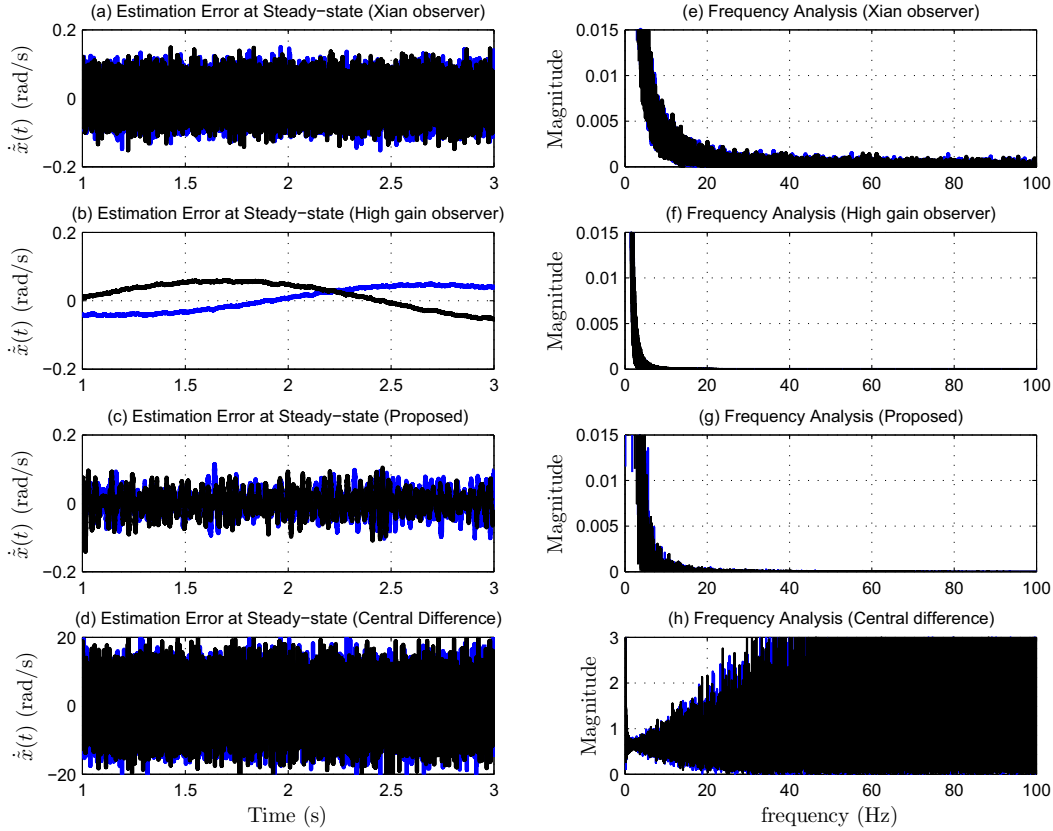


Figure 4-5. The steady-state velocity estimation error $\dot{\hat{x}}(t)$ using (a) [1], (b) [2], (c) the proposed method, and (d) the center difference method on simulations, in presence of sensor noise (SNR 60dB). The right figures (e)-(h) indicate the respective frequency analysis of velocity estimation $\dot{\hat{x}}(t)$.

is also a purely robust feedback method, where all uncertainties are damped out by a sliding mode term resulting in higher frequency velocity estimates than the developed observer, as seen from both experiment and simulation results.

4.7 Conclusion

A novel design of an adaptive observer using DNNs for uncertain nonlinear systems is proposed. The DNN works in conjunction with a dynamic filter without any off-line training

Table 4-1. Transient ($t = 0 - 1$ sec) and steady state ($t = 1 - 10$ sec) velocity estimation errors $\dot{\hat{x}}(t)$ for different velocity estimation methods in presence of noise 50dB.

	Central difference	Method in [1]	Method in [2]	Proposed
Transient RMS Error	66.2682	0.1780	0.1040	0.1309
Steady State RMS Error	8.1608	0.0565	0.0538	0.0504

phase. A sliding feedback term is added to the DNN structure to account for reconstruction errors and external disturbances. The observation states are proven to asymptotically converge to the system states and a similar observer structure is extended to high-order uncertain systems. Simulations and experiments show the improvement of the proposed method in comparison to several other estimation methods.

CHAPTER 5
GLOBAL OUTPUT FEEDBACK TRACKING CONTROL FOR UNCERTAIN
SECOND-ORDER NONLINEAR SYSTEMS

A DNN observer-based OFB controller for uncertain nonlinear systems with bounded disturbances is developed. A two-fold objective, asymptotic estimation of unmeasurable states and asymptotic tracking control, is set up. The asymptotic estimation of the unmeasurable state is achieved by exploiting the DNN-based observer in Chapter 4, wherein the dynamic filter and the weight update laws are modified for the new objective. A robust controller includes a NN feedforward term, along with the estimated state feedback and sliding mode terms through the Lyapunov-based stability analysis to yield an asymptotic tracking result. The developed method yields the first OFB technique simultaneously achieving asymptotic tracking and asymptotic estimation of unmeasurable states for the class of uncertain nonlinear systems with bounded disturbances. Experiments on a two-link robot manipulator are used to investigate the performance of the proposed control approach.

5.1 Dynamic System and Properties

Consider a control-affine second order Euler-Lagrange like nonlinear system of the form

$$\ddot{x} = f(x, \dot{x}) + G(x)u + d, \quad (5-1)$$

where $x(t) \in \mathbb{R}^n$ is the measurable output with a finite initial condition $x(0) = x_0$, $u(t) \in \mathbb{R}^n$ is the control input, $f(x, \dot{x}) \in \mathbb{R}^n$, $G(x) \in \mathbb{R}^{n \times n}$ are continuous functions, and $d(t) \in \mathbb{R}^n$ is an exogenous disturbance. The following assumptions about the system in (5-1) will be utilized in the subsequent development.

Assumption 5.1. *The time derivatives of the system output $\dot{x}(t), \ddot{x}(t)$ are unmeasurable.*

Assumption 5.2. *The unknown function $f(x, \dot{x})$ is C^1 , and the function $G(x)$ is known, invertible and the matrix inverse $G^{-1}(x)$ is bounded.*

Assumption 5.3. *The disturbance $d(t)$ is differentiable, and $d(t), \dot{d}(t) \in \mathcal{L}_\infty$.*

Based on the universal approximation property of MLNNs, the unknown function $f(x, \dot{x})$ in (5–1) can be replaced by a MLNN, and the system can be represented as

$$\ddot{x} = W^T \sigma(V_1^T x + V_2^T \dot{x}) + \varepsilon + Gu + d, \quad (5-2)$$

where $W \in \mathbb{R}^{N+1 \times n}$, $V_1, V_2 \in \mathbb{R}^{n \times N}$ are unknown ideal weight matrices of the MLNN having N hidden layer neurons, $\sigma(t) \triangleq \sigma(V_1^T x(t) + V_2^T \dot{x}(t)) \in \mathbb{R}^{N+1}$ is the activation function (sigmoid, hyperbolic tangent etc.), and $\varepsilon(x, \dot{x}) \in \mathbb{R}^n$ is a function reconstruction error. The following assumptions will be used in the DNN-based observer and controller development and stability analysis.

Assumption 5.4. *The ideal NN weights are bounded by known positive constants [46], i.e.*

$$\|W\| \leq \bar{W}, \|V_1\| \leq \bar{V}_1, \|V_2\| \leq \bar{V}_2.$$

Assumption 5.5. *The activation function $\sigma(\cdot)$ and its partial derivatives $\sigma'(\cdot)$, $\sigma''(\cdot)$ are bounded [46]. This assumption is satisfied for typical activation functions (e.g., sigmoid, hyperbolic tangent).*

Assumption 5.6. *The function reconstruction error $\varepsilon(x, \dot{x})$, and its first time derivative are bounded [46], as $\|\varepsilon(x, \dot{x})\| \leq \bar{\varepsilon}_1$, $\|\dot{\varepsilon}(x, \dot{x}, \ddot{x})\| \leq \bar{\varepsilon}_2$, where $\bar{\varepsilon}_1, \bar{\varepsilon}_2$ are known positive constants.*

5.2 Estimation and Control Objectives

The contribution in this chapter is the development of a robust DNN-based observer such that the estimated states asymptotically converge to the states of the system (5–1), and a discontinuous controller enables the system state to asymptotically track a desired time-varying trajectory $x_d(t) \in \mathbb{R}^n$, despite uncertainties and disturbances in the system. To quantify these objectives, an estimation error $\tilde{x}(t) \in \mathbb{R}^n$ and a tracking error $e(t) \in \mathbb{R}^n$ are defined as

$$\tilde{x} \triangleq x - \hat{x}, \quad (5-3)$$

$$e \triangleq x - x_d, \quad (5-4)$$

where $\hat{x}(t) \in \mathbb{R}^n$ is the state of the DNN observer which is introduced in the subsequent development. The desired trajectory $x_d(t)$ and its derivatives $x_d^{(i)}(t)$ ($i = 1, 2$), are assumed to exist and be

bounded. To compensate for the lack of direct measurements of $\dot{x}(t)$, the filtered estimation error $r_{es}(t) \in \mathbb{R}^n$ and the filtered tracking error $r_{tr}(t) \in \mathbb{R}^n$ are defined as

$$r_{es} \triangleq \dot{\tilde{x}} + \alpha \tilde{x} + \eta, \quad (5-5)$$

$$r_{tr} \triangleq \dot{e} + \alpha e + \eta, \quad (5-6)$$

where $\alpha \in \mathbb{R}$ is a positive constant gain, and $\eta(t) \in \mathbb{R}^n$ is an output of the dynamic filter

$$\begin{aligned} \eta &= p - (k + \alpha)\tilde{x}, \\ \dot{p} &= -(k + 2\alpha)p - v + ((k + \alpha)^2 + 1)\tilde{x} + e, \\ \dot{v} &= p - \alpha v - (k + \alpha)\tilde{x}, \\ p(0) &= (k + \alpha)\tilde{x}(0), \quad v(0) = 0, \end{aligned} \quad (5-7)$$

where $v(t) \in \mathbb{R}^n$ is another output of the filter, $p(t) \in \mathbb{R}^n$ is used as an internal filter variable, and $k \in \mathbb{R}$ is a positive constant control gain. The filtered estimation error $r_{es}(t)$ and the filtered tracking error $r_{tr}(t)$ are not measurable since the expressions in (5-5) and (5-6) depend on $\dot{x}(t)$.

5.3 DNN-based Robust Observer

The MLDNN architecture is developed to observe the system in (5-1)

$$\ddot{\hat{x}} = \hat{W}^T \hat{\sigma} + Gu - (k + 3\alpha)\eta + \beta_1 \text{sgn}(\tilde{x} + v), \quad (5-8)$$

where $\begin{bmatrix} \hat{x}(t)^T & \dot{\hat{x}}(t)^T \end{bmatrix}^T \in \mathbb{R}^{2n}$ are the states of the DNN observer, $\hat{W}(t) \in \mathbb{R}^{N+1 \times n}$, $\hat{V}_1(t), \hat{V}_2(t) \in \mathbb{R}^{n \times N}$ are the weight estimates, $\hat{\sigma}(t) \triangleq \sigma(\hat{V}_1(t)^T \hat{x}(t) + \hat{V}_2(t)^T \dot{\hat{x}}(t)) \in \mathbb{R}^{N+1}$ and $\beta_1 \in \mathbb{R}$ is a positive constant control gain.

The weight update laws for the DNN in (5–8) are developed based on the subsequent stability analysis as

$$\begin{aligned}\dot{\hat{W}} &= \Gamma_w \text{proj}[\hat{\sigma}_d(\tilde{x} + e + 2\mathbf{v})^T], \\ \dot{\hat{V}}_1 &= \Gamma_{v1} \text{proj}[x_d(\tilde{x} + e + 2\mathbf{v})^T \hat{W}^T \hat{\sigma}'_d], \\ \dot{\hat{V}}_2 &= \Gamma_{v2} \text{proj}[\dot{x}_d(\tilde{x} + e + 2\mathbf{v})^T \hat{W}^T \hat{\sigma}'_d],\end{aligned}\tag{5–9}$$

where $\Gamma_w \in \mathbb{R}^{(N+1) \times (N+1)}$, $\Gamma_{v1}, \Gamma_{v2} \in \mathbb{R}^{n \times n}$, are constant symmetric positive-definite adaptation gains, the terms $\hat{\sigma}_d(t), \hat{\sigma}'_d(t)$ are defined as $\hat{\sigma}_d(t) \triangleq \sigma(\hat{V}_1(t)^T x_d(t) + \hat{V}_2(t)^T \dot{x}_d(t))$, $\hat{\sigma}'_d(t) \triangleq d\sigma(\zeta)/d\zeta|_{\zeta=\hat{V}_1^T x_d + \hat{V}_2^T \dot{x}_d}$, and $\text{proj}(\cdot)$ is a smooth projection operator [88], [89] used to guarantee that the weight estimates $\hat{W}(t), \hat{V}_1(t), \hat{V}_2(t)$ remain bounded.

To facilitate the subsequent analysis, (5–5) and (5–7) can be used to express the time derivative of $\eta(t)$ as

$$\dot{\eta} = -(k + \alpha)r_{es} - \alpha\eta + \tilde{x} + e - \mathbf{v}.\tag{5–10}$$

The closed-loop dynamics of the filtered estimation error in (5–5) can be determined by using (5–2), (5–3), (5–5), (5–8) and (5–10) as

$$\begin{aligned}\dot{r}_{es} &= W^T \sigma - \hat{W}^T \hat{\sigma} + \varepsilon + d + (k + 3\alpha)\eta - \beta_1 \text{sgn}(\tilde{x} + \mathbf{v}) \\ &\quad + \alpha(r_{es} - \alpha\tilde{x} - \eta) - (k + \alpha)r_{es} - \alpha\eta + \tilde{x} + e - \mathbf{v}.\end{aligned}\tag{5–11}$$

Adding and subtracting $W^T \sigma_d + W^T \hat{\sigma}_d + \hat{W}^T \hat{\sigma}_d$ where $\sigma_d(t) \triangleq \sigma(V_1^T x_d(t) + V_2^T \dot{x}_d(t))$, the expression in (5–11) can be rewritten as

$$\dot{r}_{es} = \tilde{N}_1 + N - kr_{es} - \beta_1 \text{sgn}(\tilde{x} + \mathbf{v}) + (k + \alpha)\eta - \tilde{x},\tag{5–12}$$

where the auxiliary function $\tilde{N}_1(e, \tilde{x}, \mathbf{v}, r_{es}, r_{1r}, \hat{W}, \hat{V}_1, \hat{V}_2, t) \in \mathbb{R}^n$ is defined as

$$\tilde{N}_1 \triangleq W^T(\sigma - \sigma_d) - \hat{W}^T(\hat{\sigma} - \hat{\sigma}_d) - (\alpha^2 - 2)\tilde{x} - \mathbf{v} + e,\tag{5–13}$$

and $N(x_d, \dot{x}_d, \hat{W}, \hat{V}_1, \hat{V}_2, t) \in \mathbb{R}^n$ is segregated into two parts as

$$N \triangleq N_D + N_B. \quad (5-14)$$

In (5-14), $N_D(t), N_B(\hat{W}, \hat{V}_1, \hat{V}_2, t) \in \mathbb{R}^n$ are defined as

$$N_D \triangleq \varepsilon + d, \quad (5-15)$$

and

$$N_B \triangleq N_{B_1} + N_{B_2}. \quad (5-16)$$

In (5-16), $N_{B_1}(\hat{W}, \hat{V}_1, \hat{V}_2, t), N_{B_2}(\hat{W}, \hat{V}_1, \hat{V}_2, t) \in \mathbb{R}^n$ are defined as

$$\begin{aligned} N_{B_1} &\triangleq W^T O(\tilde{V}_1^T x_d + \tilde{V}_2^T \dot{x}_d)^2 + \tilde{W}^T \hat{\sigma}'_d(\tilde{V}_1^T x_d + \tilde{V}_2^T \dot{x}_d), \\ N_{B_2} &\triangleq \tilde{W}^T \hat{\sigma}_d + \hat{W}^T \hat{\sigma}'_d(\tilde{V}_1^T x_d + \tilde{V}_2^T \dot{x}_d), \end{aligned} \quad (5-17)$$

where $\tilde{W}(t) \triangleq W - \hat{W}(t) \in \mathbb{R}^{N+1 \times n}$, $\tilde{V}_1(t) \triangleq V_1 - \hat{V}_1(t) \in \mathbb{R}^{n \times N}$, $\tilde{V}_2(t) \triangleq V_2 - \hat{V}_2(t) \in \mathbb{R}^{n \times N}$ are the estimate mismatches for the ideal NN weights, and $O(\tilde{V}_1^T x_d + \tilde{V}_2^T \dot{x}_d)^2 \in \mathbb{R}^{N+1}$ is the higher order term in the Taylor series of the vector functions $\sigma_d(\cdot)$ in the neighborhood of $\hat{V}_1^T x_d + \hat{V}_2^T \dot{x}_d$ as

$$\sigma_d = \hat{\sigma}_d + \hat{\sigma}'_d(\tilde{V}_1^T x_d + \tilde{V}_2^T \dot{x}_d) + O(\tilde{V}_1^T x_d + \tilde{V}_2^T \dot{x}_d)^2. \quad (5-18)$$

Motivation for segregating the terms in (5-12), (5-14) and (5-16) is derived from the fact that different terms have different bounds. The term $\tilde{N}_1(\cdot)$ includes all terms which can be upper bounded by states, whereas $N(\cdot)$ includes all terms which can be upper bounded by constants. The difference between the terms $N_D(\cdot)$ and $N_B(\cdot)$ in (5-14) which both can be upper-bounded by constants is that the first time derivative of $N_D(\cdot)$ is further upper-bounded by a constant, whereas the term $\dot{N}_B(\cdot)$ is state dependent. The term $N_B(\cdot)$ is further segregated as (5-16) to aid in the weight update law design for the DNN in (5-9). In subsequent stability analysis, the term $N_{B_1}(\cdot)$ is cancelled by the error feedback and the sliding mode term, while the term $N_{B_2}(\cdot)$ is partially compensated for by the weight update laws and partially cancelled by the error feedback and the sliding mode term.

Using (5-3)-(5-6), Assumptions 5.4-5.5, the $proj(\cdot)$ algorithm in (5-9) and the Mean Value Theorem, the auxiliary function $\tilde{N}_1(t)$ in (5-13) can be upper-bounded as

$$\|\tilde{N}_1\| \leq \zeta_1 \|z\|, \quad (5-19)$$

where $\zeta_1 \in \mathbb{R}$ is a computable positive constant, and $z(\tilde{x}, e, r_{es}, r_{tr}, v, \eta) \in \mathbb{R}^{6n}$ is defined as

$$z \triangleq [\tilde{x}^T \ e^T \ r_{es}^T \ r_{tr}^T \ v^T \ \eta^T]^T. \quad (5-20)$$

Based on Assumptions 5.3-5.6, the Taylor series expansion in (5-18), and the weight update laws in (5-9), the following bounds can be developed

$$\begin{aligned} \|N_D\| &\leq \zeta_2, \quad \|N_{B_1}\| \leq \zeta_3, \quad \|N_{B_2}\| \leq \zeta_4, \\ \|\dot{N}_D\| &\leq \zeta_5, \quad \|\dot{N}_B\| \leq \zeta_6 + \zeta_7 \|z\|, \end{aligned} \quad (5-21)$$

where $\zeta_i \in \mathbb{R}, i = 2, 3, \dots, 7$, are computable positive constants.

5.4 Robust Adaptive Tracking Controller

The control objective is to force the system state to asymptotically track the desired trajectory $x_d(t)$, despite the uncertainties and disturbances in the system. Quantitatively, this objective is to regulate the filtered tracking controller $r_{tr}(t)$ to zero. Using (5-2), (5-4), (5-6) and (5-10), the open-loop dynamics of the derivative of the filtered tracking error in (5-6) is expressed as

$$\begin{aligned} \dot{r}_{tr} &= W^T \sigma + G(x)u + \varepsilon + d - \ddot{x}_d + \alpha(r_{tr} - \alpha e - \eta) \\ &\quad - (k + \alpha)r_{es} - \alpha\eta + \tilde{x} + e - v. \end{aligned} \quad (5-22)$$

The control input $u(t)$ is now designed as a composition of the DNN term, the estimated states $\hat{x}(t), \dot{\hat{x}}(t)$, and the sliding mode term as

$$u(t) = G^{-1}[\ddot{x}_d - \hat{W}^T \hat{\sigma}_d - (k + \alpha)(\hat{e} + \alpha\hat{e}) - \beta_2 \text{sgn}(e + v)], \quad (5-23)$$

where $\beta_2 \in \mathbb{R}$ is a positive constant control gain and the tracking error estimate $\hat{e}(t) \in \mathbb{R}^n$ is defined as

$$\hat{e} \triangleq \hat{x} - x_d.$$

Based on the fact that the estimated states are measurable, the tracking error estimate $\hat{e}(t)$ and its derivative $\dot{\hat{e}}(t)$ are measurable; moreover, the filtered tracking error $r_{tr}(t)$ is related to the filtered estimation error $r_{es}(t)$ via the tracking error estimate $\hat{e}(t)$ as

$$r_{tr} = r_{es} + \dot{\hat{e}} + \alpha \hat{e}. \quad (5-24)$$

Hence, adding and subtracting $W^T \sigma_d + W^T \hat{\sigma}_d$ and using (5-22)-(5-24), the closed-loop error system becomes

$$\dot{r}_{tr} = \tilde{N}_2 + N - kr_{tr} - \beta_2 \text{sgn}(e + v) - e, \quad (5-25)$$

where the auxiliary function $\tilde{N}_2(e, \tilde{x}, \eta, v, r_{tr}, t) \in \mathbb{R}^n$ is defined as

$$\tilde{N}_2 \triangleq W^T (\sigma - \sigma_d) - (\alpha^2 - 2)e - v + \tilde{x} - 2\alpha\eta, \quad (5-26)$$

and the function $N(\cdot)$ is introduced in (5-14). Similarly, using (5-4), (5-6), Assumptions 5.4-5.5, the $proj(\cdot)$ algorithm in (5-9), and the Mean Value Theorem [74], the auxiliary function $\tilde{N}_2(\cdot)$ in (5-26) can be upper-bounded as

$$\|\tilde{N}_2\| \leq \zeta_8 \|z\|, \quad (5-27)$$

where $\zeta_8 \in \mathbb{R}$ is a computable positive constant.

To facilitate the subsequent stability analysis, let $y(z, P, Q) \in \mathbb{R}^{6n+2}$ be defined as

$$y \triangleq [z^T \quad \sqrt{P} \quad \sqrt{Q}]^T. \quad (5-28)$$

In (5–28), the auxiliary function $P(r_{es}, r_{tr}, \tilde{x}, e, v, \dot{\tilde{x}}, \dot{e}, \dot{v}, t) \in \mathbb{R}$ is the Filippov solution to the differential equation

$$\dot{P} \triangleq L, \quad (5-29)$$

$$\begin{aligned} P_0 &\triangleq P(\tilde{x}(0), e(0), v(0), 0) \\ &= \beta_1 \sum_{j=1}^n |\tilde{x}_j(0) + v_j(0)| + \beta_2 \sum_{j=1}^n |e_j(0) + v_j(0)| - (\tilde{x}(0) + e(0) + 2v(0))^T N(0), \end{aligned}$$

where the subscript $j = 1, 2, \dots, n$ denotes the j^{th} element of $\tilde{x}(0)$, $e(0)$ or $v(0)$, and the auxiliary function $L(r_{es}, r_{tr}, \tilde{x}, e, v, \dot{\tilde{x}}, \dot{e}, \dot{v}, t) \in \mathbb{R}$ is defined as

$$\begin{aligned} L &\triangleq -r_{es}^T (N_D + N_{B_1} - \beta_1 \text{sgn}(\tilde{x} + v)) - r_{tr}^T (N_D + N_{B_1} - \beta_2 \text{sgn}(e + v)) \\ &\quad - (\tilde{x} + e + 2v)^T N_{B_2} + \beta_3 \|z\|^2, \end{aligned} \quad (5-30)$$

where β_1, β_2 are introduced in (5–8) and (5–23), and $\beta_3 \in \mathbb{R}$ is a positive constant. The control gains $\beta_i, i = 1, 2, 3$ are chosen according to the sufficient conditions

$$\beta_1, \beta_2 > \max(\zeta_2 + \zeta_3 + \zeta_4, \zeta_2 + \zeta_3 + \frac{\zeta_5}{\alpha} + \frac{\zeta_6}{\alpha}), \quad \beta_3 > 2\zeta_7, \quad (5-31)$$

where $\zeta_i, i = 1, 2, \dots, 7$ are introduced in (5–19) and (5–21). Provided the sufficient conditions in (5–31) are satisfied, the following inequality can be obtained $P(\cdot) \geq 0^1$. The auxiliary function $Q(\tilde{W}, \tilde{V}_1, \tilde{V}_2) \in \mathbb{R}$ in (5–28) is defined as

$$Q(t) \triangleq \frac{\alpha}{2} \text{tr}(\tilde{W}^T \Gamma_w^{-1} \tilde{W}) + \frac{\alpha}{2} \text{tr}(\tilde{V}_1^T \Gamma_{v1}^{-1} \tilde{V}_1) + \frac{\alpha}{2} \text{tr}(\tilde{V}_2^T \Gamma_{v2}^{-1} \tilde{V}_2), \quad (5-32)$$

where $\text{tr}(\cdot)$ denotes the trace of a matrix. Since the gains $\Gamma_w, \Gamma_{v1}, \Gamma_{v2}$ are symmetric, positive-definite matrices, $Q(\cdot) \geq 0$.

¹ See Appendix B for proof

5.5 Lyapunov Stability Analysis for DNN-based Observation and Control

Theorem 5.1. *The DNN-based observer and controller proposed in (5–8) and (5–23), respectively, along with the weight update laws in (5–9) ensure asymptotic estimation and tracking in sense that*

$$\begin{aligned} \|\tilde{x}(t)\| &\rightarrow 0 \text{ and } \left\| \dot{\tilde{x}}(t) \right\| \rightarrow 0 \text{ as } t \rightarrow \infty, \\ \|e(t)\| &\rightarrow 0 \text{ and } \|\dot{e}(t)\| \rightarrow 0 \text{ as } t \rightarrow \infty, \end{aligned}$$

provided the gain conditions in (5–31) are satisfied, and the control gains α and $k = k_1 + k_2$ introduced in (5–5)-(5–7) are selected as

$$\lambda \triangleq \min(\alpha, k_1) > \frac{\zeta_1^2 + \zeta_8^2}{4k_2} + \beta_3, \quad (5-33)$$

where $\zeta_1, \zeta_8, \beta_3$ are introduced in (5–19), (5–27), and (5–30), respectively.

Proof. Consider the Lyapunov candidate function $V_L(y, t) : \mathcal{D} \times (0, \infty) \rightarrow \mathbb{R}$, which is a Lipschitz continuous regular positive definite function defined as

$$V_L \triangleq \frac{1}{2} \tilde{x}^T \tilde{x} + \frac{1}{2} e^T e + \frac{1}{2} v^T v + \frac{1}{2} \eta^T \eta + \frac{1}{2} r_{es}^T r_{es} + \frac{1}{2} r_{tr}^T r_{tr} + P + Q, \quad (5-34)$$

which satisfies the following inequalities:

$$U_1(y) \leq V_L(y, t) \leq U_2(y). \quad (5-35)$$

In (5–35), $U_1(y), U_2(y) \in \mathbb{R}$ are continuous positive definite functions defined as

$$U_1(y) \triangleq \frac{1}{2} \|y\|^2, \quad U_2(y) \triangleq \|y\|^2.$$

The generalized time derivative of (5–34) exists almost everywhere (a.e.), and $\dot{V}_L(y) \in^{a.e.} \dot{\tilde{V}}_L(y)$ (see Chapter 3 for further details) where

$$\dot{\tilde{V}}_L = \bigcap_{\xi \in \partial V_L(y)} \xi^T K \left[\begin{array}{c} \dot{\tilde{x}}^T \\ \dot{e}^T \\ \dot{v}^T \\ \dot{\eta}^T \\ \dot{r}_{es}^T \\ \dot{r}_{tr}^T \\ \frac{1}{2} P^{-\frac{1}{2}} \dot{P} \\ \frac{1}{2} Q^{-\frac{1}{2}} \dot{Q} \end{array} \right]^T, \quad (5-36)$$

where ∂V_L is the generalized gradient of $V_L(y)$ [96]. Since $V_L(y)$ is a locally Lipschitz continuous regular function that is smooth in y , (5–36) can be simplified as [97]

$$\begin{aligned}\dot{\tilde{V}}_L &= \nabla V^T K \left[\begin{array}{c} \dot{\tilde{x}}^T \quad \dot{e}^T \quad \dot{v}^T \quad \dot{\eta}^T \quad \dot{r}_{es}^T \quad \dot{r}_{tr}^T \quad \frac{1}{2} P^{-\frac{1}{2}} \dot{P} \quad \frac{1}{2} Q^{-\frac{1}{2}} \dot{Q} \end{array} \right]^T \\ &= \left[\tilde{x}^T \quad e^T \quad v^T \quad \eta^T \quad r_{es}^T \quad r_{tr}^T \quad 2P^{\frac{1}{2}} \quad 2Q^{\frac{1}{2}} \right] K [\Psi]^T,\end{aligned}$$

where

$$\Psi \triangleq \left[\begin{array}{c} \dot{\tilde{x}}^T \quad \dot{e}^T \quad \dot{v}^T \quad \dot{\eta}^T \quad \dot{r}_{es}^T \quad \dot{r}_{tr}^T \quad \frac{1}{2} P^{-\frac{1}{2}} \dot{P} \quad \frac{1}{2} Q^{-\frac{1}{2}} \dot{Q} \end{array} \right].$$

Using the calculus for $K[\cdot]$ from [98] (Theorem 1, Properties 2, 5, 7), and substituting the dynamics from (5–5)-(5–7), (5–10), (5–12), (5–25), (5–29), (5–30) and (5–32), $\dot{\tilde{V}}_L(y)$ can be rewritten as

$$\begin{aligned}\dot{\tilde{V}}_L &\subset \tilde{x}^T (r_{es} - \alpha \tilde{x} - \eta) + e^T (r_{tr} - \alpha e - \eta) + \eta^T [-(k + \alpha)r_{es} - \alpha \eta + \tilde{x} + e - v] \\ &\quad + v^T (\eta - \alpha v) + r_{es}^T \{ \tilde{N}_1 + N - kr_{es} - \beta_1 K[\text{sgn}(\tilde{x} + v)] + (k + \alpha)\eta - \tilde{x} \} \\ &\quad + r_{tr}^T \{ \tilde{N}_2 + N - kr_{tr} - \beta_2 K[\text{sgn}(e + v)] - e \} - r_{es}^T \{ N_D + N_{B_1} - \beta_1 K[\text{sgn}(\tilde{x} + v)] \} \\ &\quad - r_{tr}^T \{ N_D + N_{B_1} - \beta_2 K[\text{sgn}(e + v)] \} + \beta_3 \|z\|^2 - (\tilde{x} + \dot{e} + 2\dot{v})^T N_{B_2} \\ &\quad - \alpha \text{tr}(\tilde{W}^T \Gamma_w^{-1} \dot{\tilde{W}}) - \alpha \text{tr}(\tilde{V}_1^T \Gamma_{v_1}^{-1} \dot{\tilde{V}}_1) - \alpha \text{tr}(\tilde{V}_2^T \Gamma_{v_2}^{-1} \dot{\tilde{V}}_2).\end{aligned}\tag{5–37}$$

Using the fact that $K[\text{sgn}(e + v)] = \text{SGN}(e + v)$ and $K[\text{sgn}(\tilde{x} + v)] = \text{SGN}(\tilde{x} + v)$ (see Chapter 3 for further details), the set in (5–37) can reduce to the scalar inequality. Substituting the weight update laws in (5–9) and canceling common terms, the above expression can be upper bounded as

$$\dot{\tilde{V}}_L \stackrel{a.e.}{\leq} -\alpha \tilde{x}^T \tilde{x} - \alpha e^T e - \alpha v^T v - \alpha \eta^T \eta - kr_{es}^T r_{es} - kr_{tr}^T r_{tr} + r_{es}^T \tilde{N}_1 + r_{tr}^T \tilde{N}_2 + \beta_3 \|z\|^2.\tag{5–38}$$

Using (5-19) and (5-27), substituting $k = k_1 + k_2$, and completing the squares, the expression in (5-38) can be further bounded as

$$\begin{aligned} \dot{V}_L &\stackrel{a.e.}{\leq} -\alpha \|\tilde{x}\|^2 - \alpha \|e\|^2 - \alpha \|v\|^2 - \alpha \|\eta\|^2 - k_1 \|r_{es}\|^2 - k_1 \|r_{tr}\|^2 + \left(\frac{\zeta_1^2 + \zeta_8^2}{4k_2} + \beta_3 \right) \|z\|^2 \\ &\stackrel{a.e.}{\leq} -\left(\lambda - \frac{\zeta_1^2 + \zeta_8^2}{4k_2} - \beta_3 \right) \|z\|^2 \stackrel{a.e.}{\leq} -U(y), \end{aligned} \quad (5-39)$$

where $U(y) = c \|z\|^2$, for some positive constant c , is a continuous positive semi-definite function, and λ is defined in (5-33). The inequalities in (5-35) and (5-39) show that $V_L(y) \in \mathcal{L}_\infty$; hence, $\tilde{x}(t), e(t), v(t), \eta(t), r_{es}(t), r_{tr}(t), P(t)$ and $Q(t) \in \mathcal{L}_\infty$. Using (5-5) and (5-6), it can be shown that $\dot{\tilde{x}}(t), \dot{e}(t) \in \mathcal{L}_\infty$. Based on the assumption that $x_d(t), \dot{x}_d(t) \in \mathcal{L}_\infty$, and $e(t), \dot{e}(t) \in \mathcal{L}_\infty$, $x(t), \dot{x}(t) \in \mathcal{L}_\infty$ by (5-4); moreover, using (5-3) and $\tilde{x}(t), \dot{\tilde{x}}(t) \in \mathcal{L}_\infty$, $\hat{x}(t), \dot{\hat{x}}(t) \in \mathcal{L}_\infty$. Based on Assumptions 5.2 and 5.5, the projection algorithm in (5-9), the boundedness of the $\text{sgn}(\cdot)$ and $\sigma(\cdot)$ functions, and $x_d(t), \dot{x}_d(t), \hat{x}(t), \dot{\hat{x}}(t) \in \mathcal{L}_\infty$, the control input $u(t)$ is bounded from (5-23). Similarly, $\dot{v}(t), \dot{\eta}(t), \dot{r}_{es}(t), \dot{r}_{tr}(t) \in \mathcal{L}_\infty$ by using (5-7), (5-10), (5-11), (5-25); hence $\dot{z}(t) \in \mathcal{L}_\infty$, using (5-20); hence, $U(y)$ is uniformly continuous. It can be concluded that

$$c \|z\|^2 \rightarrow 0 \text{ as } t \rightarrow \infty,$$

and using the definition of $z(t)$ in (5-20), the following result can be shown

$$\begin{aligned} \|\tilde{x}\|, \|e\| &\rightarrow 0 \text{ as } t \rightarrow \infty, \\ \|r_{es}\|, \|r_{tr}\|, \|v\|, \|\eta\| &\rightarrow 0 \text{ as } t \rightarrow \infty. \end{aligned}$$

Using (5-5) and (5-6), and standard linear analysis, it can be further shown that

$$\left\| \begin{array}{c} \dot{\tilde{x}} \\ \dot{e} \end{array} \right\| \rightarrow 0 \text{ as } t \rightarrow \infty.$$

□

5.6 Experiment Results

The performance of the proposed OFB control method is tested on a two-link robot manipulator depicted in Fig. 4-1, where the dynamics given by (4-41). The desired trajectory for each link of the manipulator is given as (in degrees)

$$\begin{aligned}x_{1d} &= 30 \sin(1.5t)(1 - \exp(-0.01t^3)), \\x_{2d} &= 30 \sin(2.0t)(1 - \exp(-0.05t^3)).\end{aligned}$$

The control gains are chosen as $k = \text{diag}(25, 90)$, $\alpha = \text{diag}(22, 30)$, $\beta_1 = 0.2$, $\beta_2 = 0.2$ and, $\Gamma_w = 0.2\mathbb{I}_{8 \times 8}$, $\Gamma_{v1} = \Gamma_{v2} = 0.2\mathbb{I}_{2 \times 2}$, where $\mathbb{I}_{n \times n}$ denotes an identity matrix of appropriate dimensions. The NNs was implemented with 7 hidden layer neurons and the NN weights are initialized as uniformly distributed random numbers in the interval $[0.1, 0.3]$. The initial conditions of the system and the observer were selected as $x(t) = [0 \ 0]^T$, $\dot{x}(t) = [0 \ 0]^T$, and $\hat{x}(t) = \dot{\hat{x}}(t) = [0 \ 0]^T$, respectively.

The performance of the proposed OFB controller is compared with two controllers: a classical PID controller, and the discontinuous OFB controller in [1]. A standard backwards difference algorithm is used to numerically determine velocity from the encoder readings to implement the PID controller. Control gains for the discontinuous controller in [1] were selected as $K_1 = 0.2$, $K_2 = \text{diag}(410, 38)$, and control gains for the PID controller were selected as $K_d = \text{diag}(120, 30)$, $K_p = \text{diag}(750, 90)$, and $K_i = \text{diag}(650, 100)$. The tracking errors and control torques for all controllers are illustrated in Figs. 5-1 and 5-2, respectively. Table 5-1 shows the RMS errors and RMS torques at steady-state for all methods. The developed controller is shown to exhibit lower tracking errors with less control authority than the comparative controllers. Moreover, the DNN-based observer yields a better velocity estimation in comparison with the high frequency content results from a backwards difference method as depicted in Fig. 5-3. Hence, the experiments illustrate that using the velocity estimation from a DNN-based observer, which adaptively compensates for unknown uncertainties in the system, results in

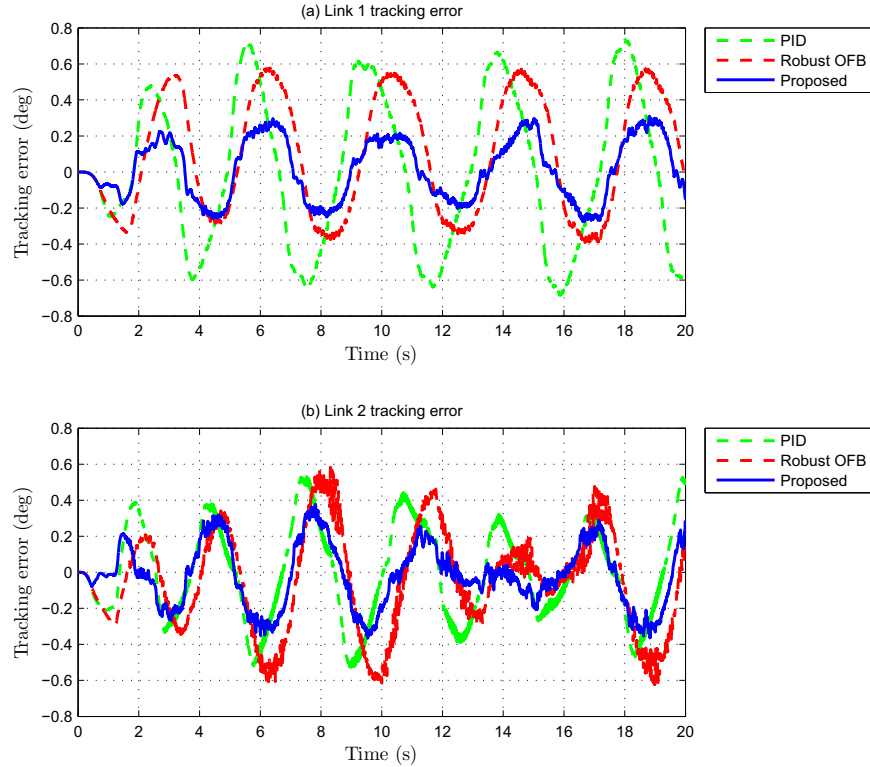


Figure 5-1. The tracking errors $e(t)$ of (a) Link 1 and (b) Link 2 using classical PID, robust discontinuous OFB controller [1], and proposed controller.

Table 5-1. Steady-state RMS errors and torques for each of the analyzed control designs.

	SSRMS Error 1	SSRMS Error 2	SSRMS Torque 1	SSRMS Torque 2
Classical PID	0.4538	0.2700	6.5805	2.4133
Robust OFB [1]	0.3552	0.2947	8.6509	1.2585
Proposed	0.1743	0.1740	6.3484	0.6944

improved control performance with lower frequency content in comparison to the compared methods.

5.7 Conclusion

A DNN observer-based OFB control of a class of second-order nonlinear uncertain systems is developed. The DNN-based observer works in conjunction with a dynamic filter to estimate the unmeasurable state. The DNN is updated on-line by weight update laws based on the estimation error, tracking error, and filter output. The controller is a combination of the NN feedforward term, and the estimated state feedback and sliding mode terms. Global asymptotic estimation of the unmeasurable state and global asymptotic tracking results are achieved,

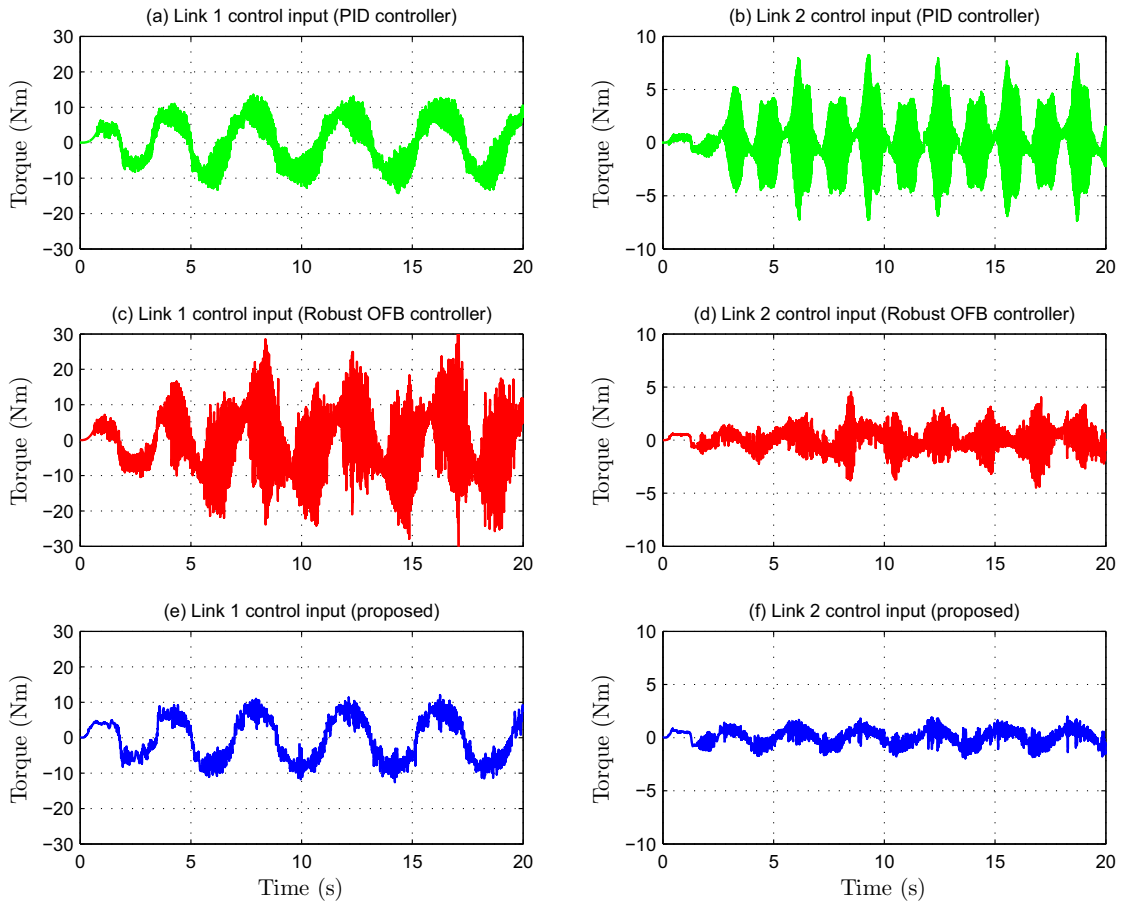


Figure 5-2. Control inputs for Link 1 and Link 2 using (a), (b) classical PID, (c), (d) robust discontinuous OFB controller [1], and (e), (f) the proposed controller.

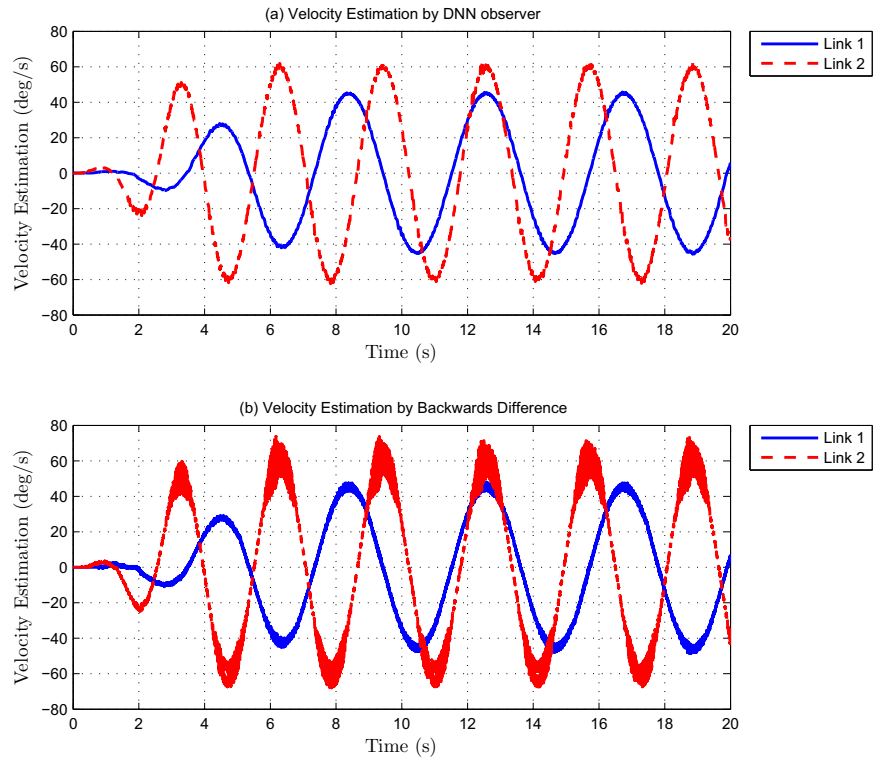


Figure 5-3. Velocity estimation $\dot{x}(t)$ using (a) DNN-based observer and (b) numerical backwards difference.

simultaneously. Results from an experiment using a two-link robot manipulator demonstrate the performance of the proposed OFB controller.

CHAPTER 6
OUTPUT FEEDBACK CONTROL FOR AN UNCERTAIN NONLINEAR SYSTEM WITH
SLOWLY VARYING INPUT DELAY

OFB control for a nonlinear system with time-varying actuator delay is a challenging problem because of both the need to compensate for the lack of the system state and the need to develop some form of prediction of the nonlinear dynamics. In this chapter, an OFB tracking controller is developed for a general second-order system with time-varying input delay, uncertainties, and additive bounded disturbances. The developed controller is a modified PD controller working in association with an integral component. The PD components are formulated using the difference between a desired trajectory and an estimated state acquired from a DNN based observer to compensate the inaccessibility of the true system state. The integral component is a predictor-like feedback term to compensate for the input delay. A stability analysis using Lyapunov-Krasovskii functionals is provided to prove UUB tracking and UUB estimation of the unavailable state. A simulation of a two-link robot manipulator is provided to illustrate the effectiveness of the proposed control strategy.

6.1 Dynamic System and Properties

Consider a control-affine second order nonlinear system of the form

$$\ddot{x} = f(x, \dot{x}) + G(x)u(t - \tau(t)) + d(t), \quad (6-1)$$

where $x(t) \in \mathbb{R}^n$ is a measurable output with a finite initial condition $x(0) = x_0$, $u(t - \tau(t)) \in \mathbb{R}^n$ represents a generalized delayed control input, where $\tau(t) \in \mathbb{R}$ is a non-negative time-varying delay, $f(x, \dot{x}) \in \mathbb{R}^n$, $G(x) \in \mathbb{R}^{n \times n}$ are unknown continuous functions, and $d(t) \in \mathbb{R}^n$ is an exogenous disturbance. The subsequent development is based on the assumptions that the state $x(t)$ is measurable, the time-varying input delay $\tau(t)$ is known, and the control input vector and its past values (i.e., $u(t - \theta) \forall \theta \in [0, \tau(t)]$) are measurable. Throughout the chapter, a time dependent delayed function is denoted as $\xi(t - \tau(t))$ or ξ_τ . Additionally, the following assumptions will be exploited.

Assumption 6.1. *The unknown function $f(x, \dot{x})$ is C^1 .*

Assumption 6.2. *The time delay is bounded such that $0 \leq \tau(t) \leq \varphi_1$, and $\|\dot{\tau}(t)\| < \frac{1}{3}$ where $\varphi_1 \in \mathbb{R}^+$ is a known constant.*

Based on the universal approximation property of MLNNs, the unknown function $f(x, \dot{x})$ in (6–1) can be replaced by a MLNN, and the system can be represented as

$$\ddot{x} = W^T \sigma(V_1^T x + V_2^T \dot{x}) + \varepsilon + Gu_\tau + d, \quad (6-2)$$

where $W \in \mathbb{R}^{N+1 \times n}$, $V_1, V_2 \in \mathbb{R}^{n \times N}$ are unknown ideal weight matrices of the MLNN having N hidden layer neurons, $\sigma(t) \triangleq \sigma(V_1^T x(t) + V_2^T \dot{x}(t)) \in \mathbb{R}^{N+1}$ is an activation function (sigmoid, hyperbolic tangent, etc.), and $\varepsilon(x, \dot{x}) \in \mathbb{R}^n$ is a function reconstruction error. Assumptions 5.3-5.6 will be also exploited in the DNN-based observer and controller development, and the stability analysis.

6.2 Estimation and Control Objectives

A contribution of this chapter is the development of a continuous DNN-based observer to estimate the unmeasurable state $\dot{x}(t)$ of the input-delayed system in (6–1). Based on this estimate, a continuous controller is designed so that the system state $x(t)$ tracks a desired time-varying trajectory $x_d(t) \in \mathbb{R}^n$, despite uncertainties and disturbances in the system. To quantify these objectives, an estimation error $\tilde{x}(t) \in \mathbb{R}^n$ and a tracking error $e(t) \in \mathbb{R}^n$ are defined as

$$\tilde{x} \triangleq x - \hat{x}, \quad (6-3)$$

$$e \triangleq x - x_d, \quad (6-4)$$

where $\hat{x}(t) \in \mathbb{R}^n$ is a state of the DNN observer which is introduced in the subsequent development. The desired trajectory $x_d(t)$ and its derivatives $x_d^{(i)}(t)$ ($i = 1, 2$), are assumed to exist and be bounded. To compensate for the lack of direct measurements of $\dot{x}(t)$, a filtered estimation error $r_{es}(t) \in \mathbb{R}^n$ and a filtered tracking error $r_{tr}(t) \in \mathbb{R}^n$ are defined as

$$r_{es} \triangleq \dot{\tilde{x}} + \alpha \tilde{x} + \eta, \quad (6-5)$$

$$r_{tr} \triangleq \dot{e} + \alpha e + Be_z + \eta, \quad (6-6)$$

where $\alpha \in \mathbb{R}^+$ is a positive constant gain, and $e_z(t) \in \mathbb{R}^n$ is an auxiliary time-delayed signal defined as

$$e_z \triangleq \int_{t-\tau(t)}^t u(\theta) d\theta. \quad (6-7)$$

The term $e_z(t)$ is a predictor-like term in sense that $e_z(t)$ transforms the input delayed system into an input delay free system (see the subsequent analysis). In (6-6), $B \in \mathbb{R}^{n \times n}$ is a known, symmetric, positive-definite, constant gain matrix that satisfies the following inequality

$$b_1 \leq \|B\| \leq b_2,$$

where $b_1, b_2 \in \mathbb{R}^+$ are known constants. The error between B and $G(x)$ is denoted by $\chi(x) \in \mathbb{R}^{n \times n}$, which is defined as

$$\chi \triangleq G - B, \quad (6-8)$$

and satisfies the following assumption

$$\|\chi\| \leq \bar{\chi}, \quad (6-9)$$

where $\bar{\chi} \in \mathbb{R}^+$ is a known constant. In (6-5) and (6-6), $\eta(t) \in \mathbb{R}^n$ is an output of the dynamic filter in (5-7). The filtered estimation error $r_{es}(t)$ and the filtered tracking error $r_{tr}(t)$ are not measurable since the expressions in (6-5) and (6-6) depend on $\dot{x}(t)$.

6.3 Robust DNN Observer Development

The following MLDNN architecture is proposed to observe the system in (6-1)

$$\ddot{\hat{x}} = \hat{W}^T \hat{\sigma} + Bu_\tau - (k + 3\alpha)\eta, \quad (6-10)$$

where $\begin{bmatrix} \hat{x}(t)^T & \dot{\hat{x}}(t)^T \end{bmatrix}^T \in \mathbb{R}^{2n}$ are the states of the DNN observer, $\hat{W}(t) \in \mathbb{R}^{N+1 \times n}$, $\hat{V}_1(t)$, $\hat{V}_2(t) \in \mathbb{R}^{n \times N}$ are weight estimates, and $\hat{\sigma}(t) \triangleq \sigma(\hat{V}_1(t)^T \hat{x}(t) + \hat{V}_2(t)^T \dot{\hat{x}}(t)) \in \mathbb{R}^{N+1}$.

The weight update laws for the DNN in (6–10) are developed based on the subsequent stability analysis as

$$\begin{aligned}\dot{\hat{W}} &= \Gamma_w \text{proj}[\hat{\sigma}(\alpha\tilde{x} + \eta)^T], \\ \dot{\hat{V}}_1 &= \Gamma_{v1} \text{proj}[\hat{x}(\alpha\tilde{x} + \eta)^T \hat{W}^T \hat{\sigma}'], \\ \dot{\hat{V}}_2 &= \Gamma_{v2} \text{proj}[\hat{x}(\alpha\tilde{x} + \eta)^T \hat{W}^T \hat{\sigma}'],\end{aligned}\tag{6–11}$$

where $\Gamma_w \in \mathbb{R}^{(N+1) \times (N+1)}$, $\Gamma_{v1}, \Gamma_{v2} \in \mathbb{R}^{n \times n}$ are constant symmetric positive-definite adaptation gains, the term $\hat{\sigma}'(t)$ is defined as $\hat{\sigma}' \triangleq d\sigma(\zeta)/d\zeta|_{\zeta=\hat{V}_1^T \hat{x} + \hat{V}_2^T \hat{x}}$, and $\text{proj}(\cdot)$ is a smooth projection operator (cf. [88], [89]) used to guarantee that the weight estimates $\hat{W}(t), \hat{V}_1(t), \hat{V}_2(t)$ remain bounded.

To facilitate the subsequent analysis, (5–7) and (6–5) can be used to express the time derivative of $\eta(t)$ as

$$\dot{\eta} = -(k + \alpha)r_{es} - \alpha\eta + \tilde{x} + e - v.\tag{6–12}$$

The closed-loop dynamics of the filtered estimation error in (6–5) can be determined by using (6–2), (6–3), (6–5), (6–8), (6–10) and (6–12) as

$$\begin{aligned}\dot{r}_{es} &= W^T \sigma - \hat{W}^T \hat{\sigma} + \varepsilon + d + \chi u_\tau + (k + 3\alpha)\eta + \\ &+ \alpha(r_{es} - \alpha\tilde{x} - \eta) - (k + \alpha)r_{es} - \alpha\eta + \tilde{x} + e - v.\end{aligned}\tag{6–13}$$

After some algebraic manipulation, the closed-loop dynamics of the filtered estimation error $r_{es}(t)$ can be further expressed as

$$\dot{r}_{es} = N_1 + N_2 - kr_{es} + \chi u_\tau + (k + \alpha)\eta - \tilde{x},\tag{6–14}$$

where the auxiliary function $N_1(\hat{x}, \hat{x}, \hat{W}, \hat{V}_1, \hat{V}_2) \in \mathbb{R}^n$ is

$$N_1 \triangleq \tilde{W}^T \hat{\sigma} + \hat{W}^T \hat{\sigma}'[\tilde{V}_1^T \hat{x} + \tilde{V}_2^T \hat{x}],\tag{6–15}$$

and $N_2(e, \tilde{x}, v, r_{es}, r_{tr}, e_z, \hat{W}, \hat{V}_1, \hat{V}_2, t) \in \mathbb{R}^n$ is

$$\begin{aligned} N_2 \triangleq & W^T (\sigma - \sigma(V_1^T \hat{x} + V_2^T \hat{\dot{x}})) + \tilde{W}^T \hat{\sigma}'[\tilde{V}_1^T \hat{x} + \tilde{V}_2^T \hat{\dot{x}}] \\ & + W^T O(\tilde{V}_1^T \hat{x} + \tilde{V}_2^T \hat{\dot{x}})^2 - (\alpha^2 - 2)\tilde{x} - v + e + \varepsilon + d, \end{aligned} \quad (6-16)$$

where $\tilde{W}(t) \triangleq W - \hat{W}(t) \in \mathbb{R}^{N+1 \times n}$, $\tilde{V}_1(t) \triangleq V_1 - \hat{V}_1(t) \in \mathbb{R}^{n \times N}$, $\tilde{V}_2(t) \triangleq V_2 - \hat{V}_2(t) \in \mathbb{R}^{n \times N}$ are estimate mismatches for the ideal NN weights, and $O(\tilde{V}_1^T \hat{x} + \tilde{V}_2^T \hat{\dot{x}})^2 \in \mathbb{R}^{N+1}$ represents a higher order term in the Taylor series of the vector function $\sigma(V_1^T \hat{x}(t) + V_2^T \hat{\dot{x}}(t))$ in the neighborhood of $\hat{V}_1^T \hat{x} + \hat{V}_2^T \hat{\dot{x}}$ as

$$\sigma(V_1^T \hat{x} + V_2^T \hat{\dot{x}}) = \hat{\sigma} + \hat{\sigma}'[\tilde{V}_1^T \hat{x} + \tilde{V}_2^T \hat{\dot{x}}] + O(\tilde{V}_1^T \hat{x} + \tilde{V}_2^T \hat{\dot{x}})^2. \quad (6-17)$$

Using (6-3)-(6-6), Assumptions 5.3-5.6, the $proj(\cdot)$ algorithm in (6-11), the Taylor series expansion in (6-17) and the Mean Value Theorem, the auxiliary functions $N_1(\cdot)$ in (6-15) and $N_2(\cdot)$ in (6-16) can be upper-bounded as

$$\begin{aligned} \|N_1\| &\leq \zeta_1 \|z\| + \zeta_2, \\ \|N_2\| &\leq \zeta_3 \|z\| + \zeta_4, \end{aligned} \quad (6-18)$$

where $\zeta_i \in \mathbb{R}^+$, $i = 1, \dots, 4$ are computable positive constants, and $z(\tilde{x}, e, r_{es}, r_{tr}, v, \eta, e_z) \in \mathbb{R}^{7n}$ is defined as

$$z \triangleq [\tilde{x}^T \ e^T \ r_{es}^T \ r_{tr}^T \ v^T \ \eta^T \ e_z^T]^T. \quad (6-19)$$

6.4 Robust Tracking Control Development

The control objective is to force the system state to track the desired trajectory $x_d(t)$, despite the uncertainties, disturbances, and time-delays in the system. Quantitatively, this objective is to regulate the tracking error $e(t)$ to zero. Using (6-2), (6-4), (6-6)-(6-8) and (6-12), the open-loop dynamics of the filtered tracking error in (6-6) can be expressed as

$$\begin{aligned} \dot{r}_{tr} = & W^T \sigma + Gu_\tau + \varepsilon + d - \ddot{x}_d + \alpha(r_{tr} - \alpha e - \eta - Be_z) \\ & + B\dot{e}_z - (k + \alpha)r_{es} - \alpha\eta + \tilde{x} + e - v. \end{aligned} \quad (6-20)$$

Based on the error system formulation in (6-7), the time derivative of $e_z(t)$ can be calculated as

$$\dot{e}_z = u - u_\tau + u_\tau \dot{\tau}. \quad (6-21)$$

Hence, the open-loop error system in (6-20) contains a delay-free control input. Based on (6-20) and the subsequent stability analysis, the control input is designed as

$$u(t) = -B^{-1}(k + \alpha)(\dot{e} + \alpha\hat{e} + Be_z), \quad (6-22)$$

where the tracking error estimate $\hat{e}(t) \in \mathbb{R}^n$ is defined as

$$\hat{e} \triangleq \hat{x} - x_d.$$

Based on the fact that the estimated states $\hat{x}(t)$, $\dot{\hat{x}}(t)$ are measurable, the tracking error estimates $\hat{e}(t)$ and its derivative $\dot{\hat{e}}(t)$ are measurable; moreover, the filtered tracking error $r_{tr}(t)$ is related to the filtered estimation error $r_{es}(t)$ via the tracking error estimate $\hat{e}(t)$ as

$$r_{tr} = r_{es} + \dot{\hat{e}} + \alpha\hat{e} + Be_z. \quad (6-23)$$

The relation in (6-23) shows that eventhough both the filtered tracking error $r_{tr}(t)$ and the filtered estimation error $r_{es}(t)$ are unmeasurable, the difference between $r_{tr}(t)$ and $r_{es}(t)$ is measurable. The DNN observer provides negative feedback of the filtered estimation error $r_{es}(t)$ to guarantee the convergence of the estimated states, and the controller in (6-22) compensates for the difference between $r_{es}(t)$ and $r_{tr}(t)$ to obtain the negative feedback of the filtered tracking error $r_{tr}(t)$; hence the convergence of the tracking error can be achieved.

Using (6-20)-(6-23), the closed-loop error system becomes

$$\dot{r}_{tr} = N_3 - kr_{tr} + \chi u_\tau + Bu_\tau \dot{\tau} - e, \quad (6-24)$$

where the auxiliary function $N_3(e, \tilde{x}, \eta, v, e_z, r_{tr}, t) \in \mathbb{R}^n$ is defined

$$N_3 \triangleq W^T \sigma - (\alpha^2 - 2)e - v + \tilde{x} - 2\alpha\eta - \alpha Be_z + \varepsilon + d - \ddot{x}_d. \quad (6-25)$$

Similarly, using (6-4), (6-6), Assumptions 5.3-5.6, the condition (6-9) and the $proj(\cdot)$ algorithm in (6-11), the auxiliary function $N_3(\cdot)$ in (6-25) can be upper-bounded as

$$\|N_3\| \leq \zeta_5 \|z\| + \zeta_6, \quad (6-26)$$

where $\zeta_5, \zeta_6 \in \mathbb{R}^+$ are computable positive constants.

To facilitate the subsequent stability analysis, let $y(z, P, Q, R) \in \mathbb{R}^{7n+3}$ be defined as

$$y \triangleq [z^T \quad \sqrt{P} \quad \sqrt{Q} \quad \sqrt{R}]^T, \quad (6-27)$$

where $P(u, t, \tau), Q(r_{es}, r_{tr}, t, \tau, \hat{\tau}) \in \mathbb{R}$ denote positive-definite LK functionals defined as

$$P \triangleq \omega \int_{t-\tau(t)}^t \left(\int_s^t \|u(\theta)\|^2 d\theta \right) ds, \quad (6-28)$$

$$Q \triangleq \frac{(6\bar{\chi} + b_1)(k + \alpha)}{4b_1} \int_{t-\tau(t)}^t \|r_{es}(\theta) - r_{tr}(\theta)\|^2 d\theta, \quad (6-29)$$

and $\omega \in \mathbb{R}^+$ is a known constant. Additionally, the auxiliary function $R(\tilde{W}, \tilde{V}_1, \tilde{V}_2) \in \mathbb{R}$ in (6-27) is defined as

$$R \triangleq \frac{1}{2} tr(\tilde{W}^T \Gamma_w^{-1} \tilde{W}) + \frac{1}{2} tr(\tilde{V}_1^T \Gamma_{v1}^{-1} \tilde{V}_1) + \frac{1}{2} tr(\tilde{V}_2^T \Gamma_{v2}^{-1} \tilde{V}_2), \quad (6-30)$$

where $tr(\cdot)$ denotes the trace of a matrix. Since the gains $\Gamma_w, \Gamma_{v1}, \Gamma_{v2}$ are symmetric, positive-definite matrices, $R(\cdot) \geq 0$. Using Assumption 5.4 and the $proj(\cdot)$ algorithm in (6-11), $R(\cdot)$ can be upper bounded as

$$R(t) \leq \bar{R}, \quad (6-31)$$

where $\bar{R} \in \mathbb{R}^+$ is a known constant. Moreover, the update laws in (6-11) are designed such that

$$\dot{R} + (\alpha \bar{x} + \eta)^T N_1 = 0. \quad (6-32)$$

6.5 Lyapunov Stability Analysis for DNN-based Observation and Control

Theorem 6.1. *The DNN-based observer and controller proposed in (6-10) and (6-22), respectively, along with the weight update laws in (6-11) ensure uniformly ultimately bounded*

estimation and tracking in sense that

$$\begin{aligned}\|\dot{\tilde{x}}(t)\| &\leq \varepsilon_1 \exp(-\varepsilon_2 t) + \varepsilon_3, \\ \|e(t)\| &\leq \varepsilon_4 \exp(-\varepsilon_5 t) + \varepsilon_6,\end{aligned}\tag{6-33}$$

where $\varepsilon_i \in \mathbb{R}^+$, $i = 1, 2, \dots, 6$ are known constants, provided $\tau(t)$ and $\dot{\tau}(t)$ are sufficiently small, the approximation matrix B are selected sufficiently close to $G(x)$, and the following sufficient conditions are satisfied

$$\begin{aligned}\omega &> \sup_{\tau, \dot{\tau}} \left(\frac{2\tau}{(1-\dot{\tau})} \left(\frac{1}{2\psi^2} + 2\zeta_1 \zeta_7 \right) \right), \quad \alpha > \frac{b_2^2 \psi^2}{2} + 2\zeta_1 \zeta_7, \\ k_1 &> \sup_{\tau, \dot{\tau}} \left((k + \alpha) \left(\frac{|\dot{\tau}| + 1}{2} + \frac{7\bar{\chi}}{2b_1} + 2\omega\tau(k + \alpha) \right) \right) + 2\zeta_1 \zeta_7,\end{aligned}\tag{6-34}$$

where $\psi \in \mathbb{R}^+$ is a known gain constant, and $k_1 \in \mathbb{R}^+$ is introduced in (6-45).

Proof. Consider the Lyapunov candidate function $V_L(y, t) : \mathcal{D} \times (0, \infty) \rightarrow \mathbb{R}$, which is a Lipschitz continuous positive-definite functional defined as

$$V_L \triangleq \frac{1}{2} \tilde{x}^T \tilde{x} + \frac{1}{2} e^T e + \frac{1}{2} v^T v + \frac{1}{2} \eta^T \eta + \frac{1}{2} r_{es}^T r_{es} + \frac{1}{2} r_{tr}^T r_{tr} + P + Q + R,\tag{6-35}$$

which satisfies the following inequalities:

$$U_1(y) \leq V_L(y, t) \leq U_2(y).\tag{6-36}$$

In (6-36), $U_1(y), U_2(y) \in \mathbb{R}$ are continuous positive-definite functions defined as

$$U_1(y) \triangleq \frac{1}{2} \|y\|^2, \quad U_2(y) \triangleq \|y\|^2.$$

Using (6-5)-(6-7), (6-12), (6-14), and (6-24), and by applying the Leibniz Rule to determine the time derivative of (6-28) and (6-29), the time derivative of (6-35) can be calculated as

$$\begin{aligned}
\dot{V}_L &= \tilde{x}^T (r_{es} - \alpha \tilde{x} - \eta) + e^T (r_{tr} - \alpha e - \eta - B e_z) + v^T (\eta - \alpha v) \\
&+ \eta^T (-(k + \alpha) r_{es} - \alpha \eta + \tilde{x} + e - v) + r_{tr}^T (N_3 - k r_{tr} + \chi u_\tau + B u_\tau \dot{\tau} - e) \\
&+ r_{es}^T (N_1 + N_2 - k r_{es} + \chi u_\tau + (k + \alpha) \eta - \tilde{x}) + \dot{R} + \omega \tau \|u\|^2 \\
&- \omega (1 - \dot{\tau}) \int_{t-\tau(t)}^t \|u(\theta)\|^2 d\theta + \frac{(6\bar{\chi} + b_1)(k + \alpha)}{4b_1} \|r_{es} - r_{tr}\|^2 \\
&- (1 - \dot{\tau}) \frac{(6\bar{\chi} + b_1)(k + \alpha)}{4b_1} \|r_{es_\tau} - r_{tr_\tau}\|^2. \tag{6-37}
\end{aligned}$$

Using (6-32), canceling common terms, and utilizing the relationship between the controller $u(t)$ with the unmeasurable errors $r_{es}(t)$, $r_{tr}(t)$ as

$$u(t) = (k + \alpha) B^{-1} (r_{es} - r_{tr}), \tag{6-38}$$

the expression in (6-37) can be expanded and regrouped as

$$\begin{aligned}
\dot{V}_L &= -\alpha \tilde{x}^T \tilde{x} - \alpha e^T e - e^T B e_z - \alpha v^T v - \alpha \eta^T \eta - k r_{es}^T r_{es} - k r_{tr}^T r_{tr} + \dot{\tilde{x}}^T N_1 \\
&+ r_{es}^T N_2 + (k + \alpha) (r_{es} + r_{tr})^T \chi B^{-1} (r_{es_\tau} - r_{tr_\tau}) + \dot{\tau} (k + \alpha) r_{tr}^T (r_{es_\tau} - r_{tr_\tau}) \\
&+ r_{tr}^T N_3 + \omega \tau (k + \alpha)^2 \|r_{es} - r_{tr}\|^2 - \omega (1 - \dot{\tau}) \int_{t-\tau(t)}^t \|u(\theta)\|^2 d\theta \\
&+ \frac{(6\bar{\chi} + b_1)(k + \alpha)}{4b_1} \|r_{es} - r_{tr}\|^2 - (1 - \dot{\tau}) \frac{(6\bar{\chi} + b_1)(k + \alpha)}{4b_1} \|r_{es_\tau} - r_{tr_\tau}\|^2. \tag{6-39}
\end{aligned}$$

Young's inequality can be used to upper bound select terms in (6-39) as

$$\begin{aligned}
\|e\| \|B\| \|e_z\| &\leq \frac{b_2^2 \psi^2}{2} \|e\|^2 + \frac{1}{2\psi^2} \|e_z\|^2, \\
\|r_{tr}\| \|r_{es_\tau} - r_{tr_\tau}\| &\leq \frac{1}{2} \|r_{tr}\|^2 + \frac{1}{2} \|r_{es_\tau} - r_{tr_\tau}\|^2, \\
\|r_{es} - r_{tr}\|^2 &\leq 2 \|r_{tr}\|^2 + 2 \|r_{es}\|^2.
\end{aligned} \tag{6-40}$$

Using (6–38), (6–40), and Assumption 6.2, (6–39) can be upper bounded as

$$\begin{aligned}
\dot{V}_L \leq & -\alpha \|\tilde{x}\|^2 - \left(\alpha - \frac{b_2^2 \psi^2}{2} \right) \|e\|^2 + \frac{1}{2\psi^2} \|e_z\|^2 - \alpha \|v\|^2 - \alpha \|\eta\|^2 \\
& - k \|r_{es}\|^2 - k \|r_{tr}\|^2 + \|\dot{\tilde{x}}\| \|N_1\| + \|r_{es}\| \|N_2\| + \|r_{tr}\| \|N_3\| \\
& + \frac{\bar{\chi}(k+\alpha)}{2b_1} \left(\|r_{es}\|^2 + \|r_{tr}\|^2 + 2 \|r_{es\tau} - r_{tr\tau}\|^2 \right) \\
& + \frac{|\dot{\tau}|(k+\alpha)}{2} \left(\|r_{tr}\|^2 + \|r_{es\tau} - r_{tr\tau}\|^2 \right) - \omega(1-\dot{\tau}) \int_{t-\tau(t)}^t \|u(\theta)\|^2 d\theta \quad (6-41) \\
& + \left(2\omega\tau(k+\alpha)^2 + \frac{(6\bar{\chi}+b_1)(k+\alpha)}{2b_1} \right) \left(\|r_{tr}\|^2 + \|r_{es}\|^2 \right) \\
& - (1-\dot{\tau})(k+\alpha) \left(\frac{3\bar{\chi}}{2b_1} + \frac{1}{4} \right) \|r_{es\tau} - r_{tr\tau}\|^2.
\end{aligned}$$

Utilizing Assumption 6.2 yields

$$\begin{aligned}
\frac{|\dot{\tau}|(k+\alpha)}{2} & \leq \frac{(1-\dot{\tau})(k+\alpha)}{4}, \\
\frac{\bar{\chi}(k+\alpha)}{b_1} & \leq \frac{3\bar{\chi}(k+\alpha)(1-\dot{\tau})}{2b_1}, \quad (6-42)
\end{aligned}$$

and using the Cauchy-Schwartz inequality, and (6–7), the integral term in (6–41) can be upper bounded as

$$-\omega(1-\dot{\tau}) \int_{t-\tau}^t \|u(\theta)\|^2 d\theta \leq -\frac{\omega(1-\dot{\tau})}{2\tau} \|e_z\|^2 - \frac{\omega(1-\dot{\tau})}{2} \int_{t-\tau}^t \|u(\theta)\|^2 d\theta. \quad (6-43)$$

Utilizing (6–18), (6–26), (6–42), (6–43), and the fact that $\|\dot{\tilde{x}}\| \leq \zeta_7 \|z\|$, where $\zeta_7 \in \mathbb{R}^+$ is defined as $\zeta_7 \triangleq \max(1, \alpha)$, the inequality in (6–41) can be expressed as

$$\begin{aligned}
\dot{V}_L \leq & -\alpha \|\tilde{x}\|^2 - \left(\alpha - \frac{b_2^2 \psi^2}{2} \right) \|e\|^2 - \left(\frac{\omega(1-\dot{\tau})}{2\tau} - \frac{1}{2\psi^2} \right) \|e_z\|^2 - \alpha \|v\|^2 \\
& - \alpha \|\eta\|^2 - k \|r_{es}\|^2 - k \|r_{tr}\|^2 + \zeta_7 (\zeta_1 \|z\| + \zeta_2) \|z\| + (\zeta_3 \|z\| + \zeta_4) \|r_{es}\| \\
& + (\zeta_5 \|z\| + \zeta_6) \|r_{tr}\| + \frac{|\dot{\tau}|(k+\alpha)}{2} \|r_{tr}\|^2 - \frac{\omega(1-\dot{\tau})}{2} \int_{t-\tau(t)}^t \|u(\theta)\|^2 d\theta \quad (6-44) \\
& + \left(2\omega\tau(k+\alpha)^2 + \frac{(7\bar{\chi}+b_1)(k+\alpha)}{2b_1} \right) \left(\|r_{tr}\|^2 + \|r_{es}\|^2 \right).
\end{aligned}$$

Let k , introduced in (5–7), be defined as

$$k \triangleq k_1 + k_2 + k_3, \quad (6-45)$$

where $k_1, k_2, k_3 \in \mathbb{R}^+$ are positive control gains, and let the auxiliary constants $\beta, \lambda \in \mathbb{R}^+$ be defined as

$$\begin{aligned} \beta &\triangleq \frac{1}{2} \min \left[\alpha - \frac{b_2^2 \psi^2}{2}, \inf_{\tau, \dot{\tau}} \left(\frac{\omega(1-\dot{\tau})}{2\tau} - \frac{1}{2\psi^2} \right), \right. \\ &\quad \left. \inf_{\tau, \dot{\tau}} \left(k_1 - (k + \alpha) \left(\frac{|\dot{\tau}| + 1}{2} + \frac{7\bar{\chi}}{2b_1} + 2\omega\tau(k + \alpha) \right) \right) \right], \\ \lambda &\triangleq \frac{(\zeta_4^2 + \zeta_6^2)}{4k_3} + \frac{\zeta_2^2 \zeta_7^2}{4\beta}, \end{aligned} \quad (6-46)$$

where $\zeta_2, \zeta_4, \zeta_6$ are introduced in (6–18) and (6–26). Using (6–45), (6–46), and completing the squares, the expression in (6–44) can be further upper bounded as

$$\begin{aligned} \dot{V}_L &\leq -2\beta \|z\|^2 + \zeta_7 (\zeta_1 \|z\| + \zeta_2) \|z\| + \frac{(\zeta_3^2 + \zeta_5^2) \|z\|^2}{4k_2} + \frac{(\zeta_4^2 + \zeta_6^2)}{4k_3} \\ &\quad - \frac{\omega(1-\dot{\tau})}{2} \int_{t-\tau(t)}^t \|u(\theta)\|^2 d\theta. \end{aligned} \quad (6-47)$$

Using the inequality [63]

$$\int_{t-\tau(t)}^t \left(\int_s^t \|u(\theta)\|^2 d\theta \right) ds \leq \tau \sup_{s \in [t-\tau, t]} \left[\int_s^t \|u(\theta)\|^2 d\theta \right] = \tau \int_{t-\tau(t)}^t \|u(\theta)\|^2 d\theta,$$

and completing the squares, the expression in (6–47) can be upper bounded as

$$\begin{aligned} \dot{V}_L &\leq - \left(\beta - \frac{(\zeta_3^2 + \zeta_5^2)}{4k_2} - \zeta_1 \zeta_7 \right) \|z\|^2 + \lambda \\ &\quad - \frac{\omega(1-\dot{\tau})}{4} \int_{t-\tau(t)}^t \|u(\theta)\|^2 d\theta - \frac{\omega(1-\dot{\tau})}{4\tau} \int_{t-\tau(t)}^t \left(\int_s^t \|u(\theta)\|^2 d\theta \right) ds. \end{aligned} \quad (6-48)$$

By further utilizing (6–28)-(6–31) and (6–38), the inequality in (6–48) can be written as

$$\begin{aligned} \dot{V}_L &\leq - \left(\beta - \frac{(\zeta_3^2 + \zeta_5^2)}{4k_2} - \zeta_1 \zeta_7 \right) \|z\|^2 + \lambda - R + \bar{R} - \frac{\omega(1-\dot{\tau})(k + \alpha)^2}{4b_2^2} Q - \frac{(1-\dot{\tau})}{4\tau} P \\ &\leq -\beta_2 \|y\|^2 + \lambda + \bar{R}, \end{aligned} \quad (6-49)$$

where $\beta_2 \in \mathbb{R}^+$ is defined as

$$\beta_2 \triangleq \min \left[\left(\beta - \frac{(\zeta_3^2 + \zeta_5^2)}{4k_2} - \zeta_1 \zeta_7 \right), \inf_{\tau, \dot{\tau}} \left(\frac{\omega(1-\dot{\tau})(k+\alpha)^2}{4b_2^2} \right), \inf_{\tau, \dot{\tau}} \left(\frac{(1-\dot{\tau})}{4\tau} \right), 1 \right].$$

Using (6-36), the inequality in (6-49) can be written as

$$\dot{V}_L \leq -\beta_2 V_L + \lambda + \bar{R}, \quad (6-50)$$

where the linear differential inequality in (6-50) can be solved as

$$V_L(y, t) \leq e^{-\beta_2 t} V_L(0) + \beta_2^{-1} (\lambda + \bar{R}) [1 - e^{-\beta_2 t}], \quad \forall t \geq 0. \quad (6-51)$$

Based on (6-35) and (6-51), it can be concluded that $e(t), \tilde{x}(t), r_{es}(t), r_{tr}(t), \eta(t), v(t) \in \mathcal{L}_\infty$, hence using the definition of $r_{es}(t)$ in (6-5) and the relation between $u(t), r_{es}(t)$ and $r_{tr}(t)$ in (6-38), $\dot{\tilde{x}}(t), u(t) \in \mathcal{L}_\infty$. \square

6.6 Simulation Results

The following dynamics of a two link robot manipulator are considered for the simulations:

$$M(x)\ddot{x} + V_m(x, \dot{x})\dot{x} + F_d\dot{x} + \tau_d(t) = u_\tau(t), \quad (6-52)$$

where $x = \begin{bmatrix} x_1 & x_2 \end{bmatrix}^T$ are the angular positions (*rad*) and $\dot{x} = \begin{bmatrix} \dot{x}_1 & \dot{x}_2 \end{bmatrix}^T$ are the angular velocities (*rad/s*) of the two links, respectively, $M(x)$ is the inertia matrix and $V_m(x, \dot{x})$ is the centripetal-Coriolis matrix, defined as

$$M = \begin{bmatrix} p_1 + 2p_3c_2 & p_2 + p_3c_2 \\ p_2 + p_3c_2 & p_2 \end{bmatrix}$$

$$V_m = \begin{bmatrix} -p_3s_2\dot{x}_2 & -p_3s_2(\dot{x}_1 + \dot{x}_2) \\ p_3s_2\dot{x}_1 & 0 \end{bmatrix},$$

where $p_1 = 3.473 \text{ kg} \cdot \text{m}^2$, $p_2 = 0.196 \text{ kg} \cdot \text{m}^2$, $p_3 = 0.242 \text{ kg} \cdot \text{m}^2$, $c_2 = \cos(x_2)$, $s_2 = \sin(x_2)$, and $F_d = \text{diag} \{5.3, 1.1\} \text{ Nm} \cdot \text{sec}$ denotes friction coefficients. An additive exogenous disturbance is applied as $\tau_d(t) = [0.2\sin(\frac{t}{2}) \ 0.1\sin(\frac{t}{4})]^T$. The desired trajectories for Links 1 and 2 for all

simulations are selected as

$$\begin{aligned}x_{d1}(t) &= 40\sin(1.5t) \left(1 - e^{-0.01t^3}\right) \text{ deg}, \\x_{d2}(t) &= 20\sin(1.5t) \left(1 - e^{-0.01t^3}\right) \text{ deg}.\end{aligned}$$

The initial conditions of the system and the observer are chosen as $x(t) = [0 \ 0]^T$, $\dot{x}(t) = [0 \ 0]^T$ and $\hat{x}(t) = \dot{\hat{x}}(t) = [0 \ 0]^T$, respectively. The controller in (6-22) assumes that the inertia matrix $M(x)$ is unknown, hence, a best guess estimate of the inertia matrix is selected as

$$B = \begin{bmatrix} 3.5 & 0.2 \\ 0.2 & 0.2 \end{bmatrix}^{-1}.$$

To illustrate performance of the developed method, simulations are executed using various time-varying delays. The time delays are selected as sinusoidal functions with increasing magnitudes, increasing varying speeds and increasing displacement offsets. For each case, Link 1 and Link 2 RMS tracking errors and RMS estimation errors are shown in Table 6-1, respectively. The results clearly show that the system performance is better with small and slowly varying time-delays.

In the theoretical analysis, the time-delay is assumed to be exactly known. However, to examine the robustness of the developed controller with respect to the time-delay parameters, the input delay entering the plant is varied from the delay used in the controller feedback.

The feedback delay of the controller is kept as the sinusoid function with a offset of 10 ms as $\tau(t) = 2\sin\left(\frac{t}{10}\right) + 10 \text{ ms}$. Table 6-2 presents simulation results where magnitudes and/or offsets of plant delays are varied from the corresponding parameters of the controller delay. The results suggest that the controller is robust to variances in delay magnitude and offset. However, the smaller variances result in better performance. Figure 6-1 illustrates the time-delay, tracking, and estimation errors and control torques associated with the +10% magnitude and +10% offset variance case. The developed approach has been proven for the exact knowledge of the time delay, but the simulation results also illustrate some robustness with regard to uncertainties in

Table 6-1. Link1 and Link 2 RMS tracking errors and RMS estimation errors.

Time-Delay $\tau(t)$ (ms)	RMS Tracking (deg)		RMS Estimation (deg/s)	
	Link1	Link2	Link 1	Link2
$2\sin\left(\frac{t}{10}\right) + 5$	0.1346	0.1820	0.0366	0.1257
$2\sin\left(\frac{t}{10}\right) + 10$	0.2278	0.3024	0.0491	0.2050
$5\sin\left(\frac{t}{2}\right) + 10$	0.2351	0.3463	0.0546	0.2350
$5\sin\left(\frac{t}{2}\right) + 20$	0.9134	0.9350	0.2097	0.6255

Table 6-2. RMS errors for cases of uncertainty in time-varying delay seen by the plant as compared to the delay of the controller.

Time-Delay Variance in Plant	RMS Tracking (deg)		RMS Estimation (deg/s)	
	Link1	Link2	Link 1	Link2
-30% magnitude	0.2237	0.2567	0.0470	0.1722
-10% magnitude	0.2278	0.2710	0.0491	0.1818
0% magnitude	0.2278	0.3024	0.0491	0.2050
10% magnitude	0.2322	0.3040	0.0516	0.2053
30% magnitude	0.2342	0.3119	0.0531	0.2105
10% offset	0.2429	0.3489	0.0577	0.2350
30% offset	0.2783	0.4815	0.0705	0.3288
10% magnitude, 10% offset	0.2641	0.3023	0.0626	0.2021

the time delay. Future studies will consider the development of OFB controllers for uncertain nonlinear systems with unknown time-varying input delays.

6.7 Conclusion

A continuous OFB controller is developed for uncertain second-order nonlinear systems affected by time-varying input delays and additive bounded disturbances. The delay is assumed to be bounded and slowly varying. A DNN-based observer works in junction with the controller to provide an estimate of the unmeasurable state. A Lyapunov-based stability analysis utilizing LK functionals is used to prove simultaneously UUB estimation of the unmeasurable state and UUB tracking in the presence of model uncertainty, disturbances and time delays. Numerical simulations demonstrate the performance of the proposed method.

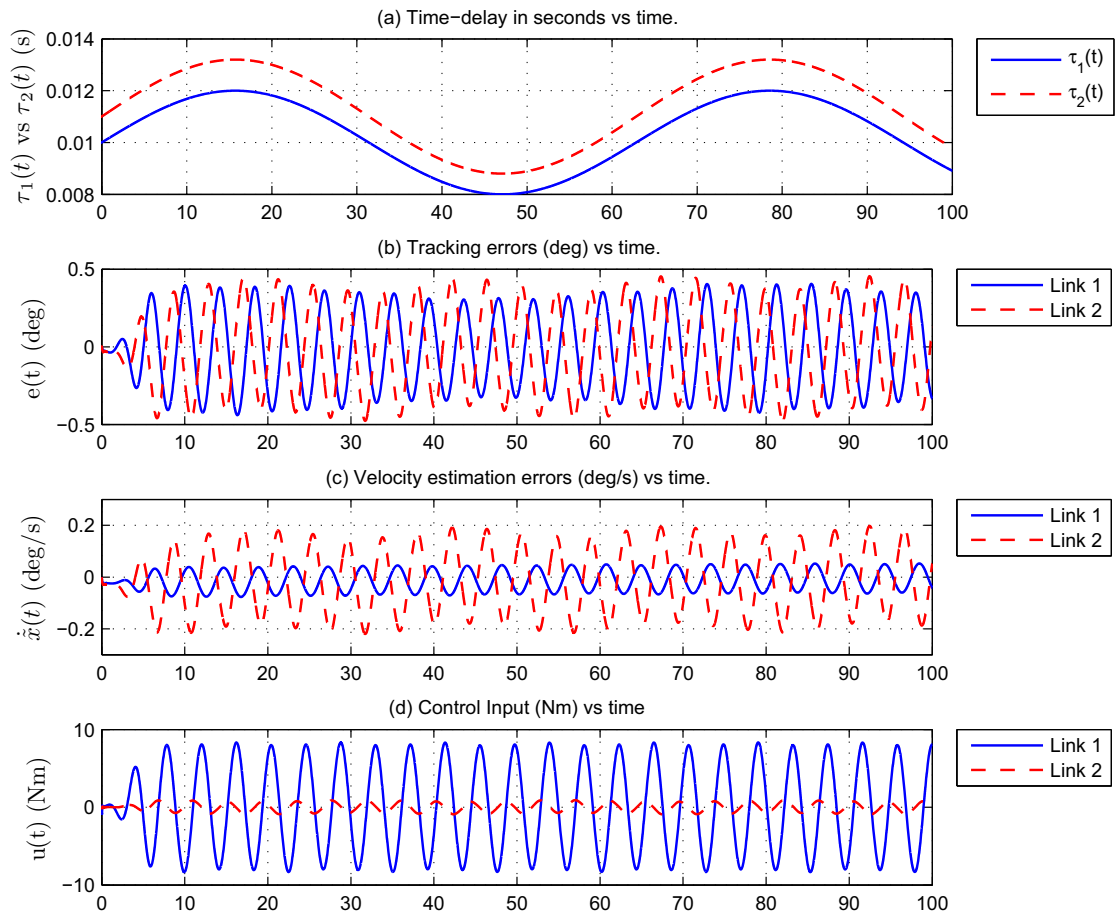


Figure 6-1. Simulation results with 10% magnitude and 10% offset variance in time-delay

CHAPTER 7 CONCLUSION AND FUTURE WORKS

This chapter concludes the dissertation by discussing the main contributions developed in each chapter. Limitations and implementation issues of the work are discussed to open possible future research directions.

7.1 Dissertation Summary

This work focuses on various applications of DNNs to control continuous-time nonlinear systems. The universal approximation property of DNNs, equipped with the ability to approximate dynamic systems, enable new opportunities to embed DNNs in control structures. The structural design and update laws for DNNs depend on each particular application. In Chapter 3, a DNN is designed as an identifier, but in Chapters 4-6, an observer design based on DNNs has been used. All DNNs are trained online to approximate system uncertainties by weight update laws developed based on the stability analysis. For disturbance rejection purposes, DNNs can be modified with the addition of some pure robust terms. Identification/estimation and tracking control objectives are considered in each chapter.

The focus of Chapter 3 is to develop an identification based adaptive tracking controller for a class of continuous-time uncertain nonlinear systems with additive bounded disturbances. This work overcomes the limitation of previous works where controllers are either discrete-time and/or yield a UUB stability result due to the presence of disturbances and unknown approximation errors. A DNN is used to approximate the nonlinear uncertain dynamics, a sliding mode included in the DNN structure accounts for the disturbances and reconstruction errors to obtain an asymptotic identification result. In addition, the DNN identifier is trained online. The asymptotic tracking result is made possible by combining a continuous RISE feedback term with a NN feedforward term. A simulation demonstrates the performance of the proposed identifier and controller. Although the proposed method guarantees asymptotic identification and asymptotic tracking, a limitation of the controller is that the input gain matrix is required to be exactly known, and system states are completely measurable.

The development of the observer in Chapter 4 is motivated by the need to estimate inaccessible system states when full state feedback is not available. In contrast to purely robust feedback methods in literature, a DNN-based robust adaptive approach is developed. The observer structure consists of a DNN to estimate the system dynamics on-line, a dynamic filter to estimate the unmeasurable state and a sliding mode feedback term to account for modeling errors and exogenous disturbances. The observed states are proven to asymptotically converge to the system states through Lyapunov-based analysis. Simulations and experiments on a two-link robot manipulator are performed to show the effectiveness of the proposed method in comparison to several other state estimation methods. The developed observer in Chapter 4 motivated the OFB control development illustrated in Chapters 5 and 6.

In Chapter 5, a DNN-based observer-controller is developed for uncertain nonlinear systems affected by bounded external disturbances, to achieve a two-fold result: asymptotic estimation of unmeasurable states and asymptotic tracking control. A combination of a NN feedforward term, along with estimated state feedback and sliding mode terms are designed for the controller. This method is an adaptive robust OFB method which is shown by experiments to reduce high-frequency content signals and improve tracking results in comparison with compared purely robust methods. Limitations of the method, however, are the requirement of the knowledge of the input gain matrix and the discontinuity of the controller.

An OFB control method for uncertain nonlinear systems with exogenous disturbances and time-varying input delays are presented in Chapter 6. To develop this approach, both the need to compensate for the lack of the system state and the need to develop some form of prediction of the nonlinear dynamics are required simultaneously. The delay is assumed to be bounded and slowly varying. A DNN-based observer is used to provide a surrogate for the inaccessible state, a predictor is utilized to inject a delay free control into the analysis, and a Lyapunov-based stability analysis facilitated by LK functionals is used to prove UUB estimation of the unmeasurable state and UUB tracking results. A continuous controller is developed, and the requirement of knowledge of the input gain matrix in Chapters 3 and 5 is relaxed in this chapter.

7.2 Future Work

This work illustrates that DNNs can be successfully applied to feedback control. While the developed methods are fairly general and applicable to a wide range of systems, several limitations still exist. This section discusses the open theoretical problems, implementation issues, and future research directions.

1. In all nonlinear systems considered in this dissertation, disturbances are assumed to be bounded and sufficiently smooth. A practically motivated problem is how to apply DNNs to design nonlinear identifiers, observers, controllers for nonlinear systems affected by stochastic disturbances. The parallels of the developed results to stochastic nonlinear systems should be pursued.
2. In Chapter 6, time-varying delays are assumed to be bounded, continuous, slowly varying and exactly known. Future efforts should try to relax these assumptions by considering the case where time delays are random, unknown, and/or the delay appears both in the control input and system states.
3. In Chapter 5, the developed OFB controller is a discontinuous controller which can cause chattering and requires infinite control bandwidth. How to design a continuous controller to obtain asymptotic results for uncertain nonlinear systems affected by exogenous bounded disturbances and the lack of full-state feedback remains an open problem.
4. In Chapters 3 and 5, the input gain matrix is assumed to be exactly known to obtain an asymptotic error convergence. Under suitable conditions, is the asymptotic error convergence achievable without the knowledge of the input gain matrix?
5. To the best of author's knowledge, all controllers in literature for uncertain nonlinear systems with a time-varying input delay only obtain UUB results. A potential full-state feedback or OFB controller for these systems to achieve an asymptotic result is still an open problem.
6. In Chapter 4, an extension of the DNN-based observer for n^{th} order nonlinear systems is introduced. In this method, however, full access to system states except for the

highest-order state is required. Relaxing this assumption while still obtaining asymptotic estimation remains an open problem.

7. The gain condition in (6-34) can be satisfied only if the time delay is sufficiently small and slowly varying and the approximation of the input gain matrix is sufficiently good. Is the system still stable and is the tracking objective achieved if the delayed time is long and fast changing or no enough knowledge to make a sufficient good guess for the input gain matrix? Can the approximation matrix adaptively approximate for the unknown input gain matrix? All of these questions could be explored in future efforts.

APPENDIX A
DYNAMIC NEURAL NETWORK-BASED ROBUST IDENTIFICATION AND CONTROL OF
A CLASS OF NONLINEAR SYSTEMS

A.1 Proof of the Inequality in Eq. (3–12)

Using Eq. (3–7) and the triangle inequality in Eq. (3–10) yields

$$\begin{aligned}
\|h\| &\leq \|W\| (\|\tilde{\sigma}_1\| + \|\tilde{\sigma}_2\|) + \|W\| \|\sigma(V^T x^*) - \sigma(\hat{V}^T x^*) - \sigma'(\hat{V}^T x^*) \tilde{V}^T x^*\| \\
&\quad + \|\varepsilon\| + \|d\| + \|\tilde{W}\| \|\sigma'(\hat{V}^T x^*)\| \|\tilde{V}\| \|x^*\| \\
&\leq \|W\| (\|\tilde{\sigma}_1\| + \|\tilde{\sigma}_2\| + \|\sigma(V^T x^*) - \sigma(\hat{V}^T x^*)\| + \|\sigma'(\hat{V}^T x^*) \tilde{V}^T x^*\|) \quad (\text{A-1}) \\
&\quad + \|\varepsilon\| + \|d\| + (\|W\| + \|\hat{W}\|) \|\sigma'(\hat{V}^T x^*)\| (\|V\| + \|\hat{V}\|) \|x^*\| \\
&\leq \bar{h}
\end{aligned}$$

where Assumptions 3.2, 3.3 - 3.5, the properties of the sample state $x^*(t)$, the projection bounds on the weight estimates in Eq. (3–11) are used. The bound $\bar{h} \in \mathbb{R}$ is computed by using the upper bounds of all terms in Eq. (A–1).

A.2 Proof of the Inequality in Eq. (3–23)

Using the update laws designing in Eq. (3–11) and the triangle inequality in Eq. (3–21) yields

$$\begin{aligned}
\|\tilde{N}\| &\leq \|A_s + \alpha I\| (\|r\| + \alpha \|e\|) + \|W\| \|\sigma(V^T x)\| \|V\| (\|r\| + \alpha \|e\|) \\
&\quad + \left\| \dot{\hat{W}} \right\| \|\sigma(\hat{V}^T x_d)\| + \|\hat{W}\| \|\sigma'(\hat{V}^T x_d)\| \left\| \dot{\hat{V}} \right\| \|x_d\| + \|e\| \\
&\leq \|A_s + \alpha I\| (\|r\| + \alpha \|e\|) + \|W\| \|\sigma(V^T x)\| \|V\| (\|r\| + \alpha \|e\|) + \|e\| \quad (\text{A-2}) \\
&\quad + \|\tilde{x}\| \left(\|\Gamma_1\| \|\sigma(\hat{V}^T \hat{x})\| \|\sigma(\hat{V}^T x_d)\| + \|\Gamma_2\| \|\hat{W}\|^2 \|\sigma'(\hat{V}^T x_d)\| \|\sigma'(\hat{V}^T x^*)\| \|x_d\| \|x^*\| \right)
\end{aligned}$$

Using the definition of $z(t)$ in Eq. (3–24) and the fact that $\|\tilde{x}\| \leq \|z\|$, $\|e\| \leq \|z\|$, $\|r\| \leq \|z\|$, the expression in (A–2) can be rewritten as

$$\begin{aligned} \|\tilde{N}\| &\leq [(\lambda_{\max}(A_s + \alpha I) + \|W\| \|\sigma(V^T x)\| \|V\|) (\alpha + 1) + 1] \|z\| \\ &\quad + \|z\| \left(\|\Gamma_1\| \|\sigma(\hat{V}^T \hat{x})\| \|\sigma(\hat{V}^T x_d)\| + \|\Gamma_2\| \|\hat{W}\|^2 \|\sigma'(\hat{V}^T x_d)\| \|\sigma'(\hat{V}^T x^*)\| \|x_d\| \|x^*\| \right) \\ &\leq \zeta_1 \|z\| \end{aligned} \tag{A–3}$$

where Assumptions 3.3 - 3.5, the properties of the sample state $x^*(t)$, the projection bounds on the weight estimates in Eq. (3–11) are used. The bound $\zeta_1 \in \mathbb{R}$ is computed by using the upper bounds of all terms in Eq. (A–3).

A.3 Proof of the Inequality in Eqs. (3–25) and (3–26)

Using the triangle inequality for the following equation yields

$$\begin{aligned} N_D &= \dot{d} + \dot{\varepsilon}, \\ \|N_D\| &\leq \|\dot{d}\| + \|\dot{\varepsilon}\| \leq \zeta_2, \\ \|\dot{N}_D\| &\leq \|\ddot{d}\| + \|\ddot{\varepsilon}\| \leq \zeta_4, \end{aligned}$$

where Assumptions 3.2 and 3.5 are used. The bound $\zeta_2, \zeta_4 \in \mathbb{R}$ are computed by using the upper bounds of the first and second derivatives of the disturbance and the reconstruction error. Similarly, the term $N_B(t)$ and its derivative can be upper-bounded as follow

$$\begin{aligned} N_B &= W^T \sigma'(V^T x) V^T \dot{x}_d - \hat{W}^T \sigma'(\hat{V}^T x_d) \hat{V}^T \dot{x}_d, \\ \|N_B\| &\leq \|W\| \|\sigma'(V^T x)\| \|V\| \|\dot{x}_d\| + \|\hat{W}\| \|\sigma'(\hat{V}^T x_d)\| \|\hat{V}\| \|\dot{x}_d\| \leq \zeta_3, \\ \dot{N}_B &= W^T \dot{\sigma}'(V^T x) V^T \dot{x}_d + W^T \sigma'(V^T x) V^T \ddot{x}_d - \dot{\hat{W}}^T \sigma'(\hat{V}^T x_d) \hat{V}^T \dot{x}_d \\ &\quad - \hat{W}^T \dot{\sigma}'(\hat{V}^T x_d) \hat{V}^T \dot{x}_d - \hat{W}^T \sigma'(\hat{V}^T x_d) \dot{\hat{V}}^T \dot{x}_d - \hat{W}^T \sigma'(\hat{V}^T x_d) \hat{V}^T \ddot{x}_d \end{aligned}$$

$$\begin{aligned}
\|\dot{N}_B\| &\leq \|W\| \|\sigma'(V^T x)\| \|V\| \|\dot{x}_d\| + \|W\| \|\sigma'(V^T x)\| \|V\| \|\ddot{x}_d\| \\
&\quad + \|\dot{W}\| \|\sigma'(\hat{V}^T x_d)\| \|\hat{V}\| \|\dot{x}_d\| + \|\hat{W}\| \|\sigma'(\hat{V}^T x_d)\| \|\hat{V}\| \|\dot{x}_d\| \\
&\quad + \|\hat{W}\| \|\sigma'(\hat{V}^T x_d)\| \|\dot{\hat{V}}\| \|\dot{x}_d\| + \|\hat{W}\| \|\sigma'(\hat{V}^T x_d)\| \|\hat{V}\| \|\ddot{x}_d\|
\end{aligned} \tag{A-4}$$

Using the Eq. (3-11), the following upper-bounds are obtained

$$\begin{aligned}
\|\dot{W}\| &\leq \|\Gamma_1\| \|\sigma(\hat{V}^T \hat{x})\| \|\tilde{x}\| \leq c_1 \|z\|, \\
\|\dot{\hat{V}}\| &\leq \|\Gamma_2\| \|x^*\| \|\tilde{x}\| \|\hat{W}\| \|\sigma'(\hat{V}^T x^*)\| \leq c_2 \|z\|,
\end{aligned}$$

and

$$\|\sigma'(V^T x)\| \leq \|\sigma''(V^T x)\| \|V\| \|\dot{x}\| = \|\sigma''(V^T x)\| \|V\| \|r - \alpha e + \dot{x}_d\| \leq c_3 + c_4 \|z\|,$$

$$\|\sigma'(\hat{V}^T x_d)\| \leq \|\sigma''(\hat{V}^T x_d)\| \left(\|\dot{\hat{V}}\| \|x_d\| + \|\hat{V}\| \|\dot{x}_d\| \right) \leq c_5 + c_6 \|z\|,$$

where $c_i \in \mathbb{R}$, ($i = 1, 2, \dots, 6$) are computable positive constants. Finally, the inequality (A-4) can be rewritten as

$$\|\dot{N}_B\| \leq \zeta_5 + \zeta_6 \|z\|,$$

where the bounds $\zeta_5, \zeta_6 \in \mathbb{R}$ are computed based on the constants c_i , ($i = 1, 2, \dots, 6$), and the upper-bounds of all other terms in the right side of (A-4).

A.4 Proof of the Inequality in Eq. (3-32)

Integrating (3-29) and using (3-22) yields

$$L(t) = \int_0^t \left(r^T (N_D + N_B - \beta_1 \text{sgn}(e)) - \beta_2 \|z\|^2 \right) d\tau + L(0).$$

Using the fact that $r = \dot{e} + \alpha e$ yields

$$\begin{aligned}
L(t) &= \int_0^t \dot{e}^T (N_D + N_B) d\tau - \int_0^t \dot{e}^T \beta_1 \text{sgn}(e) d\tau \\
&\quad + \int_0^t \alpha e^T (N_D + N_B - \beta_1 \text{sgn}(e)) d\tau - \int_0^t \beta_2 \|z\|^2 d\tau + L(0).
\end{aligned}$$

Integrating the first integral by parts and integrating the second integral, yields

$$L(t) = e^T N - e^T(0)N(0) - \int_0^t e^T (\dot{N}_B + \dot{N}_D) d\tau + \beta_1 \sum_{j=1}^n |e_j(0)| - \beta_1 \sum_{j=1}^n |e_j(t)| \\ + \int_0^t \alpha e^T (N_D + N_B - \beta_1 \text{sgn}(e)) d\tau - \int_0^t \beta_2 \|z\|^2 d\tau + L(0).$$

Using the fact that $\|e\| \leq \sum_{j=1}^n |e_j(t)|$, the following upper bound is obtained

$$L(t) \leq \|e\| \|N\| - e^T(0)N(0) + \beta_1 \sum_{j=1}^n |e_j(0)| - \beta_1 \|e\| \\ + \int_0^t \|e\| (\|\dot{N}_B\| + \|\dot{N}_D\|) d\tau + \int_0^t \alpha \|e\| (\|N_D\| + \|N_B\| - \beta_1) d\tau \\ - \int_0^t \beta_2 \|z\|^2 d\tau + L(0).$$

Using the bounds in (3–25) and (3–26), and rearranging terms, the following expression is obtained

$$L(t) \leq \beta_1 \sum_{j=1}^n |e_j(0)| - e^T(0)N(0) + L(0) - (\beta_1 - \zeta_2 - \zeta_3) \|e\| \\ - \int_0^t \alpha \|e\| (\beta_1 - \zeta_2 - \zeta_3 - \frac{\zeta_4}{\alpha} - \frac{\zeta_5}{\alpha}) d\tau - \int_0^t (\beta_2 - \zeta_6) \|z\|^2 d\tau.$$

If the sufficient conditions in (3–30) are satisfied, then the following inequality holds

$$L(t) \leq \beta_1 \sum_{j=1}^n |e_j(0)| - e^T(0)N(0) + L(0).$$

APPENDIX B
DYNAMIC NEURAL NETWORK-BASED GLOBAL OUTPUT FEEDBACK TRACKING
CONTROL FOR UNCERTAIN SECOND-ORDER NONLINEAR SYSTEMS

Proof of the Inequality in (5-31)

Integrating (5-30) and using (5-14) yields

$$H = \int_0^t L d\tau = \int_0^t \left(r_{es}^T (N_D + N_{B_1} - \beta_1 \text{sgn}(\tilde{x} + \mathbf{v})) + r_{ir}^T (N_D + N_{B_1} - \beta_2 \text{sgn}(e + \mathbf{v})) \right. \\ \left. + (\dot{\tilde{x}} + \dot{e} + 2\dot{\mathbf{v}})^T N_{B_2} - \beta_3 \|z\|^2 \right) d\tau.$$

Using the fact that $r_{es} = \dot{\tilde{x}} + \dot{\mathbf{v}} + \alpha(\tilde{x} + \mathbf{v})$ and $r_{ir} = \dot{e} + \dot{\mathbf{v}} + \alpha(e + \mathbf{v})$ yields

$$H = \int_0^t \left(\dot{\tilde{x}} + \dot{e} + 2\dot{\mathbf{v}} \right)^T (N_D + N_{B_1} + N_{B_2}) d\tau - \int_0^t (\dot{\tilde{x}} + \dot{\mathbf{v}})^T \beta_1 \text{sgn}(\tilde{x} + \mathbf{v}) d\tau \\ - \int_0^t (\dot{e} + \dot{\mathbf{v}})^T \beta_2 \text{sgn}(e + \mathbf{v}) d\tau + \int_0^t \alpha(\tilde{x} + \mathbf{v})^T (N_D + N_{B_1} - \beta_1 \text{sgn}(\tilde{x} + \mathbf{v})) d\tau \\ + \int_0^t \alpha(e + \mathbf{v})^T (N_D + N_{B_1} - \beta_2 \text{sgn}(e + \mathbf{v})) d\tau - \int_0^t \beta_3 \|z\|^2 d\tau.$$

Integrating the first integral by parts, and integrating the second and third integrals yields

$$H = (\tilde{x} + e + 2\mathbf{v})^T N - [\tilde{x}(0) + e(0) + 2\mathbf{v}(0)]^T N(0) \\ + \beta_1 \sum_{j=1}^n [|\tilde{x}_j(0) + v_j(0)| - |\tilde{x}_j + v_j|] - \int_0^t (\tilde{x} + e + 2\mathbf{v})^T (\dot{N}_D + \dot{N}_B) d\tau \\ + \beta_2 \sum_{j=1}^n [|e_j(0) + v_j(0)| - |e_j + v_j|] - \int_0^t \beta_3 \|z\|^2 d\tau \\ + \int_0^t \alpha(e + \mathbf{v})^T [N_D + N_{B_1} - \beta_2 \text{sgn}(e + \mathbf{v})] d\tau.$$

Using the fact that $\|\tilde{x} + \mathbf{v}\| \leq \sum_{j=1}^n |\tilde{x}_j + \mathbf{v}_j|$ and $\|e + \mathbf{v}\| \leq \sum_{j=1}^n |e_j + \mathbf{v}_j|$, the following upper bound is obtained

$$\begin{aligned}
H &\leq \|\tilde{x} + e + 2\mathbf{v}\| \|N\| - (\tilde{x}(0) + e(0) + 2\mathbf{v}(0))^T N(0) \\
&\quad + \beta_1 \sum_{j=1}^n |\tilde{x}_j(0) + \mathbf{v}_j(0)| - \beta_1 \|\tilde{x} + \mathbf{v}\| \\
&\quad + \beta_2 \sum_{j=1}^n |e_j(0) + \mathbf{v}_j(0)| - \beta_2 \|e + \mathbf{v}\| \\
&\quad + \int_0^t \alpha \|\tilde{x} + \mathbf{v}\| \left\| N_D + N_{B_1} + \frac{\dot{N}}{\alpha} - \beta_1 \right\| d\tau \\
&\quad + \int_0^t \alpha \|e + \mathbf{v}\| \left\| N_D + N_{B_1} + \frac{\dot{N}}{\alpha} - \beta_2 \right\| d\tau - \int_0^t \beta_3 \|z\|^2 d\tau.
\end{aligned}$$

Using the bounds in (5–31), based on the fact that $\|\tilde{x} + e + 2\mathbf{v}\| \leq \|\tilde{x} + \mathbf{v}\| + \|e + \mathbf{v}\|$, and rearranging terms, the following expression is obtained

$$\begin{aligned}
H &\leq \beta_1 \sum_{j=1}^n |\tilde{x}_j(0) + \mathbf{v}_j(0)| + \beta_2 \sum_{j=1}^n |e_j(0) + \mathbf{v}_j(0)| \\
&\quad - (\tilde{x}(0) + e(0) + 2\mathbf{v}(0))^T N(0) - (\beta_1 - \zeta_2 - \zeta_3 - \zeta_4) \|\tilde{x} + \mathbf{v}\| \\
&\quad - (\beta_2 - \zeta_2 - \zeta_3 - \zeta_4) \|e + \mathbf{v}\| - \int_0^t \alpha \|\tilde{x} + \mathbf{v}\| \left(\beta_1 - \zeta_2 - \zeta_3 - \frac{\zeta_5}{\alpha} - \frac{\zeta_6}{\alpha} \right) d\tau \\
&\quad - \int_0^t \alpha \|e + \mathbf{v}\| \left(\beta_2 - \zeta_2 - \zeta_3 - \frac{\zeta_5}{\alpha} - \frac{\zeta_6}{\alpha} \right) d\tau - \int_0^t (\beta_3 - 2\zeta_7) \|z\|^2 d\tau.
\end{aligned}$$

If the sufficient conditions in (5–31) are satisfied, then the following inequality holds

$$\begin{aligned}
H &\leq \beta_1 \sum_{j=1}^n |\tilde{x}_j(0) + \mathbf{v}_j(0)| + \beta_2 \sum_{j=1}^n |e_j(0) + \mathbf{v}_j(0)| \\
&\quad - (\tilde{x}(0) + e(0) + 2\mathbf{v}(0))^T N(0), \\
H &= \int_0^t L d\tau \leq P(0). \tag{B–1}
\end{aligned}$$

Hence, using (5–29) and (B–1), it can be shown that

$$P(t) \geq 0.$$

REFERENCES

- [1] B. Xian, M. S. de Queiroz, D. M. Dawson, and M. McIntyre, "A discontinuous output feedback controller and velocity observer for nonlinear mechanical systems," *Automatica*, vol. 40, no. 4, pp. 695–700, 2004.
- [2] L. Vasiljevic and H. Khalil, "Error bounds in differentiation of noisy signals by high-gain observers," *Systems & Control Letters*, vol. 57, no. 10, pp. 856–862, 2008.
- [3] D. White and D. Sofge, *Handbook of intelligent control: neural, fuzzy, and adaptive approaches*. Van Nostrand Reinhold Company, 1992.
- [4] W. T. Miller, R. Sutton, and P. Werbos, *Neural Networks for Control*. MIT Press, 1990.
- [5] F. L. Lewis, "Nonlinear network structures for feedback control," *Asian J. Control*, vol. 1, no. 4, pp. 205–228, 1999.
- [6] D. Pham and X. Liu, "Dynamic system identification using partially recurrent neural networks," *J. Syst. Eng.*, vol. 2, no. 2, pp. 90–97, 1992.
- [7] M. Gupta, L. Jin, and N. Homma, *Static and dynamic neural networks: from fundamentals to advanced theory*. Wiley-IEEE Press, 2003.
- [8] K. Funahashi and Y. Nakamura, "Approximation of dynamic systems by continuous-time recurrent neural networks," *Neural Networks*, vol. 6, pp. 801–806, 1993.
- [9] M. Polycarpou and P. Ioannou, "Identification and control of nonlinear systems using neural network models: Design and stability analysis," *Systems Report 91-09-01, University of Southern California*, 1991.
- [10] K. Narendra and K. Parthasarathy, "Identification and control of dynamical systems using neural networks," *IEEE Trans. Neural Networks*, vol. 1, no. 1, pp. 4–27, 1990.
- [11] E. Kosmatopoulos, M. Polycarpou, M. Christodoulou, and P. Ioannou, "High-order neural network structures for identification of dynamical systems," *IEEE Trans. Neural Networks*, vol. 6, no. 2, pp. 422 – 431, 1995.
- [12] G. A. Rovithakis and M. A. Christodoulou, "Adaptive control of unknown plants using dynamical neural networks," *IEEE Trans. Syst. Man Cybern.*, vol. 24, pp. 400–412, 1994.
- [13] A. Delgado, C. Kambhampati, and K. Warwick, "Dynamic recurrent neural network for system identification and control," *IEE Proc. Contr. Theor. Appl.*, vol. 142, no. 4, pp. 307–314, 1995.
- [14] A. S. Poznyak, W. Yu, E. N. Sanchez, and J. P. Perez, "Nonlinear adaptive trajectory tracking using dynamic neural networks," *IEEE Trans. Neural Networks*, vol. 10, no. 6, pp. 1402–1411, Nov 1999.

- [15] A. Poznyak, E. Sanchez, and W. Yu, *Differential neural networks for robust nonlinear control: identification, state estimation and trajectory tracking*. World Scientific Pub Co Inc, 2001.
- [16] X. Ren, A. Rad, P. Chan, and W. Lo, “Identification and control of continuous-time nonlinear systems via dynamic neural networks,” *IEEE Trans. Ind. Electron.*, vol. 50, no. 3, pp. 478–486, 2003.
- [17] J. Hopfield, “Neurons with graded response have collective computational properties like those of two-state neurons,” *Proc. Nat. Acad. Sci. U.S.A.*, vol. 81, no. 10, p. 3088, 1984.
- [18] X. Li and W. Yu, “Dynamic system identification via recurrent multilayer perceptrons,” *Inf. Sci. Inf. Comput. Sci.*, vol. 147, pp. 45–63, 2002.
- [19] H. Dinh, S. Bhasin, and W. E. Dixon, “Dynamic neural network-based robust identification and control of a class of nonlinear systems,” in *Proc. IEEE Conf. Decis. Control*, Atlanta, GA, 2010, pp. 5536–5541.
- [20] S. Bhasin, M. Johnson, and W. E. Dixon, “A model-free robust policy iteration algorithm for optimal control of nonlinear systems,” in *Proc. IEEE Conf. Decis. Control*, Atlanta, GA, 2010, pp. 3060–3065.
- [21] J.-J. Slotine, J. Hedrick, and E. A. Misawa, “On sliding observers for nonlinear systems,” in *American Control Conf.*, 1986, pp. 1794–1800.
- [22] C. Canudas De Wit and J.-J. Slotine, “Sliding observers for robot manipulators,” *Automatica*, vol. 27, pp. 859–864, 1991.
- [23] M. Mohamed, T. Karim, and B. Safya, “Sliding mode observer for nonlinear mechanical systems subject to nonsmooth impacts,” in *Int. Multi-Conf. Syst. Signals Devices*, 2010.
- [24] K. W. Lee and H. K. Khalil, “Adaptive output feedback control of robot manipulators using high-gain observer,” *INT. J. CONTROL*, vol. 67, pp. 869–886, 1997.
- [25] E. Shin and K. Lee, “Robust output feedback control of robot manipulators using high-gain observer,” in *IEEE Int. Conf. on Control and Appl.*, 1999.
- [26] A. Astolfi, R. Ortega, and A. Venkatraman, “A globally exponentially convergent immersion and invariance speed observer for n degrees of freedom mechanical systems,” in *Proc. Chin. Control Conf.*, 2009.
- [27] N. Lotfi and M. Namvar, “Global adaptive estimation of joint velocities in robotic manipulators,” *IET Control Theory Appl.*, vol. 4, pp. 2672–2681, 2010.
- [28] J. Davila, L. Fridman, and A. Levant, “Second-order sliding-mode observer for mechanical systems,” *IEEE Trans. Autom. Control*, vol. 50, pp. 1785–1789, 2005.
- [29] D. Dawson, Z. Qu, and J. Carroll, “On the state observation and output feedback problems for nonlinear uncertain dynamic systems,” *Syst. Contr. Lett.*, vol. 18, pp. 217–222, 1992.

- [30] Y. H. Kim and F. L. Lewis, "Neural network output feedback control of robot manipulators," *IEEE Trans. Robot. Autom.*, vol. 15, pp. 301–309, 1999.
- [31] H. Berghuis and H. Nijmeijer, "A passivity approach to controller-observer design for robots," *IEEE Trans. Robot. Autom.*, vol. 9, pp. 740–754, 1993.
- [32] K. D. Do, Z. Jiang, and J. Pan, "A global output-feedback controller for simultaneous tracking and stabilization for unicycle-type mobile robots," *IEEE Trans. Robot. Autom.*, vol. 20, pp. 589–594, 2004.
- [33] S. Y. Lim, D. M. Dawson, and K. Anderson, "Re-examining the nicosia-tomei robot observer-controller for a backstepping perspective," *IEEE Trans. Control Syst. Technol.*, vol. 4, pp. 304–310, 1996.
- [34] M. A. Arteaga and R. Kelly, "Robot control without velocity measurements: New theory and experiment results," *IEEE Trans. Robot. Autom.*, vol. 20, pp. 297–308, 2004.
- [35] K. Kaneko and R. Horowitz, "Repetitive and adaptive control of robot manipulators with velocity estimation," *IEEE Trans. Robot. Autom.*, vol. 12, pp. 204–217, 1997.
- [36] T. Burg, D. Dawson, J. Hu, and M. de Queiroz, "An adaptive partial state feedback controller for rigid robot manipulators," *IEEE Trans. Autom. Control*, vol. 41, pp. 1024–1031, 1996.
- [37] T. Burg, D. M. Dawson, and P. Vedagarbha, "A redesigned dcac controller without velocity measurements: Theory and demonstration," *Robotica*, vol. 15, no. 4, pp. 337–346, 1997.
- [38] F. Zhang, D. M. Dawson, M. S. de Queiroz, and W. E. Dixon, "Global adaptive output feedback tracking control of robot manipulators," *IEEE Trans. Automat. Control*, vol. 45, pp. 1203–1208, 2000.
- [39] S. Seshagiri and H. Khalil, "Output feedback control of nonlinear systems using rbf neural networks," *IEEE Trans. Neural Netw.*, vol. 11, pp. 69–79, 2000.
- [40] J. Y. Choi and J. A. Farrell, "Adaptive observer backstepping control using neural network," *IEEE Trans. Neural Netw.*, vol. 12, pp. 1103–1112, 2001.
- [41] A. J. Calise, N. Hovakimyan, and M. Idan, "Adaptive output feedback control of nonlinear systems using neural networks," *Automatica*, vol. 37, no. 8, pp. 1201–1211, 2001.
- [42] N. Hovakimyan, F. Nardi, A. Calise, and N. Kim, "Adaptive output feedback control of uncertain nonlinear systems using single-hidden-layer neural networks," *IEEE Trans. Neural Networks*, vol. 13, no. 6, pp. 1420–1431, Nov. 2002.
- [43] S. Islam and P. Liu, "Robust adaptive fuzzy output feedback control system for robot manipulators," *IEEE/ASME Trans. Mechatron.*, vol. 16, pp. 288–296, 2011.
- [44] J. A. Cook and B. K. Powell, "Modeling of an internal combustion engine for control analysis," *IEEE Control Syst. Mag*, pp. 20–25, 1988.

- [45] M. Kao and J. J. Moskwa, "Turbocharged diesel engine modeling for nonlinear engine control and state estimation," *ASME J. Dyn. Syst., Meas., Control*, vol. 117, pp. 20–30, 1995.
- [46] F. L. Lewis, R. Selmic, and J. Campos, *Neuro-Fuzzy Control of Industrial Systems with Actuator Nonlinearities*. Philadelphia, PA, USA: Society for Industrial and Applied Mathematics, 2002.
- [47] G. Niemeyer and J.-J. Slotine, "Telemanipulation with time delays," *Int. J. Robot. Res.*, vol. 23, pp. 873–890, 2004.
- [48] A. Aziminejad, M. Tavakoli, R. V. Patel, and M. Moallem, "Stability and performance in delayed bilateral teleoperation: Theory and experiments," *Control Eng. Pract.*, vol. 16, pp. 1329–1343, 2008.
- [49] Y. Gu, C. Zhang, and K. T. Chong, "Adaptive passive control with varying time delay," *Simul. Model. Pract. Theory*, vol. 18, pp. 1–8, 2010.
- [50] F. Hashemzadeh, I. Hassanzadeh, M. Tavakoli, and G. Alizadeh, "Adaptive control for state synchronization of nonlinear haptic telerobotic systems with asymmetric varying time delays," *J. Intell. Robot. Syst.*, 2012.
- [51] N. N. Krasovskii, *Stability of motion*. Stanford University Press, 1963.
- [52] X. Li and C. de Souza, "Delay-dependent robust stability and stabilization of uncertain linear delay systems: a linear matrix inequality approach," *IEEE Trans. Autom. Control*, vol. 42, no. 8, pp. 1144–1148, Aug 1997.
- [53] V. B. Kolmanovskii, S.-I. Niculescu, and J.-P. Richard, "On the liapunov-krasovskii functionals for stability analysis of linear delay systems," *Int. J. Control*, vol. 72, pp. 374 – 384, 1999.
- [54] B. S. Razumikhin, "On the stability of systems with a delay," *Prikl. Mat. Meh*, vol. 20, pp. 500–512, 1956.
- [55] ———, "Application of liapunov's method to problems in the stability of systems with a delay," *Automat. i Telemekh*, vol. 21, pp. 740–749, 1960.
- [56] M. Jankovic, "Control Lyapunov-Razumikhin functions and robust stabilization of time delay systems," *IEEE Trans. Autom. Control*, vol. 46, no. 7, pp. 1048–1060, 2001.
- [57] R. Bellman and K. L. Cooke, *Differential- Difference Equations*. Academic Press, 1963.
- [58] L. E. Elsgolts and S. B. Norkin, *Introduction to the theory and application of differential equations with deviating arguments*. Academic Press, 1973, vol. 105.
- [59] F. Mazenc, S. Mondie, R. Francisco, P. Conge, I. Lorraine, and F. Metz, "Global asymptotic stabilization of feedforward systems with delay in the input," *IEEE Trans. Autom. Control*, vol. 49, (5), pp. 844–850, 2004.

- [60] B. Chen, X. Liu, and S. Tong, “Robust fuzzy control of nonlinear systems with input delay,” *Chaos, Solitons & Fractals*, vol. 37, no. 3, pp. 894–901, 2008.
- [61] M. Krstic, “Input delay compensation for forward complete and strict-feedforward nonlinear systems,” *IEEE Trans. Autom. Control*, vol. 55, pp. 287–303, feb. 2010.
- [62] B. Castillo-Toledo, S. Di Gennaro, and G. Castro, “Stability analysis for a class of sampled nonlinear systems with time-delay,” in *Proc. IEEE Conf. Decis. Control*, 2010, pp. 1575–1580.
- [63] N. Sharma, S. Bhasin, Q. Wang, and W. E. Dixon, “Predictor-based control for an uncertain Euler-Lagrange system with input delay,” *Automatica*, vol. 47, no. 11, pp. 2332–2342, 2011.
- [64] L. Guo, “ H_∞ output feedback control for delay systems with nonlinear and parametric uncertainties,” *Proc. IEE Control Theory Appl.*, vol. 149, no. 3, pp. 226–236, 2002.
- [65] W. Li, Y. Dong, and X. Wang, “Robust H_∞ control of uncertain nonlinear systems with state and input time-varying delays,” in *Proc. Chin. Control Decis. Conf.*, 2010, pp. 317–321.
- [66] N. Bekiaris-Liberis and M. Krstic, “Compensation of time-varying input delay for nonlinear systems,” in *Mediterr. Conf. Control and Autom.*, Corfu, Greece, 2011.
- [67] M. Krstic, “Lyapunov stability of linear predictor feedback for time-varying input delay,” *IEEE Trans. Autom. Control*, vol. 55, pp. 554–559, 2010.
- [68] N. Fischer, R. Kamalapurkar, N. Fitz-Coy, and W. E. Dixon, “Lyapunov-based control of an uncertain Euler-Lagrange system with time-varying input delay,” in *American Control Conference*, Montréal, Canada, June 2012, pp. 3919–3924.
- [69] A. Ailon and M. Gil, “Stability analysis of a rigid robot with output-based controller and time delay,” *Systems & Control Letters*, vol. 40, no. 1, pp. 31–35, 2000.
- [70] A. Ailon, R. Segev, and S. Arogeti, “A simple velocity-free controller for attitude regulation of a spacecraft with delayed feedback,” *IEEE Trans. Autom. Control*, vol. 49, no. 1, pp. 125–130, 2004.
- [71] A. Ailon, “Asymptotic stability in a flexible-joint robot with model uncertainty and multiple time delays in feedback,” *J. Franklin Inst.*, vol. 341, no. 6, pp. 519–531, 2004.
- [72] A. Poznyak, W. Yu, E. Sanchez, and H. Sira-Ramirez, “Robust identification by dynamic neural networks using sliding mode learning,” *Appl. Math. Comput. Sci.*, vol. 8, pp. 135–144, 1998.
- [73] J. Huang and F. Lewis, “Neural-network predictive control for nonlinear dynamic systems with time-delay,” *IEEE Trans. Neural Networks*, vol. 14, no. 2, pp. 377–389, 2003.

- [74] B. Xian, D. M. Dawson, M. S. de Queiroz, and J. Chen, “A continuous asymptotic tracking control strategy for uncertain nonlinear systems,” *IEEE Trans. Autom. Control*, vol. 49, pp. 1206–1211, 2004.
- [75] P. M. Patre, W. MacKunis, K. Kaiser, and W. E. Dixon, “Asymptotic tracking for uncertain dynamic systems via a multilayer neural network feedforward and RISE feedback control structure,” *IEEE Trans. Automat. Control*, vol. 53, no. 9, pp. 2180–2185, 2008.
- [76] H. T. Dinh, R. Kamalapurkar, S. Bhasin, and W. E. Dixon, “Dynamic neural network-based robust observers for second-order uncertain nonlinear systems,” in *Proc. IEEE Conf. Decis. Control*, Orlando, FL, 2011, pp. 7543–7548.
- [77] H. T. Dinh, S. Bhasin, D. Kim, and W. E. Dixon, “Dynamic neural network-based global output feedback tracking control for uncertain second-order nonlinear systems,” in *American Control Conference*, Montréal, Canada, June 2012, pp. 6418–6423.
- [78] S. Haykin, *Neural Networks and Learning Machines*, 3rd ed. Upper Saddle River, NJ: Prentice Hall, 2008.
- [79] D. R. Hush and B. G. Horne, “Progress in supervised neural networks,” *IEEE Signal Process. Mag.*, vol. 10, no. 1, pp. 8–39, 1993.
- [80] J. Hopfield, “Neural networks and physical systems with emergent collective computational abilities,” in *Proc. Nat. Acad. Sci. USA*, vol. 79, 1982, pp. 2554–2558.
- [81] E. Sontag, “Neural nets as system models and controllers,” in *Proc. 7th Yale workshop on Adaptive and Learning Systems*, 1992, pp. 73–79.
- [82] I. Sandberg, “Approximation theorems for discrete-time systems,” *IEEE Trans. on Circuits and Syst.*, vol. 38, pp. 564–566, 1991.
- [83] ———, “Uniform approximation and the circle criterion,” *IEEE Trans. on Autom. Control*, vol. 38, pp. 1450–1458, 1993.
- [84] ———, “Uniform approximation of multidimensional myopic maps,” *IEEE Trans. on Circuits and Syst.*, vol. 44, pp. 477–485, 1997.
- [85] K. Hornick, “Approximation capabilities of multilayer feedforward networks,” *Neural Networks*, vol. 4, pp. 251–257, 1991.
- [86] G. Cybenko, “Approximation by superpositions of a sigmoidal function,” *Math. Control Signals Syst.*, vol. 2, pp. 303–314, 1989.
- [87] A. Barron, “Universal approximation bounds for superpositions of a sigmoidal function,” *IEEE Trans. Inf. Theory*, vol. 39, no. 3, pp. 930–945, 1993.
- [88] W. E. Dixon, A. Behal, D. M. Dawson, and S. Nagarkatti, *Nonlinear Control of Engineering Systems: A Lyapunov-Based Approach*. Birkhäuser: Boston, 2003.

- [89] M. Krstic, P. V. Kokotovic, and I. Kanellakopoulos, *Nonlinear and Adaptive Control Design*. John Wiley & Sons, 1995.
- [90] P. M. Patre, W. Mackunis, C. Makkar, and W. E. Dixon, “Asymptotic tracking for systems with structured and unstructured uncertainties,” *IEEE Trans. Control Syst. Technol.*, vol. 16, pp. 373–379, 2008.
- [91] A. Filippov, “Differential equations with discontinuous right-hand side,” *Am. Math. Soc. Transl.*, vol. 42 no. 2, pp. 199–231, 1964.
- [92] A. F. Filippov, *Differential Equations with Discontinuous Right-hand Sides*. Kluwer Academic Publishers, 1988.
- [93] G. V. Smirnov, *Introduction to the theory of differential inclusions*. American Mathematical Society, 2002.
- [94] J. P. Aubin and H. Frankowska, *Set-valued analysis*. Birkhäuser, 2008.
- [95] R. Leine and N. van de Wouw, “Non-smooth dynamical systems,” in *Stability and Convergence of Mechanical Systems with Unilateral Constraints*, ser. Lecture Notes in Applied and Computational Mechanics. Springer Berlin / Heidelberg, 2008, vol. 36, pp. 59–77.
- [96] F. H. Clarke, *Optimization and nonsmooth analysis*. SIAM, 1990.
- [97] D. Shevitz and B. Paden, “Lyapunov stability theory of nonsmooth systems,” *IEEE Trans. Autom. Control*, vol. 39 no. 9, pp. 1910–1914, 1994.
- [98] B. Paden and S. Sastry, “A calculus for computing Filippov’s differential inclusion with application to the variable structure control of robot manipulators,” *IEEE Trans. Circuits Syst.*, vol. 34 no. 1, pp. 73–82, 1987.

BIOGRAPHICAL SKETCH

Huyen T. Dinh was born in April, 1984 in Thai Nguyen, Vietnam. She received her Bachelor of Engineering degree in Mechatronic Engineering in 2006 from Hanoi University of Technology (HUT), Vietnam. She worked as a lecturer in Mechanical Engineering department of University of Transport and Communications, Vietnam from September 2006. She then joined the Nonlinear Controls and Robotics (NCR) research group at the University of Florida (UF) to pursue her doctoral research under the advisement of Dr. Warren Dixon since August 2008 and completed her Ph.D. in August 2012. From September 2012 onward she will be an assistant professor in the University of Transport and Communications, Vietnam.